Ph.D. Thesis

Model-specific predictions and testability in realistic supersymmetric grand unified models

(現実的な超対称大統一模型における模型特有の予言とその検証可能性)

Yoshihiro Shigekami

Theoretical Elementary Particle Physics Group,
Department of Physics, Nagoya University

Submitted: December 2017
Revised: February 2018

Abstract

The Standard Model (SM) is almost consistent with the current experimental data and completed by the discovery of a Higgs boson at the Large Hadron Collider (LHC). It is constructed by the gauge theory with $SU(3)_C \times SU(2)_L \times U(1)_Y$ gauge symmetries. However, there are still open questions which cannot solve in the SM. This means that it is needed to consider a model beyond the SM.

One of the interesting and promising extensions is a supersymmetric (SUSY) grand unified theory (GUT). In this framework, there are two types of unification. First one is a unification of interactions which means that three SM gauge couplings are unified into a single one. Second one is a unification of matters, which is occurred by embedding the SM particles in a few multiplets. For these types of unification, there are quantitative and qualitative supports from experimental results. Moreover, some of the problems or questions in the SM can be solved, e.g. the hierarchy problem, charge quantization and explanation of the fermion mass hierarchies.

On the other hand, SUSY GUT models cause new problems which are not induced in the SM. One of these is an undesired Yukawa relation. Because of the matter unification, it predicts that Yukawa couplings are also unified at the GUT scale. Although this is one of the attractive predictions of GUT, observed SM fermion masses and the Cabibbo-Kobayashi-Maskawa (CKM) matrix are hard to obtain. Another problems are flavor-changing neutral current (FCNC) and CP-violating processes induced by SUSY particles. Since parameters in a SUSY model can be arbitrary numbers or structures, there are sizable contributions from SUSY particles to these processes in general. Such contributions, however, are strongly constrained by the experimental observables.

In this thesis, we focus on $SO(10)$ and E_6 SUSY GUT models which can realize the SM fermion mass spectrum and CKM matrix. In our $SO(10)$ model, there are flavor-violating couplings with new gauge boson only for the $\bar{\mathbf{5}}$ fields because of a mixing with additional matter fields. As a result, we obtain predictions specific to our model. In addition, we consider E_6 model with a flavor $SU(2)_F$ and anomalous $U(1)_A$ gauge symmetries, in which almost all problems caused in a SUSY GUT model are solved in a natural assumption. In this model, there are non-vanishing D-term contributions which destroy the degeneracy of the sfermion mass spectrum, and these contributions are constrained by FCNC processes. We investigate the upper bound of these contributions and find that D-terms are allowed to be sizable.

The sfermion mass spectrum predicted in the $E_6 \times SU(2)_F \times U(1)_A$ SUSY GUT model is natural SUSY-type sfermion spectrum. This type of spectrum suffers from bounds of chromo-electric dipole moment (CEDM). Therefore, we also search lower bounds of sfermion masses in different types of Yukawa structure. We find that if up-type Yukawa couplings are real at the GUT scale, CEDM bounds are satisfied even when the stop mass is $\mathcal{O}(1)$ TeV.

Contents

1 Introduction

The Standard Model (SM) of particle physics is completed by the discovery of a Higgs boson at the Large Hadron Collider (LHC), whose mass is 125 GeV [1, 2]. It is well-known that the predictions of the SM for various observables are almost consistent with the experimental data. However, there are still open questions which should be solved. Some of these questions cannot solve in the framework of the SM. For example, there are the questions about the reason why the masses of the SM fermions have rich hierarchical structures, massless neutrinos which conflict with the neutrino oscillation experiments [3–16], charge quantization which is why the electron charge Q_e and proton charge Q_p have the relation $Q_e = -Q_p$ [17], the hierarchy problem which is the fine-tuning between a bare parameter and the observed value of the Higgs mass [18] and no dark matter candidates in the SM. These questions mean that a model beyond the SM is needed.

One of the interesting and promising extensions of the SM is supersymmetric (SUSY) grand unified theory (GUT). GUTs [19] predict two types of unification: unification of interactions and unification of matters. The unification of interactions means that three gauge couplings in the SM are unified into a single one. For this unification, there is a quantitative support from the observed gauge couplings. The unification of matters is realized by embedding quarks and leptons into a few multiplets, e.g. $\mathbf{10}$ and $\bar{\mathbf{5}}$ of $SU(5)$. For this unification, we have qualitative support from the observed masses of quarks and leptons, which means that the fermion mass hierarchies can be explained by assuming that $\mathbf{10}$ fields have stronger hierarchies than $\bar{\mathbf{5}}$ fields in the Yukawa couplings. Moreover, the charge quantization is also explained by the symmetry breaking $SU(5) \to SU(3)_C \times SU(2)_L \times U(1)_Y$. In addition, SUSY particles introduced in a SUSY model solve the hierarchy problem and provide dark matter candidates in the models with R-parity.

However, SUSY GUT models suffer from the another problems which are not caused in the SM. In the point of the view of a GUT model, new particles which are new gauge bosons and a color-triplet Higgs induce proton decays, e.g. $p \to e\pi$ and $p \to K\nu$. We expect that their mass scales are much higher than the weak scale from the constraints of the proton lifetime. In $SU(5)$ GUT, the color-triplet Higgs and the doublet Higgs which is regarded as the SM Higgs doublet are belonging to a single multiplet, $\mathbf{5}_H$. Therefore, a huge fine-tuning is needed to realize both of the masses. In addition, because of the matter unification, the Yukawa couplings are also unified at the GUT scale as $Y_d = Y_e^T$ in $SU(5)$ GUT and $Y_u = Y_d = Y_e^T = Y_{\nu_D}$ in $SO(10)$ GUT, where Y_{ν_D} is a Yukawa interaction for Dirac neutrinos. Although these relations which are called *Yukawa relations* in this thesis are one of the attractive hypotheses, they are inconsistent with the observed fermion masses.

In a SUSY model, a lot of parameters are introduced in order to break SUSY softly.

Some of these parameters, especially scalar cubic couplings and mass matrices for scalar fermions (sfermions), induce flavor-violating and CP-violating processes and are strongly constrained from the experimental observables. Another problem is known as the μ-problem [20] which is a question about the size of the Higgsino mass parameter μ in the Higgs sector for a minimal SUSY SM (MSSM). Therefore, we should consider these problems when one constructs a realistic model in the framework of SUSY GUT.

In this thesis, we mainly focus on the Yukawa relations and flavor and CP processes in $SO(10)$ and E_6 SUSY GUT models. As mentioned above, the Yukawa relations in the $SO(10)$ GUT are very strong since the SM fermions of one generation are unified into a single spinor multiplet, **16** [21, 22]. Therefore, it is hard to obtain the realistic fermion mass spectrum without some extension. There are mainly 3 types of solutions: to add higher-dimensional operators [23], to introduce additional Higgs fields [24, 25] and to introduce additional matter fields [26]. We proposed one of the solutions, introducing the additional matter fields, **10** of $SO(10)$ [27, 28]. In such a case, the SM modes for $\bar{\mathbf{5}}$ fields are given by linear combinations of the fields coming from **16** and **10** of $SO(10)$. Therefore, the Yukawa couplings for $\bar{\mathbf{5}}$ fields are modified from the unified one. In addition, by considering higher-dimensional operators, realistic Yukawa structures can be obtained. Note that in this thesis, a model in which realistic Yukawa structures are realized is called *realistic model*.

The elements of the mixing matrix for the $\bar{\mathbf{5}}$ fields affect the couplings of gauge bosons and $\bar{\mathbf{5}}$ fields. Because of the rank of $SO(10)$, there is additional gauge boson in the model and this gauge boson induces flavor-violating processes at the tree-level. This is because $\bar{\mathbf{5}}$ fields from **16** and **10** have different charges under the additional $U(1)'$ symmetry. We investigate predictions of this model and discuss the bounds from flavor-changing neutral current (FCNC) processes [28][1]. Note that since these flavor-violating couplings are only for $\bar{\mathbf{5}}$ fields, we expect that some predictions specific to this model can be obtained.

In a E_6 SUSY GUT model [22, 33–39], on the other hand, its fundamental multiplet **27** has not only **16** spinor multiplet but also **10** vector multiplet of $SO(10)$ as we will show in Sec. 3.3.2. This **10** field plays the same role as an extra matter field in the $SO(10)$ GUT model. Therefore, the observed fermion masses and Cabibbo-Kobayashi-Maskawa (CKM) matrix can be obtained in a natural way.

Moreover, if one consider E_6 GUT with $SU(2)_F$ flavor symmetry [40–49] and anomalous $U(1)_A$ gauge symmetry [50–59], more attractive model can be obtained, in which almost all the problems caused in SUSY GUT models are solved in a natural assumption: all the interactions which are allowed by symmetries are introduced with $\mathcal{O}(1)$ coefficients.

[1] Once additional matter fields are introduced at the low energy, proton decay mediated by X boson is enhanced since the gauge couplings at the GUT scale become larger [29–32]. If proton decay is discovered in future experiments, it is the clear evidence of a GUT.

In such a model, a sfermion mass spectrum in which all the sfermion masses except for a scalar top (stop) mass are universal is obtained. We call this spectrum modified universal sfermion masses (MUSM). If one consider the MUSM, suppressing the SUSY contributions to FCNC processes and stabilizing the weak scale can be realized at the same time. This type of sfermion mass spectrum is nothing but the natural SUSY-type one [41, 60–62].

However, in the $E_6 \times SU(2)_F \times U(1)_A$ SUSY GUT model, the degeneracy of the MUSM is destroyed because of non-vanishing D-term contributions which are dependent on the flavor [63–66]. Therefore, these contributions are constrained by FCNC processes [67]. We investigate the upper bound of its size from the most strongest constraint in the FCNC processes, which is the CP-violating parameter ϵ_K in K^0-$\overline{K^0}$ mixing [68]. In this model, there is a novel relation about the differences of the squared sfermion masses as we will mention in Sec. 5.3, which is specific to this model. We will discuss the testability of this model by using not only the allowed size of D-terms but also this novel relation [68].

In fact, the natural SUSY-type sfermion spectrum is severely constrained by chromo-electric dipole moments (CEDMs) because of the smallness of the stop mass [69–71]. Especially, the constraint from up quark CEDM is severe even if all SUSY-breaking parameters are taken to be real. This is because in such a case, this process depends on the imaginary part of diagonalizing matrices for up-type Yukawa couplings. Therefore, in order to avoid the constraints, one can consider a scenario with spontaneously CP violation [72–75], in which the up-type Yukawa couplings are real at the GUT scale. In this scenario, the down-type Yukawa couplings are complex at the GUT scale, that induces non-vanishing Kobayashi-Maskawa (KM) phase. Since the bound of mercury electric dipole moment (EDM) is recently improved [76, 77], we investigate the lower bounds of the sfermion masses from the EDM bounds in different structures of Yukawa couplings for comparison [78]. We also discuss the effects of the structure of Yukawa couplings to the CEDM.

This thesis is organized as follow. In Secs. 2 and 3, we provide a brief review of the SM and the models beyond the SM, especially SUSY and GUT. Then we will discuss specific predictions of the $SO(10)$ GUT model in Sec. 4. Next, we will discuss the size of D-term in the E_6 model and the CEDM constraints to the MUSM in Secs. 5 and 6. Finally, we will conclude this thesis in Sec. 7.

2 The Standard Model

In this section, we will briefly review the properties of the Standard Model (SM). The SM which has $G_{\rm SM} = SU(3)_C \times SU(2)_L \times U(1)_Y$ gauge symmetry contains three types of particle: fermions, vectors and scalar. In Table 1, we summarize the particle contents and their quantum numbers. In this table, i denotes the generation, $i = 1, 2, 3$. Q_i, u_{Ri},

	spin	$SU(3)_C$	$SU(2)_L$	$U(1)_Y$
$Q_i = \begin{pmatrix} u_{Li} \\ d_{Li} \end{pmatrix}$		**3**	**2**	$\frac{1}{6}$
u_{Ri}		**3**	**1**	$\frac{2}{3}$
d_{Ri}	1/2	**3**	**1**	$-\frac{1}{3}$
$L_i = \begin{pmatrix} \nu_{Li} \\ e_{Li} \end{pmatrix}$		**1**	**2**	$-\frac{1}{2}$
e_{Ri}		**1**	**1**	-1
g		**8**	**1**	0
W	1	**1**	**3**	0
B		**1**	**1**	0
$H = \begin{pmatrix} H^+ \\ H^0 \end{pmatrix}$	0	**1**	**2**	$\frac{1}{2}$

Table 1: Particle contents of the SM. $i = 1, 2, 3$ denotes the generation.

u_{Ri}, L_i and e_{Ri} are quark doublet, right-handed up-type quarks, right-handed down-type quarks, lepton doublet and right-handed charged leptons, respectively. These are the fermion as a matter. g, W and B are the gauge bosons corresponding to $SU(3)_C$, $SU(2)_L$ and $U(1)_Y$, respectively, and H is Higgs doublet.

The Lagrangian for the SM can be written as

$$\mathcal{L}_{\rm SM} = \mathcal{L}_{\rm fermion} + \mathcal{L}_{\rm gauge} + \mathcal{L}_{\rm Higgs} + \mathcal{L}_{\rm Yukawa}. \tag{2.1}$$

In $\mathcal{L}_{\rm fermion}$, the terms of covariant derivatives for the fermions are included:

$$\begin{aligned} \mathcal{L}_{\rm fermion} = {} & \overline{Q'_i}(i\gamma^\mu D_\mu)Q'_i + \overline{u'_{Ri}}(i\gamma^\mu D_\mu)u'_{Ri} + \overline{d'_{Ri}}(i\gamma^\mu D_\mu)d'_{Ri} \\ & + \overline{L'_i}(i\gamma^\mu D_\mu)L'_i + \overline{e'_{Ri}}(i\gamma^\mu D_\mu)e'_{Ri}, \end{aligned} \tag{2.2}$$

where ψ' shows the flavor eigenstate and D_μ is the covariant derivative which is defined

for each field as

$$D_\mu Q'_i = \left(\partial_\mu - ig_3 G^\alpha_\mu T^\alpha_C - ig_2 W^a_\mu T^a_L - ig' B_\mu T_Y\right) Q'_i, \tag{2.3}$$

$$D_\mu u'_{Ri} = \left(\partial_\mu - ig_3 G^\alpha_\mu T^\alpha_C - ig' B_\mu T_Y\right) u'_{Ri}, \tag{2.4}$$

$$D_\mu d'_{Ri} = \left(\partial_\mu - ig_3 G^\alpha_\mu T^\alpha_C - ig' B_\mu T_Y\right) d'_{Ri}, \tag{2.5}$$

$$D_\mu L'_i = \left(\partial_\mu - ig_2 W^a_\mu T^a_L - ig' B_\mu T_Y\right) L'_i, \tag{2.6}$$

$$D_\mu e'_{Ri} = \left(\partial_\mu - ig' B_\mu T_Y\right) e'_{Ri}. \tag{2.7}$$

Here, g_3, g_2 and g' are gauge couplings and $T^\alpha_C = \lambda^\alpha/2$, $T^a_L = \sigma^a/2$, T_Y are generators of $SU(3)_C$, $SU(2)_L$ and $U(1)_Y$, respectively. G^α_μ, W^a_μ and B_μ are gauge bosons corresponding to $SU(3)_C$, $SU(2)_L$ and $U(1)_Y$, respectively. Note that λ^α is the Gell-Mann matrices ($\alpha = 1, \cdots, 8$) and σ^a is the Pauli matrices ($a = 1, 2, 3$).

$\mathcal{L}_{\text{gauge}}$ are the kinetic terms for the gauge bosons:

$$\mathcal{L}_{\text{gauge}} = -\frac{1}{4} G^\alpha_{\mu\nu} G^{\alpha\mu\nu} - \frac{1}{4} W^a_{\mu\nu} W^{a\mu\nu} - \frac{1}{4} B_{\mu\nu} B^{\mu\nu}, \tag{2.8}$$

where

$$G^\alpha_{\mu\nu} = \partial_\mu G^\alpha_\nu - \partial_\nu G^\alpha_\mu + g_3 f^{\alpha\beta\gamma}_C G^\beta_\mu G^\gamma_\nu, \tag{2.9}$$

$$W^\alpha_{\mu\nu} = \partial_\mu W^a_\nu - \partial_\nu W^a_\mu + g_3 f^{abc}_L W^b_\mu W^c_\nu, \tag{2.10}$$

$$B^\alpha_{\mu\nu} = \partial_\mu B_\nu - \partial_\nu B_\mu. \tag{2.11}$$

f^{abc}_L and $f^{\alpha\beta\gamma}_C$ are the structure constant of $SU(2)_L$ and $SU(3)_C$, respectively.

The Lagrangian of Higgs $\mathcal{L}_{\text{Higgs}}$ can be written as

$$\mathcal{L}_{\text{Higgs}} = |D_\mu H|^2 - V(H), \quad D_\mu H = (\partial_\mu - ig_2 W^a_\mu T^a_L - ig' B_\mu T_Y) H, \tag{2.12}$$

where $V(H)$ is Higgs potential and written as

$$V(H) = \mu^2 H^\dagger H + \frac{\lambda}{2} \left(H^\dagger H\right)^2, \tag{2.13}$$

where $\lambda > 0$. If $\mu^2 > 0$, this potential has minimum at $|H| = 0$, and the VEV of H is zero. However, if $\mu^2 < 0$, there is local minimum at $|H| \neq 0$. This value can be easily computed as

$$0 = \frac{\partial V(H)}{\partial H} = \left(-|\mu^2| + \lambda H^\dagger H\right) H^\dagger \quad \Rightarrow \quad |H|^2 = \frac{|\mu^2|}{\lambda} \equiv \frac{v^2}{2} \tag{2.14}$$

Note that $H^\dagger = 0$ which is another solution of the stationary condition Eq. (2.14) is at local maximum of $V(H)$. By using suitable $SU(2)_L \times U(1)_Y$ gauge transformations, we can take the VEV of H as

$$\langle H \rangle = \frac{1}{\sqrt{2}} \begin{pmatrix} 0 \\ v \end{pmatrix}, \quad v = \sqrt{\frac{2|\mu^2|}{\lambda}}, \tag{2.15}$$

where $v = 246.22$ GeV [79]. This VEV breaks all $SU(2)_L \times U(1)_Y$ transformation other than one transformation which is corresponding to phase transformation for upper component of $SU(2)_L$ doublet:

$$(T_L^3 + T_Y)\langle H \rangle = \begin{pmatrix} 1 & 0 \\ 0 & 0 \end{pmatrix} \frac{1}{\sqrt{2}} \begin{pmatrix} 0 \\ v \end{pmatrix} = \begin{pmatrix} 0 \\ 0 \end{pmatrix}, \tag{2.16}$$

where $T_L^3 + T_Y$ is regarded as the generator of $U(1)_{\rm em}$ as seen below. As a result, the VEV of Eq. (2.15) can cause the symmetry breaking, $SU(2)_L \times U(1)_Y \to U(1)_{\rm em}$.

Before this symmetry breaking, four gauge bosons corresponding to $SU(2)_L$ and $U(1)_Y$ are all massless because of the gauge symmetries. After symmetry breaking, some of the gauge bosons get masses. Substituting Eq. (2.15) into the covariant derivative of the Higgs, gauge boson masses are obtained as

$$\begin{aligned} |D_\mu \langle H \rangle|^2 &= \left| \frac{1}{2} \begin{pmatrix} -ig_2 W_\mu^3 - ig' B_\mu & -ig_2(W_\mu^1 - iW_\mu^2) \\ -ig_2(W_\mu^1 + iW_\mu^2) & +ig_2 W_\mu^3 - ig' B_\mu \end{pmatrix} \frac{1}{\sqrt{2}} \begin{pmatrix} 0 \\ v \end{pmatrix} \right|^2 \\ &= \frac{g_2^2 v^2}{8} \left| W_\mu^1 - iW_\mu^2 \right|^2 + \frac{v^2}{8} \left| g_2 W_\mu^3 - g' B_\mu \right|^2 \\ &= \frac{g_2^2 v^2}{4} W_\mu^+ W^{-\mu} + \frac{(g_2^2 + g'^2) v^2}{8} Z_\mu Z^\mu, \end{aligned} \tag{2.17}$$

where $W_\mu^\pm \equiv \frac{W_\mu^1 \mp i W_\mu^2}{\sqrt{2}}$ and $Z_\mu \equiv \frac{g_2 W_\mu^3 - g' B_\mu}{\sqrt{g_2^2 + g'^2}}$ are the W bosons and the Z boson. Therefore, the three of four gauge bosons in the SM get masses as [79]

$$M_W \equiv \frac{1}{2} g_2 v = 80.385 \pm 0.015\,\text{GeV}, \tag{2.18}$$

$$M_Z \equiv \frac{1}{2} \sqrt{g_2^2 + g'^2}\, v = 91.1876 \pm 0.0021\,\text{GeV}, \tag{2.19}$$

and the remaining one mode, $A_\mu \equiv \frac{g' W_\mu^3 + g_2 B_\mu}{\sqrt{g_2^2 + g'^2}}$, which is the photon is massless. This is known for the Higgs mechanism. Note that Z_μ and A_μ can be written by using the

Weinberg angle, $\sin\theta_W = \frac{g'}{\sqrt{g_2^2+g'^2}}$, as

$$\begin{pmatrix} Z_\mu \\ A_\mu \end{pmatrix} = \begin{pmatrix} \cos\theta_W & -\sin\theta_W \\ \sin\theta_W & \cos\theta_W \end{pmatrix} \begin{pmatrix} W_\mu^3 \\ B_\mu \end{pmatrix}. \tag{2.20}$$

In terms of the mass eigenstates of gauge bosons, $W_\mu^\pm$, Z_μ and A_μ, the covariant derivative for the fermions can be rewritten as

$$\begin{aligned} &\partial_\mu - ig_2 W_\mu^a T_L^a - ig' B_\mu T_Y \\ &\quad = \partial_\mu - i\frac{g_2}{\sqrt{2}}\left(W_\mu^+ T^+ + W_\mu^- T^-\right) - i\frac{g_2}{\cos\theta_W} Z_\mu (T_L^3 - Q_e \sin^2\theta_W) - ieA_\mu Q_e, \end{aligned} \tag{2.21}$$

where $T^\pm = T_L^1 \pm iT_L^2$, $Q_e = T_L^3 + T_Y$ is the generator of $U(1)_{\rm em}$ and $e = g_2 \sin\theta_W$ is the positron electric charge. Therefore, we can obtain the fermion-gauge boson couplings as

$$\mathcal{L}_{\rm Yukawa} \supset g_2\left(W_\mu^+ J_W^{\mu\,+} + W_\mu^- J_W^{\mu\,-} + Z_\mu J_Z^\mu\right) + eA_\mu J_{\rm EW}^\mu, \tag{2.22}$$

where

$$J_W^{\mu\,+} = \frac{1}{\sqrt{2}}\left(\overline{\nu_{L\,i}}\gamma^\mu e'_{L\,i}\right) + \frac{1}{\sqrt{2}}\left(\overline{u'_{L\,i}}\gamma^\mu d'_{L\,i}\right), \tag{2.23}$$

$$J_W^{\mu\,-} = \frac{1}{\sqrt{2}}\left(\overline{e'_{L\,i}}\gamma^\mu \nu_{L\,i}\right), + \frac{1}{\sqrt{2}}\left(\overline{d'_{L\,i}}\gamma^\mu u'_{L\,i}\right) \tag{2.24}$$

$$J_Z^\mu = \frac{1}{\cos\theta}\sum_\psi \left[\overline{\psi'_{L\,i}}\gamma^\mu g_L^f \psi'_{L\,i} + \overline{\psi'_{R\,i}}\gamma^\mu g_R^f \psi'_{R\,i}\right], \tag{2.25}$$

$$J_{\rm EW}^\mu = \overline{e'_i}\gamma^\mu(-1)e'_i + \overline{u'_i}\gamma^\mu\left(+\frac{2}{3}\right)u'_i + \overline{d'_i}\gamma^\mu\left(-\frac{1}{3}\right)d'_i. \tag{2.26}$$

Note that $g_I^f = T_L^{3\,f} - Q_e^f \sin^2\theta_W$ $(I = L, R)$. $T_L^{3\,f}$ is $+1/2$, $-1/2$ and 0 for $f = u'_{L\,i}, \nu_{L\,i}$, for $f = d'_{L\,i}, e'_{L\,i}$ and for the right-handed particles, respectively. Q_e^f is the electric charge for the fermion f.

After symmetry breaking $SU(2)_L \times U(1)_Y \to U(1)_{\rm em}$, moreover, the fermions also get masses through Yukawa couplings. In the SM, the Yukawa couplings are

$$\mathcal{L}_{\rm Yukawa} = (Y_u)_{ij} Q'_i u^{c\prime}_{R\,j} H + (Y_d)_{ij} Q'_i d^{c\prime}_{R\,j} H^\dagger + (Y_e)_{ij} L'_i e^{c\prime}_{R\,j} H^\dagger + \text{h.c.}, \tag{2.27}$$

where $\psi_R^c \equiv (\psi^c)_L = (\psi_R)^c$. Therefore, the SM matters get masses as $M_\psi = \frac{1}{\sqrt{2}} Y_\psi v$ $(\psi = u, d, e)$ where M_ψ is a mass matrix. By diagonalizing these mass matrices, the mass eigenvalues and eigenstates are obtained. In this thesis, the mass eigenstates of the SM

fermion are defined by

$$\psi_L = L_\psi^\dagger \psi'_L, \quad \psi_R^c = R_\psi^\dagger \psi_R^{c\prime}. \tag{2.28}$$

In this definition, diagonalization of the Yukawa matrix is realized as $Y_\psi^{\rm diag} = L_\psi^T Y_\psi R_\psi$. In this definition, the CKM matrix is obtained from Eq. (2.23) as

$$V_{\rm CKM} \equiv L_u^\dagger L_d \equiv \begin{pmatrix} V_{ud} & V_{us} & V_{ub} \\ V_{cd} & V_{cs} & V_{cb} \\ V_{td} & V_{ts} & V_{tb} \end{pmatrix}. \tag{2.29}$$

$V_{\rm CKM}$ is unitary matrix, $V_{\rm CKM}^\dagger V_{\rm CKM} = 1 = V_{\rm CKM} V_{\rm CKM}^\dagger$. In general, 3×3 unitary matrix has three rotational angles and six phases. For $V_{\rm CKM}$, since five phases can be absorbed by the redefinition of the quark phases, the physical degrees of freedom are three rotational angles and one phase. Therefore, $V_{\rm CKM}$ can be parameterized by $s_{ij} \equiv \sin\theta_{ij}$, $c_{ij} \equiv \cos\theta_{ij}$ and KM phase δ as [80–82]

$$V_{\rm CKM} = \begin{pmatrix} c_{12}c_{13} & s_{12}c_{13} & s_{13}e^{-i\delta} \\ -s_{12}c_{23} - c_{12}s_{23}s_{13}e^{i\delta} & c_{12}c_{23} - s_{12}s_{23}s_{13}e^{i\delta} & s_{23}c_{13} \\ s_{12}s_{23} - c_{12}c_{23}s_{13}e^{i\delta} & -c_{12}s_{23} - s_{12}c_{23}s_{13}e^{i\delta} & c_{23}c_{13} \end{pmatrix}, \tag{2.30}$$

or

$$V_{\rm CKM} = \begin{pmatrix} 1-\frac{1}{2}\lambda^2 & \lambda & A\lambda^3(\rho - i\eta) \\ -\lambda & 1-\frac{1}{2}\lambda^2 & A\lambda^2 \\ A\lambda^3(1-\rho-i\eta) & -A\lambda^2 & 1 \end{pmatrix} + \mathcal{O}(\lambda^4). \tag{2.31}$$

The latter one is known as the Wolfenstein parametrization [83]. Two parametrizations are related as

$$s_{12} = \lambda = \frac{|V_{us}|}{\sqrt{|V_{ud}|^2 + |V_{us}|^2}}, \quad s_{23} = A\lambda^2 = \lambda \left|\frac{V_{cb}}{V_{us}}\right|, \tag{2.32}$$

$$s_{13}e^{i\delta} = V_{ub}^* = A\lambda^3(\rho + i\eta) = \frac{A\lambda^3(\bar\rho + i\bar\eta)\sqrt{1-A^2\lambda^4}}{\sqrt{1-\lambda^2}[1 - A^2\lambda^4(\bar\rho + i\bar\eta)]}. \tag{2.33}$$

From these relations, one can obtain $\bar\rho + i\bar\eta = -(V_{ud}V_{ub}^*)/(V_{cd}V_{cb}^*)$. Note that $\bar\rho$ and $\bar\eta$ are defined as $\bar\rho = \rho(1-\frac{\lambda^2}{2}) + \mathcal{O}(\lambda^4)$ and $\bar\eta = \eta(1-\frac{\lambda^2}{2}) + \mathcal{O}(\lambda^4)$.

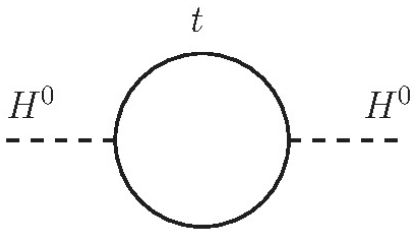

Figure 1: An example of one-loop correction for the Higgs mass.

Although the SM can explain almost all of the experimental data, there are some problems which should be solved in both of theoretical and experimental points of view. We will list some of these problems below:

- Hierarchy problem [18]

  As the gauge bosons get the masses by the Higgs mechanism, the Higgs boson also gets the mass of order of its VEV, v. This scale is experimentally known as $\mathcal{O}(100)$ GeV. In the SM, there are some quantum corrections which contribute to the Higgs mass. These corrections are dominated by the top quark contributions because of the largeness of the Yukawa coupling. Its size can be calculated by the loop diagram in Fig. 1 as

  $$\Delta m_H^2 = -\frac{3y_t^2}{8\pi^2}\Lambda^2 + \cdots , \tag{2.34}$$

  where y_t is the Yukawa coupling of the top quark and Λ is the cutoff scale of the theory. By considering these contributions, the Higgs mass is obtained by the sum of its bare parameter $m_{H\,\mathrm{bare}}^2$ and Δm_H^2. If one assume that the new physics appears at higher scale, e.g. the GUT scale, than the weak scale, it needs huge cancellation between $m_{H\,\mathrm{bare}}^2$ and Δm_H^2 in order to obtain the proper size of $m_H^2 \sim (\mathcal{O}(100)\,\mathrm{GeV})^2$.

- Neutrino masses

  In the SM, three left-handed neutrinos are all massless because there are no right-handed neutrinos. However, it has been shown that neutrinos have a small but non-zero masses in many neutrino oscillation experiments [3–16]. This is a clear evidence for the physics beyond the SM. One of the famous solutions is to introduce the SM singlet fermions as right-handed neutrinos. In this case, Majorana mass terms M_{ij} in addition to Yukawa couplings with the left-handed neutrinos can be introduced. If M_{ij} are much heavier than the weak scale, neutrino masses are suppressed by M_{ij}^{-1}, and thus tiny masses for neutrinos can be obtained. This is known as the seesaw

$m_u = 2.2^{+0.6}_{-0.4} \times 10^{-3}$	$m_c = 1.28 \pm 0.03$	$m_t = 160.0^{+4.8}_{-4.3}$
$m_d = 4.7^{+0.5}_{-0.4} \times 10^{-3}$	$m_s = 9.6^{+0.8}_{-0.4} \times 10^{-2}$	$m_b = 4.18^{+0.04}_{-0.03}$
$m_e = 5.109989 \times 10^{-4}$	$m_\mu = 0.10566$	$m_\tau = 1.77686 \pm 0.00012$

Table 2: The SM quarks and charged leptons masses in GeV [79]. We show the $\overline{\text{MS}}$ mass for the quark masses and pole mass for the lepton masses. We omit the uncertainties of m_e and m_μ.

mechanism [84, 85]. If one consider a GUT model, the right-handed neutrinos can be naturally introduced in the model.

- Charge quantization

  From Table 1, $U(1)_Y$ charges of the SM particles are quantized. Accidentally, these charges can cancel the gauge anomalies for $U(1)_Y$ and $U(1)_Y^3$. It is natural to consider that there is some mechanism behind the theory. However, this charge quantization cannot be explained in the SM. This quantization can be explained in the GUT.

- The origin of Yukawa hierarchy

  The current experimental values of the quark and lepton masses are quite hierarchical. For example, the masses of top, charm and up quark are $\mathcal{O}(100)$ GeV, $\mathcal{O}(1)$ GeV and $\mathcal{O}(1)$ MeV, respectively. In addition, the down-type quarks and charged leptons have different hierarchies and the neutrinos are almost degenerated. We summarized the masses of the quarks and charged leptons in Table 2. However, the Yukawa couplings of the SM Eq. (2.27) are just parameters and cannot be determined their values theoretically. Therefore, we must consider how we obtain this variety of hierarchies. Many models which can solve Yukawa hierarchy problem are proposed. Especially, in some SUSY GUT models, these hierarchies can be obtained in the natural assumption.

- No dark matter candidates

  There are no dark matter (DM) candidates in the SM particle contents. However, many experiments show that the DM is needed in order to explain the observable. Therefore, we should construct the models in which there are the DMs. In the SUSY models, the lightest SUSY particles can be the DM if R-parity is conserved.

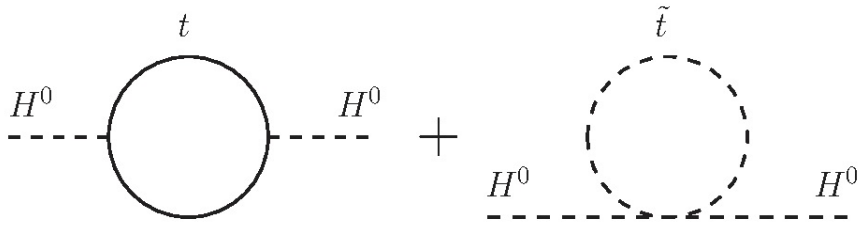

Figure 2: An example of one-loop correction for the Higgs mass in the SUSY model.

3 Models beyond the SM

In the previous section, we showed some of the problems in the SM. These problems can be solved by extending the SM. One of the most interesting and promising candidates for the model beyond the SM is a SUSY GUT. In this section, we will introduce its features and how we solve the SM problems.

3.1 Supersymmetry

The SUSY is the symmetry between bosons and fermions. There is a bosonic partner for a fermion and vice versa. These new particles are called SUSY particles. One of the important features in a SUSY model is cancellation of the quadratic divergence of quantum corrections in the Higgs mass. Because of the contributions of the SUSY particles, one-loop correction for the Higgs mass in the SUSY model can be obtained by calculating the sum of the loop diagrams in Fig. 2 as

$$\Delta m_H^2 \simeq -\frac{3y_t^2}{8\pi^2}\Lambda^2 + \left[\frac{3y_t^2}{8\pi^2}\Lambda^2 - \frac{3y_t^2}{4\pi^2}m_{\tilde{t}}^2 \ln\left(\frac{\Lambda}{m_{\tilde{t}}}\right)\right] = -\frac{3y_t^2}{4\pi^2}m_{\tilde{t}}^2 \ln\left(\frac{\Lambda}{m_{\tilde{t}}}\right), \tag{3.1}$$

where $m_{\tilde{t}}$ is the mass of the bosonic partners for the top quark, which is called stop. Note that a stop-Higgs four point coupling is y_t^2 because of the SUSY. Therefore, Λ^2 correction is canceled at one-loop level. This cancellation is caused by the difference of statistic property between the fermion and scalar fermion (sfermion).

The quantum number of SUSY particle is the same as that of corresponding SM particle. Moreover, SUSY particle and its partner have equal mass. Therefore, SUSY should be broken at the low energy since there are no signals of the SUSY particles in the experiments. This means that the Lagrangian for a SUSY model can be divided into two parts: SUSY-conserving part and SUSY-breaking part. However, if one breaks SUSY completely, the cancellation shown in Eq. (3.1) cannot occur. In order to maintain this cancellation, SUSY should be broken softly. We will explain this breaking in the framework of the minimal SUSY model.

3.1.1 Minimal Supersymmetric Standard Model

We will summarized the particle content for minimal SUSY SM (MSSM) in Table 3 (and notation is defined here). In SUSY models, two Higgs doublets are needed because of

superfiled	scalar or vector	fermion	quantum number
$\mathcal{Q}_i$	$\widetilde{Q}_i = \begin{pmatrix} \widetilde{u}_L \\ \widetilde{d}_L \end{pmatrix}_i$	$Q_i = \begin{pmatrix} u_L \\ d_L \end{pmatrix}_i$	$\left(\mathbf{3}, \mathbf{2}, \frac{1}{6}\right)$
$\mathcal{L}_i$	$\widetilde{L}_i = \begin{pmatrix} \widetilde{\nu}_{e\,L} \\ \widetilde{e}_L \end{pmatrix}_i$	$L_L = \begin{pmatrix} \nu_{e\,L} \\ e_L \end{pmatrix}_i$	$\left(\mathbf{1}, \mathbf{2}, -\frac{1}{2}\right)$
$\mathcal{U}_i$	$\widetilde{u}^*_{R\,i}$	$u^c_{R\,i}$	$\left(\bar{\mathbf{3}}, \mathbf{1}, -\frac{2}{3}\right)$
$\mathcal{D}_i$	$\widetilde{d}^*_{R\,i}$	$d^c_{R\,i}$	$\left(\bar{\mathbf{3}}, \mathbf{1}, \frac{1}{3}\right)$
$\mathcal{E}_i$	$\widetilde{e}^*_{R\,i}$	$e^c_{R\,i}$	$(\mathbf{1}, \mathbf{1}, 1)$
$\mathcal{G}$	g	$\tilde{g}$	$(\mathbf{8}, \mathbf{1}, 0)$
$\mathcal{W}$	W	$\tilde{W}$	$(\mathbf{1}, \mathbf{3}, 0)$
$\mathcal{B}$	B	$\tilde{B}$	$(\mathbf{1}, \mathbf{1}, 0)$
$\mathcal{H}_u$	$H_u = \begin{pmatrix} H^+_u \\ H^0_u \end{pmatrix}$	$\widetilde{H}_u = \begin{pmatrix} \widetilde{H}^+_u \\ \widetilde{H}^0_u \end{pmatrix}$	$\left(\mathbf{1}, \mathbf{2}, \frac{1}{2}\right)$
$\mathcal{H}_d$	$H_d = \begin{pmatrix} H^0_d \\ H^-_d \end{pmatrix}$	$\widetilde{H}_d = \begin{pmatrix} \widetilde{H}^0_d \\ \widetilde{H}^-_d \end{pmatrix}$	$\left(\mathbf{1}, \mathbf{2}, -\frac{1}{2}\right)$

Table 3: Particle contents for the MSSM. The particles with tilde show the SUSY particles. The quantum number is $(SU(3)_C, SU(2)_L, U(1)_Y)$.

two reasons: to write the Yukawa couplings and to cancel the gauge anomaly. Since we consider the model by holomorphic function of superfield rather than Lagrangian, which is called as superpotential, we cannot use the hermitian conjugation of the Higgs superfield, $\mathcal{H}^\dagger_u$. In addition, there are additional contributions to the gauge anomaly from the superpartners of the Higgs bosons, called Higgsinos. Therefore, the additional Higgs doublet whose $U(1)_Y$ charge is opposite sign to the other one must be introduced.

In the MSSM, three gauge couplings of the SM are accidentally unified around 10^{16} GeV. This is because the beta-functions of the gauge couplings are modified because of the SUSY particles. More explicitly, the coefficients of the beta-functions b_i are modified from $(41/10, -19/6, -7)$ (the SM one) to $(33/5, 1, -3)$ (the MSSM one), which b_i is defined as

$$\frac{dg_i}{dt} = \frac{b_i}{16\pi^2} g_i^3 \quad (i = 1, 2, 3), \tag{3.2}$$

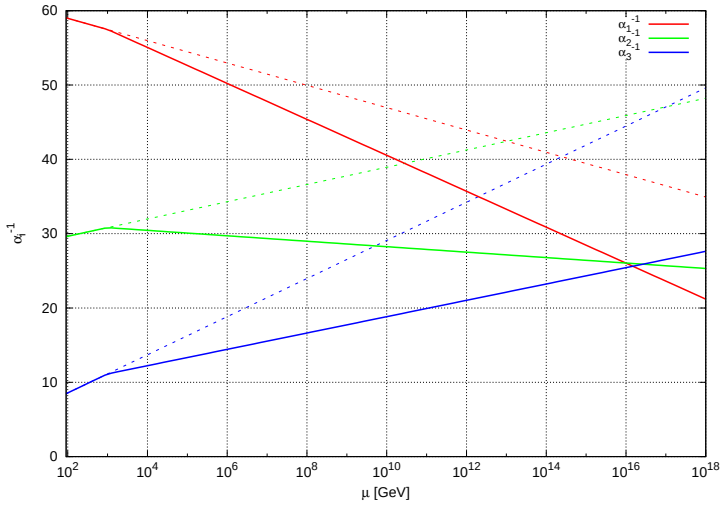

Figure 3: The SM gauge coupling running in both case of the MSSM (solid lines) and the SM (dashed line). The input parameters are the gauge couplings at M_Z scale [79]: $\alpha_1(M_Z)^{-1} = 59.04$, $\alpha_2(M_Z)^{-1} = 29.60$ and $\alpha_3(M_Z)^{-1} = 8.47$, where $\alpha_i \equiv \frac{g_i^2}{4\pi}$. We assume that the SUSY contributions appear at 1 TeV.

where $t = \ln(\mu/M_Z)$. We show the running of the SM gauge couplings in Fig. 3. Here, solid and dashed lines are the running of the MSSM and SM, respectively. In this case, the GUT scale at which three gauge couplings meet is about 10^{16} GeV. In this sense, the SUSY model is compatible with GUTs.

Next, we will show the Lagrangian in SUSY models. Note that a Lagrangian is divided by two parts as we mentioned above. The first part, SUSY conserving terms, is written as

$$\mathcal{L}_{\rm SUSY} = \left[K(\Phi_i, \Phi^{*j})\right]_D + \left(\left[\frac{1}{4} f_{ab}(\Phi_i)\hat{\mathcal{W}}^a\hat{\mathcal{W}}^b + W(\Phi_i)\right]_F + \text{h.c.}\right), \tag{3.3}$$

where $K(\Phi_i, \Phi^{*j})$ is Kähler potential, $W(\Phi_i)$ is superpotential, $f_{ab}(\Phi_i)$ is a gauge kinetic function and $\hat{\mathcal{W}}^a$ is field-strength superfield.

From the first term in Eq. (3.3), we obtain the kinetic terms for matter fields and D-terms defined as

$$\mathcal{L}_{\rm SUSY} \supset -\frac{1}{2}\sum_a D_a D_a, \quad D_a = -g_a \sum_\phi (\phi^* T^a \phi). \tag{3.4}$$

For the summation, a runs all gauge symmetry imposed in the model and ϕ runs all scalar components lived in the model. g_a and T^a are gauge coupling and generators of each gauge symmetry, respectively. Importantly, this D-term contributes to the sfermion

masses. These contributions are generated as

$$\Delta m_{\tilde{f}}^2 = \sum_a g_a^2 q_{\tilde{f}}^a q_{\phi_H}^a \langle \phi_H \rangle^2 \tag{3.5}$$

after some Higgs fields get VEV, $\langle \phi_H \rangle$. Note that $q_{\tilde{f}}^a$ and $q_{\phi_H}^a$ are the charges of $U(1)$ factor for a scalar $\tilde{f}$ and Higgs ϕ_H in the gauge symmetry, and therefore different $U(1)$ charges cause different contributions. In particular, if one considers the GUT model whose rank of the gauge symmetry is larger than that of $G_{\rm SM}$, for example $SO(10)$ and E_6, there are non-vanishing D-term contributions which are usually flavor-independent and we can obtain some signature of the GUT scenario from these contributions through scalar mass relations [63–66]. However, these contributions become flavor-dependent ones when we consider a model in which there are mixings of fields, like the mixing of $\bar{\mathbf{5}}$ of $SU(5)$ in the E_6 GUT model. Their sizes are constrained by the FCNC processes [67, 68] as we will discuss in Sec. 5.

The Yukawa interactions are obtained from the superpotential. For the MSSM, the superpotential is

$$W_{\rm MSSM} = \epsilon_{ab}\Big[(Y_u)_{ij}\mathcal{Q}_i^a\mathcal{H}_u^b\mathcal{U}_j - (Y_d)_{ij}\mathcal{Q}_i^a\mathcal{H}_d^b\mathcal{D}_j - (Y_e)_{ij}\mathcal{L}_i^a\mathcal{H}_d^b\mathcal{E}_j + \mu\mathcal{H}_u^a\mathcal{H}_d^b\Big], \tag{3.6}$$

where $\epsilon_{12} = +1$. Note that μ is the Higgsino mass parameter.

The second part of the Lagrangian is written by softly SUSY-breaking terms:

$$\begin{aligned}
\mathcal{L}_{\rm MSSM}^{\rm soft} = &-\frac{1}{2}\Big(M_3\tilde{g}\tilde{g} + M_2\tilde{W}\tilde{W} + M_1\tilde{B}\tilde{B} + \text{h.c.}\Big) \\
&-\Big((A_u)_{ij}\widetilde{Q}_i\widetilde{u}_{Rj}^* H_u - (A_d)_{ij}\widetilde{Q}_i\widetilde{d}_{Rj}^* H_d - (A_e)_{ij}\widetilde{L}_i\widetilde{e}_{Rj}^* H_d + \text{h.c.}\Big) \\
&-\left(m_{\tilde{q}}^2\right)_{ij}\widetilde{Q}_i^\dagger\widetilde{Q}_j - \left(m_{\tilde{u}}^2\right)_{ij}\widetilde{u}_{Ri}^*\widetilde{u}_{Rj} - \left(m_{\tilde{d}}^2\right)_{ij}\widetilde{d}_{Ri}^*\widetilde{d}_{Rj} \\
&-\left(m_{\tilde{l}}^2\right)_{ij}\widetilde{L}_i^\dagger\widetilde{L}_j - \left(m_{\tilde{e}}^2\right)_{ij}\widetilde{e}_{Ri}^*\widetilde{e}_{Rj} \\
&-m_{H_u}^2 H_u^* H_u - m_{H_d}^2 H_d^* H_d - (bH_u H_d + \text{h.c.}),
\end{aligned} \tag{3.7}$$

where M_i $(i = 1, 2, 3)$ is the gaugino mass, $(A_f)_{ij}$ $(f = u, d, e)$ is the 3×3 scalar cubic matrix and $(m_{\tilde{f}})_{ij}$ is the 3×3 sfermion mass squared matrix. $m_{H_u}^2$, $m_{H_d}^2$ and b are the squared mass terms which contribute to the Higgs potential. Therefore, the Higgs potential in the MSSM becomes

$$\begin{aligned}
V_H = &(|\mu|^2 + m_{H_u}^2)(|H_u^0|^2 + |H_u^+|^2) + (|\mu|^2 + m_{H_d}^2)(|H_d^0|^2 + |H_d^-|^2) \\
&+ \left[b(H_u^+ H_d^- - H_u^0 H_d^0) + \text{h.c.}\right] \\
&+ \frac{1}{8}(g_2^2 + g'^2)\left(|H_u^0|^2 + |H_u^+|^2 - |H_d^0|^2 - |H_d^-|^2\right)^2 + \frac{1}{2}g_2^2|H_u^+ H_d^{0*} + H_u^0 H_d^{-*}|^2,
\end{aligned} \tag{3.8}$$

together with the terms from Eq. (3.6). Similar to the SM, the VEVs of the Higgs doublets can be

$$\langle H_u \rangle = \begin{pmatrix} 0 \\ v_u \end{pmatrix}, \quad \langle H_d \rangle = \begin{pmatrix} v_d \\ 0 \end{pmatrix}, \tag{3.9}$$

by the $SU(2)_L$ symmetry. Note that the relation between these VEVs and the SM Higgs VEV v is $v_u^2 + v_d^2 = v^2$, and the ratio of v_u and v_d can be defined as

$$\tan\beta \equiv \frac{v_u}{v_d}. \tag{3.10}$$

The stationary conditions from Eq. (3.8), which are $\partial V_H/\partial H_u^0 = 0 = \partial V_H/\partial H_d^0$[2], lead to

$$\sin(2\beta) = \frac{2b}{m_{H_u}^2 + m_{H_d}^2 + 2|\mu|^2}, \tag{3.11}$$

$$M_Z^2 = \frac{|m_{H_d}^2 - m_{H_u}^2|}{\sqrt{1 - \sin^2(2\beta)}} - m_{H_u}^2 - m_{H_d}^2 - 2|\mu|^2. \tag{3.12}$$

In the MSSM, there are two complex Higgs doublets as we explained above. Therefore, after breaking $SU(2)_L \times U(1)_Y \to U(1)_{\rm em}$, five physical modes exist: 2 CP-even neutral scalars (h^0 and H^0), 1 CP-odd neutral scalar (A^0) and charged scalars ($H^\pm$). The masses for these modes are

$$m_{A^0}^2 = 2|\mu|^2 + m_{H_u}^2 + m_{H_d}^2, \tag{3.13}$$

$$m_{h^0,H^0}^2 = \frac{1}{2}\left(m_{A^0}^2 + M_Z^2 \mp \sqrt{(m_{A^0}^2 - M_Z^2)^2 + 4M_Z^2 m_{A^0}^2 \sin^2(2\beta)}\right), \tag{3.14}$$

$$m_{H^\pm}^2 = m_{A^0}^2 + m_W^2. \tag{3.15}$$

Note that the lighter mode h^0 is regarded as the SM Higgs boson. Therefore, these masses cause the following undesired relation at tree-level:

$$m_{h^0} < M_Z |\cos(2\beta)|. \tag{3.16}$$

Therefore, large contributions to the Higgs mass from the quantum corrections are needed to achieve the observed Higgs mass.

[2]Because of the $SU(2)_L$ gauge transformations, we can take $H_u^+ = 0$ at the minimum of the potential, without loss of generality. This means that $\partial V_H/\partial H_u^+ = 0$ leads to the result $H_d^- = 0$. Equations (3.11) and (3.12) are obtained by using $H_u^+ = 0 = H_d^-$.

3.1.2 Problems in the MSSM

Although some problems in the SM are solved by extending a model with SUSY, new problems are caused by this extension. We will summarize main problems below:

- μ-problem [20]
  In the Higgs sector of the Lagrangian for MSSM, four dimension-full parameters exist. One of them is Higgsino mass parameter, μ. Since this is a SUSY-conserving parameter, the size is thought to be order of cutoff scale, $\Lambda \gg \Lambda_{\mathrm{EW}}$. On the other hand, since the VEV of the SM Higgs boson is $\mathcal{O}(100)$ GeV, the size of μ must be the same order unless there is no miracle cancellation between parameters. This problem about the size of μ is called the μ-problem.

- SUSY FCNC problem
  In the MSSM, there are a lot of new parameters which are not in the SM in order to break SUSY softly. However, these parameters can cause flavor-changing processes. This is because the scalar cubic couplings and soft sfermions masses are 3×3 matrix and the off-diagonal element is not suppressed in general. Even if the off-diagonal elements are absent, non-zero off-diagonal elements are obtained when one takes a basis, called as super-CKM basis, in which the quarks and leptons are mass eigenstates. These off-diagonal elements are constrained by the FCNC processes and should be small to satisfy the experimental bounds. However, this smallness of the off-diagonal elements cannot be explained in the MSSM. This problem is called the SUSY FCNC problem.

- SUSY CP problem
  As same as the SUSY FCNC problem, there are a lot of new phases in the Lagrangian for MSSM since the new parameters of MSSM are generally complex. Therefore, there are CP-violating phases which are constrained by the CP-violating observables. Examples of such a observable are electric dipole moments (EDMs) and CEDMs. These observables show that some of the phases of new parameters are needed to be small for satisfying the experimental bounds. Similar to the SUSY FCNC problem, these smallness of the phases cannot be explained in the MSSM. This problem is called the SUSY CP problem.

3.2 Grand Unified Theory

Another interesting candidate for the model beyond the SM is a GUT. This predicts two types of unification. One is the unification of gauge interactions, and another one is the unification of matter fields.

In GUT models, we consider the gauge group whose rank is larger than or equal to the rank of $G_{\rm SM}$. In addition, we choose the group which has complex representations. In this thesis, we focus on $SU(5)$, $SO(10)$ and E_6 as examples of such a group. In this subsection, we review the general properties of the $SU(5)$ GUT. We will introduce $SO(10)$ and E_6 GUT in the next subsection as a context of the SUSY GUT model.

3.2.1 Properties of $SU(5)$ GUT

$SU(5)$ is the smallest group for GUT models and it is useful to know its features in discussing other GUT theories. First of all, we introduce basic properties of $SU(5)$ algebra. The rank of $SU(5)$ is 4 which is the same as that of the SM gauge group. Therefore, one has to keep the rank when the $SU(5)$ symmetry is broken. This can be realized by a VEV of the adjoint Higgs, $\mathbf{24}_A$. If $\langle \mathbf{24}_A \rangle$ is proportional to $\mathrm{diag}(2,2,2,-3,-3)v_A$, a proper symmetry breaking $SU(5) \to SU(3) \times SU(2) \times U(1)$ is realized. This fact can be understood by considering the generators of $SU(5)$. In $SU(5)$, there are 24 generators denoted as T^A. Some of these generators are remaining unbroken after symmetry breaking. By checking whether a commutator $[T^A, \langle \mathbf{24}_A \rangle]$ is zero, the remaining generators are[3]

$$T_3^\alpha = \begin{pmatrix} \frac{1}{2}\lambda^\alpha & 0_{3\times 2} \\ 0_{2\times 3} & 0_{2\times 2} \end{pmatrix}, \qquad (\alpha = 1, \cdots, 8) \tag{3.17}$$

$$T_2^a = \begin{pmatrix} 0_{3\times 3} & 0_{3\times 2} \\ 0_{2\times 3} & \frac{1}{2}\sigma^a \end{pmatrix}, \qquad (a = 1, 2, 3) \tag{3.18}$$

$$T_1 = \sqrt{\frac{3}{5}} \begin{pmatrix} -\frac{1}{3} \times 1_{3\times 3} & 0_{3\times 2} \\ 0_{2\times 3} & \frac{1}{2} \times 1_{2\times 2} \end{pmatrix} = \sqrt{\frac{3}{5}} T_Y, \tag{3.19}$$

Therefore, T_3^α and T_2^a are corresponding to the generators of the $SU(3)_C$ and $SU(2)_L$, respectively. T_Y can be regarded as the generator of $U(1)_Y$.

By using Eqs. (3.17), (3.18) and (3.19), decompositions of some representations of $SU(5)$ can be obtained as follows:

$$\mathbf{5} \;\to\; \left(\mathbf{3}, \mathbf{1}, -\frac{1}{3}\right) + \left(\mathbf{1}, \mathbf{2}, \frac{1}{2}\right), \tag{3.20}$$

$$\bar{\mathbf{5}} \;\to\; \left(\bar{\mathbf{3}}, \mathbf{1}, \frac{1}{3}\right) + \left(\mathbf{1}, \mathbf{2}, -\frac{1}{2}\right), \tag{3.21}$$

[3] T_2^3 and T_Y are obtained by linear combination of two of Cartan matrices, H_i. These are $H_3 \equiv \frac{1}{2\sqrt{6}}\mathrm{diag}(1,1,1,-3,0)$ and $H_4 \equiv \frac{1}{2\sqrt{10}}\mathrm{diag}(1,1,1,1,-4)$. By using these Cartan matrices, one can obtain the following generators: $T_2^3 = -\frac{1}{4}(\sqrt{6}H_3 - \sqrt{10}H_4)$ and $T_Y = -\frac{1}{4}(\sqrt{10}H_3 + \sqrt{6}H_4)$.

$$\mathbf{10} \;\rightarrow\; \left(\mathbf{3},\mathbf{2},\frac{1}{6}\right)+\left(\bar{\mathbf{3}},\mathbf{1},-\frac{2}{3}\right)+(\mathbf{1},\mathbf{1},1)\,, \tag{3.22}$$

$$\mathbf{24} \;\rightarrow\; (\mathbf{1},\mathbf{1},0)+(\mathbf{1},\mathbf{3},0)+(\mathbf{8},\mathbf{1},0)+\left(\mathbf{3},\mathbf{2},-\frac{5}{6}\right)+\left(\bar{\mathbf{3}},\mathbf{2},\frac{5}{6}\right), \tag{3.23}$$

where the number in each parenthesis shows the quantum number as $(SU(3), SU(2), U(1))$. Therefore, $\bar{\mathbf{5}}$ and $\mathbf{10}$ can be used as the matter fields, and the SM matter fields are partially unified as $d_R^c, L \rightarrow \bar{\mathbf{5}}$ and $Q, u_R^c, e_R^c \rightarrow \mathbf{10}$. Interestingly, the proper hypercharges of the SM fields are automatically obtained (see Table 1). Therefore, the charge quantization can be explained in the $SU(5)$ GUT. From here, we denote $\bar{\mathbf{5}}_i$ and $\mathbf{10}_i$ as matter fields. $i = 1, 2, 3$ is a index of the generation. The remaining SM fields are the gauge and Higgs bosons. We can unify the SM gauge bosons into $\mathbf{24}$ with new bosons whose charges are $\left(\mathbf{3},\mathbf{2},-\frac{5}{6}\right)$ and $\left(\bar{\mathbf{3}},\mathbf{2},\frac{5}{6}\right)$ which are known as X and Y bosons. These new fields are one of the predictions of the $SU(5)$ GUT scenario. The Higgs doublet lives in $\mathbf{5}$ with new color-triplet scalar field, denoted as H_T whose quantum number is $\left(\mathbf{3},\mathbf{1},-\frac{1}{3}\right)$. In this thesis, we denote $\mathbf{24}_G$ and $\mathbf{5}_H$ as gauge boson field and Higgs field in $SU(5)$ GUT, respectively.

As we mentioned above, we should introduce another new field $\mathbf{24}$ as an additional Higgs to break $SU(5)$ to $G_{\rm SM}$. Its VEV is

$$\langle \mathbf{24}_A \rangle = \begin{pmatrix} 2 & & & & \\ & 2 & & & \\ & & 2 & & \\ & & & -3 & \\ & & & & -3 \end{pmatrix} v_A, \tag{3.24}$$

where v_A is $SU(5)$ breaking scale. This VEV can be obtained by computing the minima of a scalar potential for $\mathbf{24}_A$, which is written as

$$V_A = -|m_A^2|\mathrm{tr}\left[\mathbf{24}_A^2\right] + \lambda_1\left(\mathrm{tr}\left[\mathbf{24}_A^2\right]\right)^2 + \lambda_2 \mathrm{tr}\left[\mathbf{24}_A^4\right]. \tag{3.25}$$

Here, we assume Z_2 parity for the $\mathbf{24}_A$. Since $\mathbf{24}$ is an hermitian matrix in special unitary group, $\langle \mathbf{24}_A \rangle$ can be diagonalized by proper $SU(5)$ transformation. Because of

the condition of the traceless, $\langle \mathbf{24}_A \rangle$ can be

$$\langle \mathbf{24}_A \rangle = \begin{pmatrix} a_1 & & & & \\ & a_2 & & & \\ & & a_3 & & \\ & & & a_4 & \\ & & & & a_5 \end{pmatrix}, \quad \sum_{i=1}^{5} a_i = 0. \tag{3.26}$$

For the VEV calculation, one should compute the local minimum of V_A,

$$V_A|_{\text{VEV}} = -|m_A^2| \sum_{i=1}^{5} a_i^2 + \lambda_1 \left(\sum_{i=1}^{5} a_i^2 \right)^2 + \lambda_2 \sum_{i=1}^{5} a_i^4 - \kappa \sum_{i=1}^{5} a_i, \tag{3.27}$$

where κ is a Lagrange multiplier. Therefore, one obtain the following conditions:

$$\begin{cases} \dfrac{\partial V_A|_{\text{VEV}}}{\partial a_i} = -2|m_A^2| a_i + 4\lambda_1 a_i \displaystyle\sum_{j=1}^{5} a_j^2 + 4\lambda_2 a_i^3 - \kappa = 0, \\ \dfrac{\partial V_A|_{\text{VEV}}}{\partial \kappa} = -\displaystyle\sum_{i=1}^{5} a_i = 0. \end{cases} \tag{3.28}$$

Equation 3.28 leads to the solution in which the potential is minimized when $a_1 = a_2 = a_3 = 2$ and $a_4 = a_5 = -3$. As a result, the solution for $SU(5) \to G_{\text{SM}}$ can be obtained when

$$\lambda_2 > 0, \quad \lambda_1 > -\frac{7}{30}\lambda_2, \tag{3.29}$$

and v_A in Eq. (3.25) is

$$v_A^2 = \frac{2|m_A^2|}{30\lambda_1 + 7\lambda_2}. \tag{3.30}$$

In order to write down Yukawa interactions for the $SU(5)$ GUT, one must know irreducible decompositions of the multiple for $\mathbf{10} \times \mathbf{10}$ and $\mathbf{10} \times \bar{\mathbf{5}}$:

$$\mathbf{10} \times \mathbf{10} = \bar{\mathbf{5}} + \bar{\mathbf{45}} + \mathbf{50}, \tag{3.31}$$

$$\mathbf{10} \times \bar{\mathbf{5}} = \mathbf{5} + \mathbf{45}. \tag{3.32}$$

Therefore, Yukawa interactions for the $SU(5)$ GUT is obtained by

$$\mathcal{L}_{\text{Y}} = (Y_u)_{ij} \mathbf{10}_i \mathbf{10}_j \mathbf{5}_H + (Y_{d,e})_{ij} \mathbf{10}_i \bar{\mathbf{5}}_j \bar{\mathbf{5}}_H. \tag{3.33}$$

From this, the hierarchies of Yukawa interactions are explained by an assumption that **10** fields have stronger hierarchy than $\bar{\mathbf{5}}$ fields. Moreover, if one introduces $SU(5)$ singlet fields $\mathbf{1}_i$ as right-handed neutrinos, extra Yukawa couplings for the neutrinos can be written as

$$\mathcal{L}_{\rm Y}^{\nu} = (Y_{\nu_D})_{ij}\bar{\mathbf{5}}_i\mathbf{1}_j\mathbf{5}_H + (M_{\nu_R})_{ij}\mathbf{1}_i\mathbf{1}_j, \tag{3.34}$$

where $(M_{\nu_R})_{ij}$ is the Majorana mass matrix. When $(M_{\nu_R})_{ij} \gg M_Z$, right-handed neutrinos $\mathbf{1}_i$ are integrated out and the neutrino Yukawa couplings are obtained as

$$-\left(Y_{\nu_D}M_{\nu_R}^{-1}Y_{\nu_D}^T\right)_{ij}\bar{\mathbf{5}}_i\bar{\mathbf{5}}_j\mathbf{5}_H\mathbf{5}_H. \tag{3.35}$$

From the above assumption, it is understood that the hierarchy of neutrino masses is the weakest. Therefore, not only tiny but also almost degenerated masses for neutrinos can be explained. Note that extra singlets considered here is naturally introduced in $SO(10)$ GUTs.

In $SU(5)$ GUT, gauge coupling unification is predicted: three gauge couplings in the SM are unified into one gauge coupling, g_5, as like

$$\sqrt{\frac{5}{3}}g' = g_2 = g_3 \equiv g_5. \tag{3.36}$$

Note that the relation between g' and g_5 is determined by Eq. (3.19):

$$g_5T_1 = g_5\sqrt{\frac{3}{5}}T_Y = g'T_Y \quad \Rightarrow \quad g_5 = \sqrt{\frac{5}{3}}g' \tag{3.37}$$

after $SU(5)$ breaking. Since $SU(2)$, $SU(3)$ and $SU(5)$ are the same normalization, relations between the gauge couplings are $g_2 = g_3 = g_5$. In fact, the gauge coupling unification is not realized in a non-SUSY minimal model as shown in Fig. 3 (dashed lines).

3.2.2 Problems in $SU(5)$ GUT

Although the $SU(5)$ GUT is the interesting extension of the SM, there are some problems which should be solved. We will list some of these below:

- Unification of the Yukawa couplings for down-type quarks and charged leptons
  From Eq. (3.33), an interesting relation at the GUT scale, $Y_d = Y_e^T$, is obtained. This is one of predictions of the $SU(5)$ GUT. This relation leads to the following relations at the low energy because of the renormalization group equation (RGE)

effects:

$$3m_e \simeq m_d, \quad 3m_\mu \simeq m_s, \quad 3m_\tau \simeq m_b. \tag{3.38}$$

However, current experimental observables show the different relations, $9m_e \sim m_d$、$m_\mu \sim m_s$、$3m_\tau \sim m_b$. There are some methods to avoid undesired relation Eq. (3.38). The examples are to introduce the extra Higgs fields and extra matter fields.

- Proton decay [19, 86]
  In the $SU(5)$ GUT, there are new particles which couple both of the quarks and leptons. These are X, Y bosons and the color-triplet Higgs H_T. These particles cause the proton decay at the tree-level. On the other hand, the current bound of the proton lifetime τ_p is very long (for $p \to e\pi$ mode, $\tau_p > 8.2 \times 10^{33}$ years [79]). This bound implies that the masses of new gauge bosons are needed to be larger than the GUT scale, $\Lambda_{\rm GUT}$. However, the mass of X (Y) boson is generated by the VEV of $\mathbf{24}_A$ in a similar way to the Higgs mechanism in the SM, so that $m_{X(Y)} \simeq \Lambda_{\rm GUT}$ and the bound of the proton lifetime is not satisfied. The lower bound for mass of H_T is weaker than that for masses of X and Y bosons since the decay width of the proton decay induced by H_T is evaluated by the Yukawa couplings rather than the gauge coupling. However, its bound is much higher than the weak scale. Therefore, the bound from the proton lifetime is one of the strong constraints for $SU(5)$ GUT models.

- Doublet-triplet splitting (DTS) problem (see [87] for a review)
  The Higgs potential related to $\mathbf{5}_H$ can be written as

$$V_{5_H} = m_{5_H}^2 |\mathbf{5}_H|^2 + |\lambda_{5_H}|(|\mathbf{5}_H|^2)^2 + \alpha |\mathbf{5}_H|^2 \mathrm{tr}\left[\mathbf{24}_A^2\right] + \beta \mathbf{5}_H^\dagger \mathbf{24}_A^2 \mathbf{5}_H, \tag{3.39}$$

  where α and β are the couplings between $\mathbf{5}_H$ and $\mathbf{24}_A$. By substituting $\langle \mathbf{24}_A \rangle$ in Eq. (3.24), the masses of H_T and the SM Higgs doublet are

$$m_{H_T}^2 = m_{5_H}^2 + (30\alpha + 4\beta)\, v_A^2, \tag{3.40}$$

$$m_H^2 = m_{5_H}^2 + (30\alpha + 9\beta)\, v_A^2. \tag{3.41}$$

  For the proton lifetime, m_{H_T} must be much larger than the weak scale, while m_H should be $\mathcal{O}(100)$ GeV because of the observed Higgs mass, 125 GeV. Therefore, there is a fine-tuning between $m_{H_T}^2$ and m_H^2 to realize both of the values. This fine-tuning is known as the doublet-triplet splitting (DTS) problem.

3.3 SUSY GUT models

The supersymmetric extension of the GUT models can be straightforwardly done. One of the interesting features is the realization of gauge coupling unification as shown in Fig. 3. In this subsection, we will introduce the $SO(10)$ and E_6 SUSY GUT and focus on the method for obtaining the realistic Yukawa couplings.

3.3.1 $SO(10)$ SUSY GUT

In $SO(10)$ GUTs, one can construct models with less number of fields since the representations of $SU(5)$ are unified. Low-dimensional representations of $SO(10)$ are **10** (vector), **16** (spinor) and **45** (adjoint), and the decompositions of these fields under $SO(10) \to SU(5) \times U(1)_V$ are

$$\begin{aligned} \mathbf{10} &\to \mathbf{5}_{-2} + \bar{\mathbf{5}}_2, \\ \mathbf{16} &\to \mathbf{10}_1 + \bar{\mathbf{5}}_{-3} + \mathbf{1}_5, \\ \mathbf{45} &\to \mathbf{24}_0 + \mathbf{10}_{-4} + \overline{\mathbf{10}}_4 + \mathbf{1}_0. \end{aligned} \tag{3.42}$$

Interestingly, the matter fields of $SU(5)$, $\mathbf{10}_i$ and $\bar{\mathbf{5}}_i$, can be unified into one spinor field, $\mathbf{16}_i$ in $SO(10)$ GUT models. In addition, since $\mathbf{16}_i$ has a singlet of $SU(5)$ which is the SM singlet, right-handed neutrinos are naturally introduced. These are the features of the $SO(10)$ GUT. In SUSY GUT models, two Higgs doublets H_u and H_d belong to $\mathbf{5}_H$ and $\bar{\mathbf{5}}_H$ of $SU(5)$. Therefore, from Eq. (3.42), these two Higgs doublets can be unified in one $\mathbf{10}_H$ of $SO(10)$. Clearly, the gauge boson field $\mathbf{24}_G$ in $SU(5)$ GUT are in $\mathbf{45}_G$ of $SO(10)$. The other Higgs field in $SU(5)$ GUT $\mathbf{24}_A$ can be embedded in $\mathbf{45}_A$.

Since the rank of $SO(10)$ is 5, an extra Higgs fields are needed. For this reason, $\mathbf{16}_H$ and $\overline{\mathbf{16}}_H$ are introduced to break $SO(10)$ to $SU(5)$. Therefore, a minimal model in $SO(10)$ GUT has three $\mathbf{16}_i$ as the matter fields, $\mathbf{45}_G$ as the gauge field and $\mathbf{10}_H$, $\mathbf{16}_H$, $\overline{\mathbf{16}}_H$ and $\mathbf{45}_A$ as Higgs fields.

In the minimal model, Yukawa interactions can be written as

$$W_{\text{Yukawa}} = Y_{ij} \mathbf{16}_i \mathbf{16}_j \mathbf{10}_H, \tag{3.43}$$

where $i, j = 1, 2, 3$ are the indices for the generations. Because of the matter unification, the Yukawa couplings are also unified, and in the $SO(10)$ GUT case, the following relation are obtained at the GUT scale:

$$Y_u = Y_d = Y_e^T = Y_{\nu_D}. \tag{3.44}$$

Here, Y_{ν_D} is a Yukawa interaction for Dirac neutrinos. This relation is an attractive hypothesis, although this cannot realize the observed fermion masses.

The Yukawa relation Eq. (3.44) can be avoided by introducing extra fields as a matter. In the $SO(10)$ GUT, one can use **10** fields as the extra matter field. In this case, the extra Yukawa couplings and mass term for **10** are

$$W_{\rm ex} = Y_i' \mathbf{16}_i \mathbf{10}\, \mathbf{16}_H + M_{10} \mathbf{10}\, \mathbf{10}. \tag{3.45}$$

After the symmetry breaking $SO(10) \to SU(5)$ by the VEV of the SM singlet in $\mathbf{16}_H$, matter fields in $\mathbf{16}_i$ and **10** mix with each other. Since **10** is decomposed to $\mathbf{5} + \bar{\mathbf{5}}$ in $SU(5)$, only $\bar{\mathbf{5}}$ fields mix. To see this explicitly, we will write down the mass matrix for the down-type quarks as an example. After breaking the symmetry, the mass matrix for the down-type quarks becomes 4×4 matrix:

$$\mathcal{L}_d = \begin{pmatrix} \overline{d_{R\,i}^{(16)}} & \overline{d_R^{(10)}} \end{pmatrix} \begin{pmatrix} Y_{ij} v_d & Y_i' \langle \mathbf{1}_H \rangle \\ 0 & M_{10} \end{pmatrix} \begin{pmatrix} d_{L\,j}^{(16)} \\ d_L^{(10)} \end{pmatrix}, \tag{3.46}$$

where $d_{L(R)\,i}^{(16)}$ and $d_{L(R)}^{(10)}$ are the down-type quarks from $\mathbf{16}_i$ and **10**, respectively. $\mathbf{1}_H$ in Eq. (3.46) is coming from $\mathbf{16}_H$ and its VEV breaks $SO(10)$ to $SU(5)$. It is clear that $d_{L(R)\,i}^{(16)}$ and $d_{L(R)}^{(10)}$ mix with each other when $SO(10)$ is broken. Therefore, the mass of one linear combination of $d_{L(R)\,i}^{(16)}$ and $d_{L(R)}^{(10)}$ is order of M_{10} (or $\langle \mathbf{1}_H \rangle$) which is expected to be superheavy, and the other three linear combinations have small masses ($\mathcal{O}(v_d)$). These modes are defined by the mixing matrices which diagonalize the 4×4 mass matrix in Eq. (3.46). Important point is that the down-type Yukawa couplings Y_d are obtained by multiplying these mixing matrix to Y_{ij}. There is similar mixing in the charged lepton sector, while up-type quark does not mix, $Y_u \sim Y_{ij}$. In addition, if one consider the effects of higher-dimensional operators to Yukawa couplings, unrealistic Yukawa relation Eq. (3.44) can be avoided and it is able to obtain the realistic Yukawa couplings which can realize the observed fermion masses. More detailed discussion is applied in Sec. 4.

3.3.2 E_6 SUSY GUT

E_6 GUT models have interesting features. Its fundamental representation, **27**, is decomposed as

$$\mathbf{27} = (\mathbf{10}, 1, 1) + (\bar{\mathbf{5}}, 1, -3) + (\mathbf{1}, 1, 5) + (\mathbf{5}, -2, -2) + (\bar{\mathbf{5}}', -2, 2) + (\mathbf{1}', 4, 0) \tag{3.47}$$

in $E_6 \supset SU(5) \times U(1)_{V'} \times U(1)_V$ notation. $(\bar{\mathbf{5}}', -2, 2)$ from **10** of $SO(10)$ plays an important role in obtaining realistic mass hierarchy and mixings of the SM, as we explained

in Sec. 3.3.1. From the E_6 algebra, E_6 singlet can be constructed by the product of three **27**s. Therefore, Higgs field is introduced as $\mathbf{27}_\Phi$ in E_6 GUT models and the Yukawa interactions are

$$W_Y = Y_{ij}\mathbf{27}_i\mathbf{27}_j\mathbf{27}_\Phi. \tag{3.48}$$

However, another Higgs field $\mathbf{27}_C$ is needed to break $E_6 \to G_{\rm SM}$ because the rank of E_6 is 6. Thus, the Yukawa interactions become the sum of the two Yukawa terms:

$$W_Y = Y^\Phi_{ij}\mathbf{27}_i\mathbf{27}_j\mathbf{27}_\Phi + Y^C_{ij}\mathbf{27}_i\mathbf{27}_j\mathbf{27}_C. \tag{3.49}$$

Note that we assume that $\mathbf{27}_\Phi$ and $\mathbf{27}_C$ breaks $E_6 \to SO(10)$ and $SO(10) \to SU(5)$ respectively. Therefore, $\mathbf{1}_\Phi \in \mathbf{27}_\Phi$ and $\mathbf{16}_C \in \mathbf{27}_C$ get non-zero VEVs. More interestingly, in the E_6 GUT, the assumption that **10** field has stronger hierarchy than $\bar{\mathbf{5}}$ of $SU(5)$ is obtained by the mixing of $\bar{\mathbf{5}}$ fields and by assuming the hierarchy of $Y^{\Phi,C}_{ij}$. From Eq. (3.47), three generations of **27** have six $\bar{\mathbf{5}}$s of $SU(5)$, and the SM modes are obtained as the light modes of the mixing of these $\bar{\mathbf{5}}$ fields. On the other hand, there are three **10**s of $SU(5)$ in three generations of **27**. Therefore, all **10** fields are regarded as the SM modes, and we expect that $Y^{\Phi,C}_{ij}$ have the hierarchical structures which realize the up-type quark mass hierarchy. For this reason, we assume

$$Y^\Phi_{ij} \sim Y^C_{ij} \sim \begin{pmatrix} \lambda^6 & \lambda^5 & \lambda^3 \\ \lambda^5 & \lambda^4 & \lambda^2 \\ \lambda^3 & \lambda^2 & 1 \end{pmatrix}, \tag{3.50}$$

where $\lambda = 0.22$. Because of the VEVs of $\mathbf{27}_\Phi$ and $\mathbf{27}_C$, Yukawa matrix for $\mathbf{5}$-$\bar{\mathbf{5}}$ sector becomes

$$\begin{array}{c} \\ \mathbf{5}_1 \\ \mathbf{5}_2 \\ \mathbf{5}_3 \end{array} \begin{array}{c} \begin{array}{cccccc} \bar{\mathbf{5}}'_1 & \bar{\mathbf{5}}'_2 & \bar{\mathbf{5}}'_3 & \bar{\mathbf{5}}_1 & \bar{\mathbf{5}}_2 & \bar{\mathbf{5}}_3 \end{array} \\ \begin{pmatrix} \lambda^6 & \lambda^5 & \lambda^3 & \lambda^{6+r} & \lambda^{5+r} & \lambda^{3+r} \\ \lambda^5 & \lambda^4 & \lambda^2 & \lambda^{5+r} & \lambda^{4+r} & \lambda^{2+r} \\ \lambda^3 & \lambda^2 & 1 & \lambda^{3+r} & \lambda^{2+r} & \lambda^r \end{pmatrix} \end{array}, \tag{3.51}$$

where $\lambda^r \equiv \langle \mathbf{16}_C \rangle / \langle \mathbf{1}_\Phi \rangle$ and $0 < r < 1$ because of $\langle \mathbf{16}_C \rangle < \langle \mathbf{1}_\Phi \rangle$. From this matrix, roughly speaking, $\bar{\mathbf{5}}'_2$, $\bar{\mathbf{5}}'_3$ and $\bar{\mathbf{5}}_3$ become superheavy with $\mathbf{5}_i$ fields. If $r = 0.5$, the realistic down-type Yukawa hierarchy is obtained as

$$Y_d \sim \begin{pmatrix} \lambda^6 & \lambda^{5.5} & \lambda^5 \\ \lambda^5 & \lambda^{4.5} & \lambda^4 \\ \lambda^3 & \lambda^{2.5} & \lambda^2 \end{pmatrix}, \tag{3.52}$$

and the SM modes denoted as $\bar{\mathbf{5}}_i^0$ become

$$(\bar{\mathbf{5}}_1^0, \bar{\mathbf{5}}_2^0, \bar{\mathbf{5}}_3^0) \sim (\bar{\mathbf{5}}_1, \bar{\mathbf{5}}_1', \bar{\mathbf{5}}_2). \tag{3.53}$$

Therefore, in E_6 GUTs, the assumption Eq. (3.51) and the ratio of VEVs, $\lambda^{0.5}$, lead to realistic mass hierarchy for the SM fermions. If one considers E_6 GUT with anomalous $U(1)_A$ gauge symmetry which is considered in Sec. 5, the hierarchy in Eq. (3.51) is obtained by the charge assignment of $U(1)_A$.

4 Flavor physics induced by Z' from $SO(10)$ SUSY GUT model

In this section, we will show predictions of a realistic $SO(10)$ SUSY GUT model. As we mentioned above, some methods to avoid the unrealistic relation Eq. (3.44) are needed in $SO(10)$ GUT models. In this thesis, we adopt the method that extra matter fields are introduced and some of the SM modes are obtained by linear combinations of the matter fields [27, 28].

We assume that $SO(10)$ is broken to $G_{\rm SM} \times U(1)'$ at the GUT scale by $SO(10)$-adjoint chiral superfields, **45** and **45′**, and $U(1)'$ symmetry is broken around 100 TeV by an extra Higgs fields, $\mathbf{16}_H$ and $\overline{\mathbf{16}}_H$. In this model, the SUSY-breaking scale is also $\mathcal{O}(100)$ TeV to achieve the 125 GeV Higgs mass [88–96], if the SUSY spectrum is not unique [97–100]. On the other hand, the gaugino masses (and Higgsino masses) are small to be around 1 TeV because of the gauge coupling unification. Therefore, there are three scales in this model, the $U(1)'$ breaking scale, gaugino mass scale and weak scale.

4.1 Setup

4.1.1 Requirements for the realistic Yukawa couplings

As we explained in Sec. 3.3.1, the matter superfields belong to the **16** representation, and the Yukawa couplings in the minimal $SO(10)$ SUSY GUT are described by one 3×3 matrix, h_{ij}:

$$W_{\rm min} = h_{ij}\mathbf{16}_i\mathbf{16}_j\mathbf{10}_H, \tag{4.1}$$

where $\mathbf{10}_H$ is the chiral superfield for the Higgs. In addition to $\mathbf{16}_i$, three **10**-representational chiral superfields, $\mathbf{10}_i$, are introduced as matter fields [27, 28]. Therefore, additional Yukawa couplings and mass terms for $\mathbf{10}_i$ can be written as

$$W_{\rm ex} = g_{ij}\mathbf{16}_i\mathbf{10}_j\mathbf{16}_H + \mu_{10\,ij}\mathbf{10}_i\mathbf{10}_j. \tag{4.2}$$

Note that $\mathbf{16}_H$ is an extra Higgs field to break the remaining $U(1)'$ symmetry, and μ-term is just omitted. In order to sketch the idea, let me focus on the down-type quark sector. Because of the decompotisions in Eq. (3.42), there are two kinds of down-type quarks in this setup. We denote these as $d^{(16)}_{L,R\,i}$ and $d^{(10)}_{L,R\,i}$ which are originated from the $\mathbf{16}_i$ and $\mathbf{10}_i$, respectively. As a result, we find the 6×6 mass matrix for the down-type quarks as

follow:

$$\mathcal{L}_d = -\begin{pmatrix}\overline{d_{R\,i}^{(16)}} & \overline{d_{R\,i}^{(10)}}\end{pmatrix}\begin{pmatrix}h_{ij}v_d & g_{ij}\langle \mathbf{1}_\Phi\rangle \\ 0 & \mu_{10\,ij}\end{pmatrix}\begin{pmatrix}d_{L\,j}^{(16)} \\ d_{L\,j}^{(10)}\end{pmatrix}, \tag{4.3}$$

where v_d denotes the nonzero VEV of the down-type Higgs doublet and $\mathbf{1}_\Phi$ is the scalar component of the SM singlet in $\mathbf{16}_H$. As seen in Eq. (4.3), $d_i^{(16)}$ and $d_i^{(10)}$ mix with each other once $\mathbf{1}_\Phi$ gets VEV. Therefore, the lightest modes for linear combinations of $d_i^{(16)}$ and $d_i^{(10)}$ can be interpreted as the SM down-type quarks. Note that at the same time, $U(1)'$ is broken spontaneously.

We define the mixing of the right-handed down-type quarks as

$$\begin{pmatrix}d_{R\,i} \\ d_{R\,i}^H\end{pmatrix} = (U_d)_{ij}\begin{pmatrix}d_{R\,j}^{(16)} \\ d_{R\,j}^{(10)}\end{pmatrix} = \begin{pmatrix}(\hat{U}_{16}^d)_{ij} & (\Delta U_d)_{ij} \\ (\Delta U_d')_{ij} & (\hat{U}_{10}^d)_{ij}\end{pmatrix}\begin{pmatrix}d_{R\,j}^{(16)} \\ d_{R\,j}^{(10)}\end{pmatrix}, \tag{4.4}$$

where d_R and d_R^H are the right-handed SM quarks and extra heavy quarks, respectively. U_d is a 6×6 unitary matrix, and $\hat{U}_{16,10}^d$ and $\Delta U_d^{(\prime)}$ are 3×3 matrices. Because of the unitarity of U_d, these 3×3 matrices satisfy the following conditions:

$$(\hat{U}_{16}^d)_{ik}(\hat{U}_{16}^d)_{jk}^* + (\Delta U_d)_{ik}(\Delta U_d)_{jk}^* = \delta_{ij}, \tag{4.5}$$

$$(\hat{U}_{16}^d)_{ik}(\Delta U_d')_{jk}^* + (\Delta U_d)_{ik}(\hat{U}_{10}^d)_{jk}^* = 0, \tag{4.6}$$

$$(\Delta U_d')_{ik}(\Delta U_d')_{jk}^* + (\hat{U}_{10}^d)_{ik}(\hat{U}_{10}^d)_{jk}^* = \delta_{ij}. \tag{4.7}$$

U_d is fixed by the parameters in the $W_{\rm ex}$, following Eqs. (4.3) and (4.4). In this section, we simply focus on the mixing in the limit that $h_{ij}v_d$ are much smaller than $g_{ij}\langle\mathbf{1}_\Phi\rangle$ and $\mu_{10\,ij}$. In this case, the left-handed SM quarks $d_{L\,i}$ are given by $d_{L\,j}^{(16)}$. Thus, in order to diagonalize the mass matrix for down-type quarks in Eq. (4.3), there are additional conditions for the elements of mixing matrix:

$$(\hat{U}_{16}^d)_{ik}g_{kj}\langle\mathbf{1}_\Phi\rangle + (\Delta U_d)_{ik}\mu_{10\,kj} = 0. \tag{4.8}$$

As a result, the Yukawa couplings for the SM down-type quarks, h_{ij}^d, is obtained by using the $\hat{U}_{16}^d$ parameters as

$$h_{ij}^d = (\hat{U}_{16}^d)_{ik}h_{kj}. \tag{4.9}$$

h_{ij} is the Yukawa couplings in the minimal case (Eq. (4.1)) and it is expected to explain the up-type SM quark mass matrix because the up-type quarks are belonging to $\mathbf{10}$ of $SU(5)$ and there are no mixing with the additional matter fields. Therefore, one can use

$\hat{U}^d_{16}$ to realize the mass hierarchy between the up-type and down-type quarks. However, since the relation in Eq. (4.5) means that the elements of $\hat{U}^d_{16}$ cannot be larger than 1, it is difficult to obtain the realistic hierarchy. In order to achieve it in this setup, one can introduce higher-dimensional operators involving $\mathbf{45}_H$ and $\mathbf{45}'_H$ fields, as discussed in Ref. [27]. Thus, Eq. (4.9) can be modified as

$$h^d_{ij} = (\hat{U}^d_{16})_{ik}(h^u_{kj} + \epsilon\, c^d_{kj}), \tag{4.10}$$

where h^u_{ij} are the Yukawa couplings for the up-type SM quarks and slightly deviated from h_{ij} by the higher-dimensional operators. ϵ is the suppression factor from the ratio between the VEVs of $\mathbf{45}_H$ and $\mathbf{45}'_H$ and the unknown cutoff scale at which the higher-dimensional operators are appeared. c^d_{ij} are the free parameters in our model and assumed to be $\mathcal{O}(1)$.

Since the lepton doublets also belong to $\bar{\mathbf{5}}$ of $SU(5)$, the similar relation of the Yukawa couplings are obtained in the same manner. The Yukawa couplings for the charged lepton are

$$h^\ell_{ij} = (\hat{U}^\ell_{16})_{ik}(h^u_{kj} + \epsilon\, c^\ell_{kj}), \tag{4.11}$$

where $\hat{U}^\ell_{16}$ is the 3×3 matrix which is defined as

$$\begin{pmatrix} \ell_{L\,i} \\ \ell^H_{L\,i} \end{pmatrix} = (U_\ell)_{ij} \begin{pmatrix} \ell^{(16)}_{L\,j} \\ \ell^{(10)}_{L\,j} \end{pmatrix} = \begin{pmatrix} (\hat{U}^\ell_{16})_{ij} & (\Delta U_\ell)_{ij} \\ (\Delta U'_\ell)_{ij} & (\hat{U}^\ell_{10})_{ij} \end{pmatrix} \begin{pmatrix} \ell^{(16)}_{L\,j} \\ \ell^{(10)}_{L\,j} \end{pmatrix}. \tag{4.12}$$

Therefore, the realistic Yukawa couplings are achieved by $U^{d,\ell}_{16}$ and $c^{d,\ell}_{ij}$.

The up-type quark Yukawa couplings h^u_{ij} can be diagonalized without loss of generality and therefore we can write it as

$$h^u_{ij} = \frac{m^u_i}{v_u}\delta_{ij}, \tag{4.13}$$

where v_u is the VEV of the up-type Higgs doublet and m^u_i are the up-type quark masses. In this case, the Yukawa couplings Eqs. (4.10) and (4.11) can be described as

$$h^d_{ij} = \frac{m^d_i}{v_d}\,(V^*_{\rm CKM})_{ji} = (\hat{U}^d_{16})_{ik}\left(\frac{m^u_k}{v_u}\,\delta_{kj} + \epsilon\, c^d_{kj}\right), \tag{4.14}$$

$$h^\ell_{ij} = \frac{m^\ell_i}{v_d}\,(V^*_R)_{ji} = (\hat{U}^\ell_{16})_{ik}\left(\frac{m^u_k}{v_u}\,\delta_{kj} + \epsilon\, c^\ell_{kj}\right), \tag{4.15}$$

where m^f_i $(f = d, \ell)$ are the SM fermion masses and $V_{\rm CKM}$ is the CKM matrix. V_R is the unitary matrix and identical to $V_{\rm CKM}$ in the $SU(5)$ limit.

m_e	0.5110 MeV [17]	λ	$0.22543^{+0.00042}_{-0.00031}$ [101]
m_μ	105.7 MeV [17]	A	$0.8227^{+0.0066}_{-0.0136}$ [101]
m_τ	1.777 GeV [17]	$\overline{\rho}$	$0.1504^{+0.0121}_{-0.0062}$ [101]
$m_d(2\text{ GeV})$	$4.8^{+0.5}_{-0.3}$ MeV [17]	$\overline{\eta}$	$0.3540^{+0.0069}_{-0.0076}$ [101]
$m_s(2\text{ GeV})$	95±5 MeV [17]	M_Z	91.1876(21) GeV [17]
$m_b(m_b)$	4.18±0.03 GeV [17]	M_W	80.385(15) GeV [17]
$\frac{2m_s}{(m_u+m_d)}(2\text{ GeV})$	27.5±1.0 [17]	$\sin^2\theta_W$	0.23126(5) [17]
$m_c(m_c)$	1.275±0.025 GeV [17]	G_F	$1.1663787(6)\times10^{-5}$ GeV^{-2} [17]
m_t	173.21±0.51 ± 0.71 GeV [17]	α	1/137.036 [17]
		$\alpha_s(M_Z)$	0.1193(16) [17]

Table 4: The input parameters used in our analysis. The CKM matrix, $V_{\rm CKM}$, is written in terms of λ, A, $\overline{\rho}$ and $\overline{\eta}$ [17].

Note that $h^{d,\ell}_{ij}$ in Eqs. (4.10) and (4.11) are generated after integrating out the heavy modes around the $U(1)'$ breaking scale. Therefore, we must consider the RGE corrections from the $U(1)'$ breaking scale ($\mathcal{O}(100)$ TeV) to the low energy scale (M_Z) in order to compare the predictions with the quark and lepton masses and mixing observed at low energy scale.

We obtain the realistic Yukawa couplings at the $U(1)'$ breaking scale as follow. First, we calculate the Yukawa couplings at the M_Z scale from the central values of the experimental measurements summarized in Table 4. In this stage, Mathematica package RunDec [102] are used to evaluate the running quark masses. Lepton pole masses are translated to $\overline{\rm MS}$ running masses at the M_Z scale, following Ref. [103]. Next, we evolve the Yukawa couplings at the M_Z scale into the ones at 1 TeV by using the SM RGE running at the two-loop level [103]. Here, we assume that all gaugino masses reside around 1 TeV. Then, we convert the $\overline{\rm MS}$ scheme into the $\overline{\rm DR}$ scheme at 1 TeV according to Ref. [104]. Finally, we obtain the Yukawa couplings at 100 TeV from the ones at 1 TeV by the RGE running including the gaugino contributions. As a result, we obtain the SM fermion masses and CKM matrix at 100 TeV as

$$\begin{aligned}(m^u_i) &= (8.4\times10^{-4}\,\text{GeV},\ 0.43\,\text{GeV},\ 1.2\times10^{2}\,\text{GeV}),\\ (m^d_i) &= (1.9\times10^{-3}\,\text{GeV},\ 3.8\times10^{-2}\,\text{GeV},\ 1.9\,\text{GeV}),\\ (m^\ell_i) &= (5.0\times10^{-4}\,\text{GeV},\ 0.11\,\text{GeV},\ 1.8\,\text{GeV}),\end{aligned} \tag{4.16}$$

and

$$V_{\rm CKM} = \begin{pmatrix} 9.7\times10^{-1} & 2.3\times10^{-1} & 1.5\times10^{-3} - 3.6\times10^{-3}i \\ -2.3\times10^{-1} - 1.6\times10^{-4}i & 9.7\times10^{-1} & 4.4\times10^{-2} \\ 8.5\times10^{-3} - 3.5\times10^{-3}i & -4.3\times10^{-2} - 8.2\times10^{-4}i & 1.0 \end{pmatrix}. \tag{4.17}$$

Note that the fermion masses at 100 TeV in Eq. (4.16) are obtained by just multiplying the running Yukawa couplings by the Higgs VEV $v = 174$ GeV and we use $\tan\beta = 3$ for Eqs. (4.16) and (4.17). h^f_{ij} at 100 TeV are given by Eqs. (4.13), (4.14) and (4.15), taking $\tan\beta$ into account.

Before discussing the Z' couplings, we would like to mention about the neutrino masses. In the $SO(10)$ GUT, because of the matter unification including right-handed neutrinos which are regarded as $\mathbf{1}$ of $SU(5)$, Yukawa couplings for the neutrinos can be also written by h_{ij} in Eq. (4.1). Unfortunately, tiny neutrino masses and large mixing cannot be realized from this Yukawa couplings. In order to obtain these tiny masses, we usually consider a seesaw mechanism [84, 85]. However, in this model, $U(1)'$ remains up to the SUSY-breaking scale ($\mathcal{O}(100)$ TeV), so that the Majorana mass terms which is $M_{ij}\mathbf{1}_i\mathbf{1}_j$ are forbidden by the $U(1)'$ symmetry and thus, we could not use the conventional seesaw mechanism.

Here, we can use another mechanism for the neutrino masses, according to the inverted hierarchy [105–107]. We introduce three $SO(10)$ singlet fields denoted as S_i. Therefore, we can write Yukawa couplings in addition to Eqs. (4.1) and (4.2) as

$$W_{\rm add} = f_{ij}\mathbf{16}_i\overline{\mathbf{16}}_H S_j + \mu_{16}\mathbf{16}_H\overline{\mathbf{16}}_H + \mu_H\mathbf{10}_H\mathbf{10}_H + \mu_{S\,ij}S_iS_j. \tag{4.18}$$

Here, we assume that μ_{16} and μ_H are around the SUSY-breaking scale and μ_S is much smaller than μ_{16} and μ_H[4]. In one generation of matter fields of this model, there is four neutral particles which belongs to following multiplets:

$$\begin{array}{cccc} & SU(5) & SO(10) & \\ \nu^{(16)}_{L\,i} & \in \mathbf{10}_i & \in \mathbf{16}_i & \\ \nu^{(16)}_{R\,i} & \in \mathbf{1}_i & \in \mathbf{16}_i & , \\ \nu^{(10)}_{L\,i} & \in \mathbf{5}_i & \in \mathbf{10}_i & \\ \overline{\nu^{(10)}_{L\,i}} & \in \bar{\mathbf{5}}'_i & \in \mathbf{10}_i & \end{array} \tag{4.19}$$

in addition to S_i. After the EW symmetry breaking, the mass matrix for these neutral

[4]The hierarchy between μ_S and the other mass parameters can be explained by assigning the global $U(1)_{\rm PQ}$ symmetry [108, 109] and introducing the other $SO(10)$ singlet fields.

particles is given from Eqs. (4.1), (4.2) and (4.18) as

$$M_\nu = \begin{pmatrix} 0 & h_{ij}v_u & 0 & g_{ij}\langle \mathbf{1}_\Phi \rangle & 0 \\ h_{ij}v_u & 0 & 0 & 0 & f_{ij}\langle \bar{\mathbf{1}}_\Phi \rangle \\ 0 & 0 & 0 & \mu_{10\,ij} & 0 \\ g_{ij}\langle \mathbf{1}_\Phi \rangle & 0 & \mu_{10\,ij} & 0 & 0 \\ 0 & f_{ij}\langle \bar{\mathbf{1}}_\Phi \rangle & 0 & 0 & \mu_{S,ij} \end{pmatrix}, \tag{4.20}$$

where this matrix is in the basis of $(\nu_{L\,i}^{(16)}, \nu_{R\,i}^{(16)}, \nu_{L\,i}^{(10)}, \overline{\nu_{L\,i}^{(10)}}, S_i)$, and $\langle \bar{\mathbf{1}}_\Phi \rangle$ is the VEV of the scalar component of the SM singlet in $\overline{\mathbf{16}}_H$. Therefore, the neutrino mass matrix is obtained as

$$(m_\nu)_{ij} = \left(h f^{-1} \mu_S f^{-1} h\right)_{ij} \left(\frac{v_u}{\langle \bar{\mathbf{1}}_\Phi \rangle}\right)^2, \tag{4.21}$$

following Refs. [105–107]. By assuming that h and f are $\mathcal{O}(1)$, $\langle \bar{\mathbf{1}}_\Phi \rangle = \mathcal{O}(100)$ TeV, $v_u = \mathcal{O}(100)$ GeV and $\mu_S = \mathcal{O}(1)$ MeV, the neutrino masses becomes $\mathcal{O}(1)$ eV and the masses of other neutral particles are around the SUSY-breaking scale. Therefore, the realistic mass spectrum for the neutrinos can be obtained in this model. We expect that the other observables in neutrino sector can be obtained since there are enough parameters to fit it. We do not consider the neutrino masses and mixing further because our arguments are independent of the neutrino sector.

4.1.2 Flavor-violating Z' couplings

As shown in Eqs. (4.4) and (4.12), the SM right-handed down-type quarks and left-handed leptons are given by the linear combinations of the parts of $\mathbf{16}_i$ and $\mathbf{10}_i$ in this setup. Important point is that $\bar{\mathbf{5}}$ fields from $\mathbf{10}$ and $\mathbf{16}$ have different $U(1)'$ charges, as like in Eq. (3.42):

$$\mathbf{10} \to \mathbf{5}_2 + \bar{\mathbf{5}}_{-2}, \tag{4.22}$$

$$\mathbf{16} \to \mathbf{10}_{-1} + \bar{\mathbf{5}}_3 + \mathbf{1}_{-5}, \tag{4.23}$$

where subscripts show the $U(1)'$ charges. Therefore, after the $U(1)'$ symmetry breaking and mixing of the $\bar{\mathbf{5}}$ fields, Z' interactions become flavor-violating as follows. Before the

$U(1)'$ symmetry breaking, the Z' interactions are[5]

$$\mathcal{L}_{Z'} = g'\hat{Z}'_\mu \Big(3\,\overline{\ell^{(16)}_{Li}}\gamma^\mu \ell^{(16)}_{Li} - 2\,\overline{\ell^{(10)}_{Li}}\gamma^\mu \ell^{(10)}_{Li} - 3\,\overline{d^{(16)}_{Ri}}\gamma^\mu d^{(16)}_{Ri} + 2\,\overline{d^{(10)}_{Ri}}\gamma^\mu d^{(10)}_{Ri} \\ -\overline{Q'_i}\gamma^\mu Q'_i + \overline{u'_{Ri}}\gamma^\mu u'_{Ri} + \overline{e'_{Ri}}\gamma^\mu e'_{Ri} \Big)\,, \tag{4.24}$$

where Q'_i, u'_{Ri} and e'_{Ri} are the flavor eigenstates of the left-handed quarks, right-handed up-type quarks and right-handed charged leptons, respectively. Once $\mathbf{1}_\Phi$ gets VEV, the field mixings Eqs. (4.4) and (4.12) are induced. Thus, the Z' interactions with the SM modes become

$$\mathcal{L}_{Z'} = g'\hat{Z}'_\mu \left(A^\ell_{ij}\overline{\ell_{Li}}\gamma^\mu \ell_{Lj} - A^d_{ij}\overline{d_{Ri}}\gamma^\mu d_{Rj} - \overline{Q_i}\gamma^\mu Q_i + \overline{u_{Ri}}\gamma^\mu u_{Ri} + \overline{e_{Ri}}\gamma^\mu e_{Ri} \right), \tag{4.25}$$

where Q_i, u_{Ri} and e_{Ri} are the mass eigenstates of the left-handed quarks, right-handed up-type quarks and right-handed charged leptons, respectively. Note that $\hat{Z}'_\mu$ is not the mass eigenstate. We will mention the mixing of Z' below. $A^{d,l}_{ij}$ are the flavor-violating couplings and defined as

$$A^d_{ij} = 5(\hat{U}^d_{16})_{ik}(\hat{U}^d_{16})^*_{jk} - 2\delta_{ij}, \quad A^\ell_{ij} = 5(\hat{U}^\ell_{16})^*_{ik}(\hat{U}^\ell_{16})_{jk} - 2\delta_{ij}. \tag{4.26}$$

Note that the unitary condition Eq. (4.5) is used. Figures 4 and 5 show our predictions for the flavor-violating couplings, A^d_{dd}, A^d_{sd}, A^d_{bd} and A^d_{bs}. For these predictions, we use $\tan\beta = 3$ and the SM fermion masses and CKM matrix at 100 TeV in Eqs. (4.16) and (4.17). The red (blue) points correspond to arbitrary complex values of $\epsilon\, c^d_{ij}$ satisfying $|\epsilon\, c^d_{ij}| < 10^{-2}$ ($|\epsilon\, c^d_{ij}| < 10^{-3}$).

Note that we found that the SM mode for the down quark d_{R1} are mainly coming from $\mathbf{10}_i$s of $SO(10)$ since the prediction that $A^d_{dd} \simeq -2$ obtained from the left panel of Fig. 4 leads to $|(\hat{U}^d_{16})_{1i}|^2 \ll 1$. This is because (1, 1)-element of the contributions of higher-dimensional operators $v_u \epsilon\, c^d_{11}$ is larger than the up quark mass. Therefore, $(\hat{U}^d_{16})_{11}$ should be small in order to obtain the down quark mass because of the relation in Eq. (4.14). Roughly speaking, $(\hat{U}^d_{16})_{12}$ and $(\hat{U}^d_{16})_{13}$ are also suppressed by $m_d(V^*_{\rm CKM})_{21}/m_c$ and $m_d(V^*_{\rm CKM})_{31}/m_t$, respectively. From Figs. 4 and 5, on the other hand, the strange and bottom quarks seem to consist of both of $\mathbf{16}_i$ and $\mathbf{10}_i$, depending on the size of the coefficients of higher-dimensional operators.

Equation 4.14 says that $(\hat{U}^{d(\ell)}_{16})_{ij}$ is proportional to the down-type quark (charged lepton) mass of i-th generation. This leads to $A^{d,\ell}_{ij} \propto m^{d,\ell}_i m^{d,\ell}_j$ $(i \neq j)$ from Eq. (4.26), so that flavor-violating couplings involving 3rd generation, especially (2, 3)-element, tend to

[5]Since the right-handed fields are embedded in the GUT multiplets as the charge conjugation fields, there is additional minus sign for their $U(1)'$ charges.

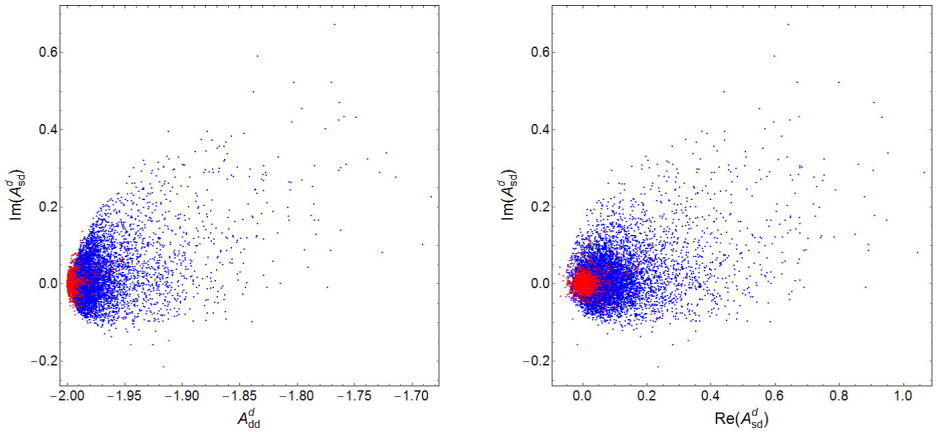

Figure 4: Our predictions for A^d_{dd} (left) and A^d_{sd} (right) [28]. The coefficients of higher-dimensional operators satisfy $|\epsilon\, c^d_{ij}| < 10^{-2}$ (red) and $|\epsilon\, c^d_{ij}| < 10^{-3}$ (blue).

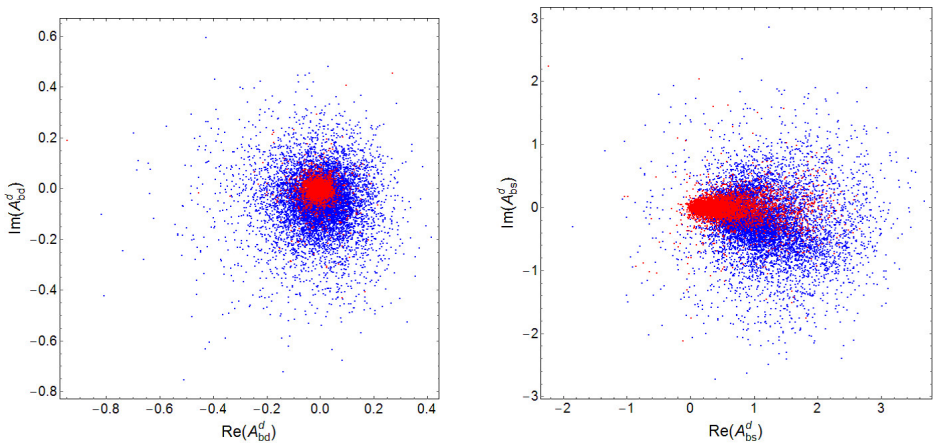

Figure 5: Our predictions for A^d_{bd} (left) and A^d_{bs} (right) [28]. The coefficients of higher-dimensional operators satisfy $|\epsilon\, c^d_{ij}| < 10^{-2}$ (red) and $|\epsilon\, c^d_{ij}| < 10^{-3}$ (blue).

be large in this model. This is one of our predictions. By using the expressions of $\hat{U}^{d,\ell}_{16}$ from Eqs. (4.14) and (4.15), $A^{d,\ell}_{ij}$ are obtained by the observables and model parameters, $\epsilon\, c^{d,\ell}_{ij}$. When ϵ is small, the approximate expressions for the flavor-violating couplings are

$$\begin{aligned}
&\mathrm{Re}(A^d_{sd}) \sim 5\tan^2\beta \frac{m^d_d\, m^d_s}{\left|v_u \epsilon\, c^d_{11}\right|^2}\lambda,\ \ \mathrm{Im}(A^d_{sd}) \sim 5\tan^2\beta \frac{m^d_d\, m^d_s}{\left|v_u \epsilon\, c^d_{11}\right|^2}\,\mathrm{Im}\left(\frac{v_u \epsilon\, c^{d*}_{12}}{m^u_c}\right),\\
&A^d_{bd} \sim 5\tan^2\beta \frac{m^d_d\, m^d_b}{\left|v_u \epsilon\, c^d_{11}\right|^2}\left(\frac{v_u \epsilon\, c^{d*}_{12}}{m^u_c}\right) A\lambda^2,\\
&\mathrm{Re}(A^d_{bs}) \sim 5\tan^2\beta \frac{m^d_s\, m^d_b}{(m^u_c)^2}\lambda^2,\ \ \mathrm{Im}(A^d_{bs}) \sim 5\tan^2\beta \frac{m^d_s\, m^d_b}{\left|v_u \epsilon\, c^d_{11}\right|^2}\,\mathrm{Im}\left(\frac{v_u \epsilon\, c^{d*}_{12}}{m^u_c}\right) A\lambda^3,
\end{aligned} \tag{4.27}$$

where A and λ are the parameters for the CKM matrix in the Wolfenstein parametrization [83]. In the $SU(5)$ limit, the approximate expressions for A^{ℓ}_{ij} are obtained by replacing d with ℓ.

Note that $\hat{Z}'_\mu$ in Eq. (4.25) is not the mass eigenstate, and mixes with Z boson denoted by $\hat{Z}_\mu$. The mass mixing is generated by the $U(1)'$-charged Higgs doublets [27]:

$$\begin{pmatrix} \hat{Z}_\mu \\ \hat{Z}'_\mu \end{pmatrix} = \begin{pmatrix} \cos\theta & -\sin\theta \\ \sin\theta & \cos\theta \end{pmatrix} \begin{pmatrix} Z_\mu \\ Z'_\mu \end{pmatrix}, \tag{4.28}$$

where $\sin\theta$ is approximately estimated as

$$\tan 2\theta \simeq 4\,\frac{g'}{g_Z}\frac{M_Z^2}{M_{Z'}^2}. \tag{4.29}$$

We have to include this effect, when we discuss the phenomenology in our model.

4.2 Flavor physics

In this subsection, we investigate the predictions of the $SO(10)$ GUT model discussed above from flavor physics. One of the important features of this model is that some of the FCNC processes involving Z'_μ and Z_μ are induced at the tree-level. Moreover, all elements of the flavor-violating couplings could be $\mathcal{O}(1)$, corresponding to the higher-dimensional operators. Therefore, we have to check the consistency with the flavor-violating processes, especially concerned with the first and second generations, e.g. K^0-$\overline{K^0}$ mixing and $\mu \to 3e$. These processes are the most sensitive to the new physics contributions. Furthermore, since the flavor-violating coupling A^d_{bs} tends to be larger than the other flavor-violating couplings, we investigate not only K physics but also B physics and search the specific prediction of this model.

4.2.1 $\Delta F = 2$ processes

First, we start to investigate the constraints from the $\Delta F = 2$ processes in K and $B_{(s)}$ systems. In the SM, the source of the CP violation is only come from the CP phase in the CKM matrix. The SM predictions for CP and flavor-violating processes are usually tiny because of the suppression caused by the Glashow-Iliopoulos-Maiani mechanism. In fact, the SM prediction of K^0-$\overline{K^0}$ mixing is quite small but consistent with the experimental observations, although theoretical uncertainties in the SM predictions are still sizable. That is, the size of new physics contributions to the K physics is strongly constrained in order to satisfy the experimental results. Similar to K^0-$\overline{K^0}$ mixing, we can obtain the constraints to new physics contributions from B meson mixings, B^0-$\overline{B^0}$ and B^0_s-$\overline{B^0_s}$

mixings.

In this model, the $\Delta F = 2$ processes, like the meson mixing, are caused by Z' and Z interactions at tree-level. The induced operators are

$$\mathcal{H}^{\Delta F=2} = \frac{1}{2} \sum_{q=K,B,B_s} \widetilde{C}_1^q \widetilde{Q}_1^q \tag{4.30}$$

where the each operator and Wilson coefficient are given by

$$\begin{aligned}
\widetilde{Q}_1^K &= (\overline{s_R}\gamma_\mu d_R)(\overline{s_R}\gamma^\mu d_R), \quad \widetilde{C}_1^K = \frac{(A_{sd}^d)^2}{\Lambda_{Z'}^2}, \\
\widetilde{Q}_1^B &= (\overline{b_R}\gamma_\mu d_R)(\overline{b_R}\gamma^\mu d_R), \quad \widetilde{C}_1^B = \frac{(A_{bd}^d)^2}{\Lambda_{Z'}^2}, \\
\widetilde{Q}_1^{B_s} &= (\overline{b_R}\gamma_\mu s_R)(\overline{b_R}\gamma^\mu s_R), \quad \widetilde{C}_1^{B_s} = \frac{(A_{bs}^d)^2}{\Lambda_{Z'}^2},
\end{aligned} \tag{4.31}$$

where $\Lambda_{Z'}$ is defined as

$$\frac{1}{\Lambda_{Z'}^2} \equiv \left(\frac{g'^2 \cos^2\theta}{M_{Z'}^2} + \frac{g'^2 \sin^2\theta}{M_Z^2} \right). \tag{4.32}$$

Note that the operators which consist of left-handed quarks, such as $(\overline{s_L}\gamma_\mu d_L)(\overline{s_L}\gamma^\mu d_L)$, contribute the meson mixing in the SM. As we mentioned above, the CP phase appears in the $(t,\, d)$-element of the CKM matrix in the SM. On the other hand, the flavor-violating couplings A_{ij}^d are generally complex in this model. Therefore, Z' interactions are strongly constrained by the CP-violating processes.

Hereafter, we set $\Lambda_{Z'} = 1.4 \times 10^3$ TeV (500 TeV), which corresponds to $M_{Z'} = 100$ TeV (36 TeV) and $g' \simeq 0.073$ [27]. In order to achieve the 125 GeV Higgs mass, we take $\tan\beta = 3$ [88–96].

• $\Delta S = 2$ processes

Based on Ref. [110], we investigate the upper bound on the Z' interaction from the K^0-$\overline{K^0}$ mixing. The physical observables on the mixing are the CP-violating parameter ϵ_K and mass difference ΔM_K. These observables can be expressed as

$$\epsilon_K = \frac{\kappa_\epsilon e^{i\varphi_\epsilon}}{\sqrt{2}(\Delta M_K)_{\rm exp}} \mathrm{Im}(M_{12}^K), \;\; \Delta M_K = 2\mathrm{Re}(M_{12}^K), \tag{4.33}$$

where κ_ϵ and φ_ϵ are given by the observations: $\kappa_\epsilon = 0.94 \pm 0.02$ and $\varphi_\epsilon = 0.2417 \times \pi$. M_{12}^K can be decomposed as follows in this model:

$$M_{12}^K = \left(M_{12}^K\right)_{\rm SM} + \Delta M_{12}^K. \tag{4.34}$$

m_K	497.611(13) MeV [17]	m_{B_s}	5.3663(6) GeV [17]
F_K	156.1(11) MeV [114]	m_B	5.2795(3) GeV [17]
$\hat{B}_K$	0.764(10) [114]	F_{B_s}	227.7 ± 6.2 MeV [114]
$(\Delta M_K)_{\rm exp}$	$3.484(6)\times10^{-12}$ MeV [17]	F_B	190.6 ± 4.6 MeV [114]
$\lvert\epsilon_K\rvert$	$(2.228(11))\times10^{-3}$ [17]	$\hat{B}_{B_s}$	1.33(6) [114]
$\mathrm{BR}(K^+\to\pi^0 e^+\nu)$	5.07(4) % [17]	$\hat{B}_B$	1.26(11) [114]
$\tau(K^+)$	$(1.238(2))\times10^{-8}$ s [17]	η_B	0.55 [112]
$\tau(K_L)$	$(5.116(21))\times10^{-8}$ s [17]	η_Y	1.012 [115]
η_1	1.87(76) [111]	Γ_μ^{-1}	$2.1969811(22)\times10^{-6}$ s
η_2	0.5765(65) [112]		
η_3	0.496(47) [113]		

Table 5: The input parameters relevant to our analyses in flavor physics.

ΔM_{12}^K is the Z' contribution. It is given by the matrix element $\langle\widetilde{Q}_1^K\rangle$ as

$$\Delta M_{12}^K = \frac{1}{2}\widetilde{C}_1^K(\mu)\langle\widetilde{Q}_1^K\rangle. \tag{4.35}$$

Note that $\langle\widetilde{Q}_1^K\rangle$ can be extracted from the SM prediction, because the only difference is the chirality. $\widetilde{C}_1^K(\mu)$ is the Wilson coefficient derived from Eq. (4.31) and the RGE correction. The running correction is shown in Appendix B.

The SM prediction is described as

$$(M_{12}^K)_{\rm SM} = \frac{G_F^2}{12\pi^2}F_K^2\hat{B}_K m_K M_W^2\left\{\lambda_c^2\eta_1 S_0(x_c)+\lambda_t^2\eta_2 S_0(x_t)+2\lambda_c\lambda_t\eta_3 S(x_c,x_t)\right\}. \tag{4.36}$$

x_i and λ_i denote m_i^2/M_W^2 and $(V_{CKM})_{is}^*(V_{CKM})_{id}$, respectively. $\eta_{1,2,3}$ correspond to the Next-Leading-Order and Next-to-Next-Leading-Order QCD corrections [111–113]. The values we adopt are summarized in Table 5. The functions, $S_0(x_t)$ and $S(x_c,x_t)$, are shown in Appendix C.

The physical observables in K^0-$\overline{K^0}$ mixing are experimentally measured well, while there is the large uncertainty from the matrix element and the CKM matrix in the SM predictions. We use the central values in Tables 4 and 5 and calculate the predictions of this model as the deviations from the SM predictions, which are defined as

$$\delta\epsilon_K \equiv \frac{\epsilon_K}{(\epsilon_K)_{\rm SM}} - 1 \ \text{ and } \ \delta(\Delta M_K) \equiv \frac{\Delta M_K}{(\Delta M_K)_{\rm SM}} - 1. \tag{4.37}$$

Due to the large uncertainties of the SM predictions, it is difficult to obtain the explicit

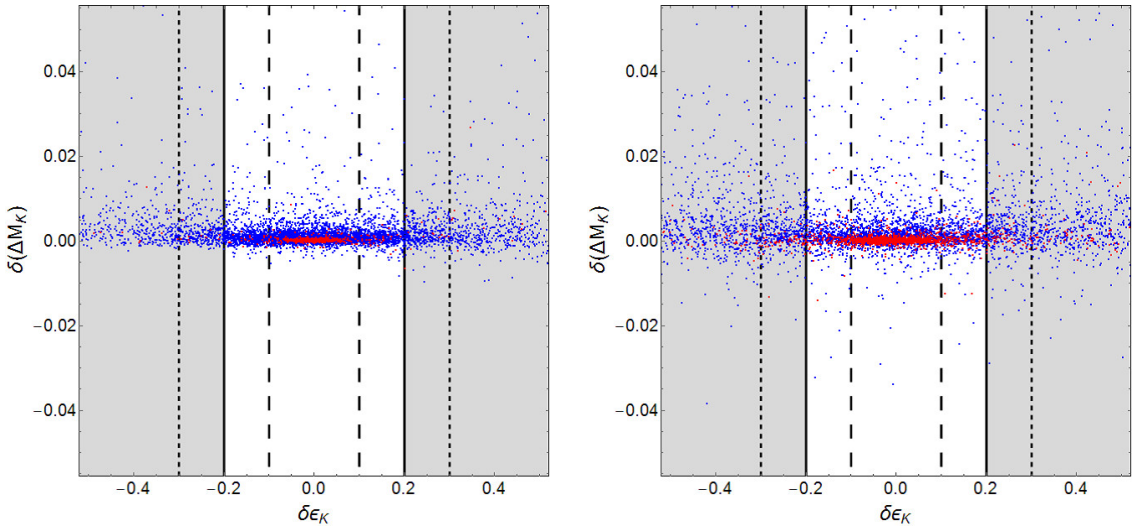

Figure 6: Our predictions for $\delta\epsilon_K$ and $\delta(\Delta M_K)$ with $\Lambda_{Z'} = 1400$ TeV (left panel) and $\Lambda_{Z'} = 500$ TeV (right panel) [28]. The coefficients of higher-dimensional operators satisfy $|\epsilon\, c^d_{ij}| < 10^{-2}$ (red) and $|\epsilon\, c^d_{ij}| < 10^{-3}$ (blue). Black dashed, solid and dotted line show the deviation from SM by 10%, 20% and 30%, respectively.

exclusion limits of $|\delta\epsilon_K|$ and $|\delta(\Delta M_K)|$. In Ref. [116], the CKM fitter group shows that the experimental upper bounds on $|\delta\epsilon_K|$ and $|\delta(\Delta M_K)|$ are at most $\mathcal{O}(30)$ %. It will be developed up to $\mathcal{O}(20)$ % at the Belle II experiment [116].

In Fig. 6, the predictions of $\delta\epsilon_K$ and $\delta(\Delta M_K)$ are shown in the cases with $\Lambda_{Z'} = 1400$ TeV (left panel) and $\Lambda_{Z'} = 500$ TeV (right panel). The black dashed, solid and dotted line show the deviation from SM by 10%, 20% and 30%, respectively. Clearly, ϵ_K largely deviates from the SM prediction, even if $\Lambda_{Z'}$ is $\mathcal{O}(10^3)$ TeV. Therefore, the consistency with ϵ_K should be considered whenever we discuss the other observables. Note that one can find that $\delta(\Delta M_K)$ tends to be positive from Fig. 6. This is because the real part of the flavor-violating coupling A^d_{sd} tends to be positive from Fig. 4. This tendency is one of the predictions of this model, although its deviation is very small and almost dominated by the SM prediction.

• $\Delta B = 2$ processes

Next, we derive predictions of B^0-$\overline{B^0}$ and B^0_s-$\overline{B^0_s}$ mixings in a similar way of K^0-$\overline{K^0}$ mixing. In the case of the B meson mixings, relevant observables are mass differences, ΔM_B and ΔM_{B_s}. These are written by $\widetilde{C}_1^{B_{d,s}}$ as follow:

$$\Delta M_{B_q} = 2\left|(M_{12}^{B_q})_{\rm SM} + \frac{1}{6}\widetilde{C}_1^{B_q} m_{B_q} F_{B_q} \hat{B}_{B_q}\right| \ (q = d,\ s), \tag{4.38}$$

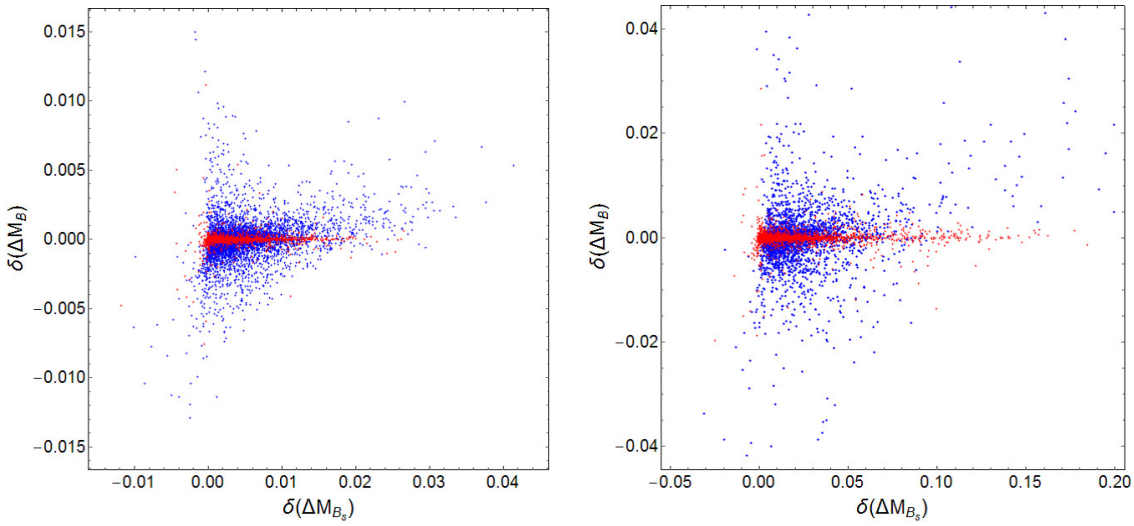

Figure 7: Our predictions for $\delta(\Delta M_{B_s})$ and $\delta(\Delta M_B)$ with $\Lambda_{Z'} = 1400$ TeV (left) and $\Lambda_{Z'} = 500$ TeV (right) [28]. The coefficients of higher-dimensional operators satisfy $|\epsilon\, c^d_{ij}| < 10^{-2}$ (red) and $|\epsilon\, c^d_{ij}| < 10^{-3}$ (blue). In these figures, we only show the points that $|\delta\epsilon_K| \leq 0.3$ is satisfied.

where $(M_{12}^{B_q})_{\rm SM}$ is given by the top-loop contribution:

$$(M_{12}^{B_q})_{\rm SM} = \frac{G_F^2}{12\pi^2} F_{B_q}^2 \hat{B}_{B_q} m_{B_q} M_W^2 \lambda_{B_q}^2 \eta_B S_0(x_t). \tag{4.39}$$

The input parameters are listed in Table 5 and $\lambda_{B_q} = (V_{CKM})^*_{tb}(V_{CKM})_{tq}$. As the K^0-$\overline{K^0}$ mixing, there are still large uncertainties in the SM predictions, coming mainly from the errors of hadronic mixing matrix elements and the CKM matrix elements, and therefore, the new physics constraints would be not so easy to obtain. Recently, the Fermilab and MILC Collaborations have shown their results on the SM predictions of ΔM_B and ΔM_{B_s} [117] and about 10 % errors are still inevitable. The LHCb and Belle II experiments will improve the measurement, as discussed in Ref. [116].

As shown in Fig. 5, A^d_{bs} tends to be large compared to the other flavor-violating couplings. Therefore, we may obtain the important predictions of this model from ΔM_{B_s}, although the deviation is relatively smaller than the K^0-$\overline{K^0}$ mixing because of the size of the SM prediction. Figure 7 shows our predictions for the deviations of ΔM_B and ΔM_{B_s} in the cases with $\Lambda_{Z'} = 1400$ TeV (left panel) and $\Lambda_{Z'} = 500$ TeV (right panel). $\delta(\Delta M_{B_{d,s}})$ are defined as the same manner in Eq. (4.37). In these figures, all points satisfy $|\delta\epsilon_K| \leq 0.3$. If $m_{Z'}$ is around $\mathcal{O}(10)$ TeV, $\delta(\Delta M_B)$ could reach 10 %, which maybe cause the tension with the current measurement [116]. Note that the distribution of the predictions in Fig. 7 can be understood from Fig. 5. We would like to emphasize that the

features of the flavor-violating couplings are specific to this model, so that not only the K^0-$\overline{K^0}$ mixing but also B^0-$\overline{B^0}$ mixing is important to test this model.

4.2.2 $\Delta F = 1$ processes

In addition to $\Delta F = 2$ processes, the Z' interactions of this model contribute to $\Delta F = 1$ processes, including the rare decays of K and B mesons. We study the semi-leptonic and leptonic decays of K and the leptonic decays of B and B_s. In this thesis, we focus on the processes such as $K_L^0 \to \pi\nu\overline{\nu}$, $K_L^0 \to \ell_i^+\ell_j^-$ and $B_{d,s}^0 \to \mu^+\mu^-$. For these decays, some experiments, for example the KOTO, Belle II and LHCb, will develop their measurements. Therefore, we can expect that some hints to new physics will be given in the near future.

• $\Delta S = 1$ processes

To begin with, let us study the $\Delta S = 1$ processes which play a crucial role in testing this model. For the rare K meson decays which is caused at the tree-level in this model, the effective Hamiltonian is given by the Z' exchanging and Z boson exchanging through the Z-Z' mixing caused by Eq. (4.29):

$$\mathcal{H}^{\Delta S=1} = (C_I^f)_{ij}(\overline{s_R}\gamma_\mu d_R)(\overline{f_I^i}\gamma^\mu f_I^j), \tag{4.40}$$

where f denotes $f = \nu$, ℓ, u, d and $I = L$, R is the chirality of the fermions. $(C_I^f)^{ij}$ at $\mu = M_{Z'}$ is obtained as

$$(C_I^f)_{ij} = -A_{sd}^d \left\{ \frac{(Q_I^f)_{ij}}{\Lambda_{Z'}^2} + \frac{\delta_{ij}}{\Lambda_Z^2}\left(T_I^{3\,f} - Q_e^f \sin^2\theta_W\right)\right\}, \tag{4.41}$$

where Λ_Z^2 is defined as

$$\frac{1}{\Lambda_Z^2} \equiv g' g_Z \sin\theta\cos\theta\left(\frac{1}{M_Z^2} - \frac{1}{M_{Z'}^2}\right), \tag{4.42}$$

and can be approximately evaluated as $\Lambda_Z^2 \simeq \Lambda_{Z'}^2/2$ according to Eq. (4.29) in the limit $M_{Z'} \gg M_Z$. From Eq. (4.25), we obtain each $(Q_I^F)_{ij}$ as

$$\left((Q_L^{\nu,l})_{ij},\, (Q_R^l)_{ij}\right) = (A_{ij}^l,\, +\delta_{ij}), \tag{4.43}$$

$$\left((Q_L^{u,d})_{ij},\, (Q_R^u)_{ij},\, (Q_R^d)_{ij}\right) = (-\delta_{ij},\, +\delta_{ij},\, -A_{ij}^d). \tag{4.44}$$

T_I^f and Q_e^f are defined in Sec. 2.

$K_L^0 \to \pi^0 \nu \overline{\nu}$ and $K^+ \to \pi^+ \nu \overline{\nu}$

The rare decay of neutral K meson, e.g. $K_L^0 \to \pi^0 \nu \overline{\nu}$, is one of the important measurements of the CP-violating processes. For this mode, the SM predicts very small branching ratio which the current experimental bound does not reach yet: $\mathrm{BR}(K_L^0 \to \pi^0 \nu\overline{\nu}) < 2.6 \times 10^{-8}$ [118]. The KOTO experiment at the J-PARC will cover the region in the near future. On the other hand, the decay of the charged K meson, $K^+ \to \pi^+ \nu \overline{\nu}$, has been already measured as $\mathrm{BR}(K^+ \to \pi^+ \nu\overline{\nu}) = 1.73^{+1.15}_{-1.05} \times 10^{-10}$ [119]. The NA62 experiment at the CERN will update this result.

In the SM, the branching ratio for the both modes are given by the following operators:

$$\mathcal{H}_{\mathrm{SM}}^{\Delta S=1} = C_{\mathrm{SM}} (\overline{s_L} \gamma_\mu d_L)(\overline{\nu_L}^i \gamma^\mu \nu_L^i). \tag{4.45}$$

C_{SM} is given by the Z penguin diagram and the box diagram involving W boson, and described as[6]

$$C_{\mathrm{SM}} = \frac{G_F}{\sqrt{2}} \frac{2\,\alpha}{\pi \sin^2\theta_W} \left(\lambda_c X_c + \lambda_t X(x_t)\right). \tag{4.46}$$

$X_c/\lambda^4 = (0.42 \pm 0.03)$ is proposed in Ref. [110]. $X(x_t)$ is the short-distance contribution given by the Z-penguin diagrams and box diagrams involving top quark respectively. In Appendix C, we summarize the LO description. In this model, there are the Z' contribution to this process, as we shown in Eqs. (4.40) and (4.41). By using the isospin symmetry and taking the ratio to $K^+ \to \pi^0 e^+ \nu$, one can estimate the branching ratio of $K_L^0 \to \pi^0 \nu \overline{\nu}$ as

$$\mathrm{BR}(K_L^0 \to \pi^0 \nu \overline{\nu}) = \frac{\mathcal{A}_{ij}\mathcal{A}_{ij}^*}{8|(V_{CKM})_{us}|^2 G_F^2} \times \frac{\tau(K_L^0)}{\tau(K^+)} \times r_{K_L^0} \times \mathrm{BR}(K^+ \to \pi^0 e^+ \nu), \tag{4.47}$$

where $\mathcal{A}_{ij}$ is defined as

$$\mathcal{A}_{ij} \equiv \frac{1}{\sqrt{2}} \left\{ \delta_{ij}(C_{\mathrm{SM}} - C_{\mathrm{SM}}^*) + (C_L^\nu)_{ij} - (C_L^\nu)_{ji}^* \right\}, \tag{4.48}$$

$\tau(K_L^0)$ and $\tau(K^+)$ are the lifetime of K_L^0 and K^+ and $r_{K_L^0}$ is the isospin breaking effect which is estimated as $r_{K_L^0} \simeq 0.955$ according to Ref. [121]. Note that the SM prediction is $\mathrm{BR}(K_L^0 \to \pi^0\nu\overline{\nu}) = 2.43(39)(6) \times 10^{-11}$ [122].

Since $K_L^0 \to \pi^0 \nu \overline{\nu}$ is the CP-violating process, the decay depends on the imaginary part of the tree-level FCNCs. It is expected that the Z' contribution to $K^+ \to \pi^0 e^+ \nu$ is small in this model. Therefore, we use the well measured experimental value for $\mathrm{BR}(K^+ \to \pi^0 e^+ \nu)$ as the input parameter. Note that the contribution from penguin diagram in C_{SM} is also modified by $\cos^2\theta$ defined in Eq. (4.28) (or Eq. (4.29)), but we ignore such

[6] One can see the current status of the calculations in Ref. [120].

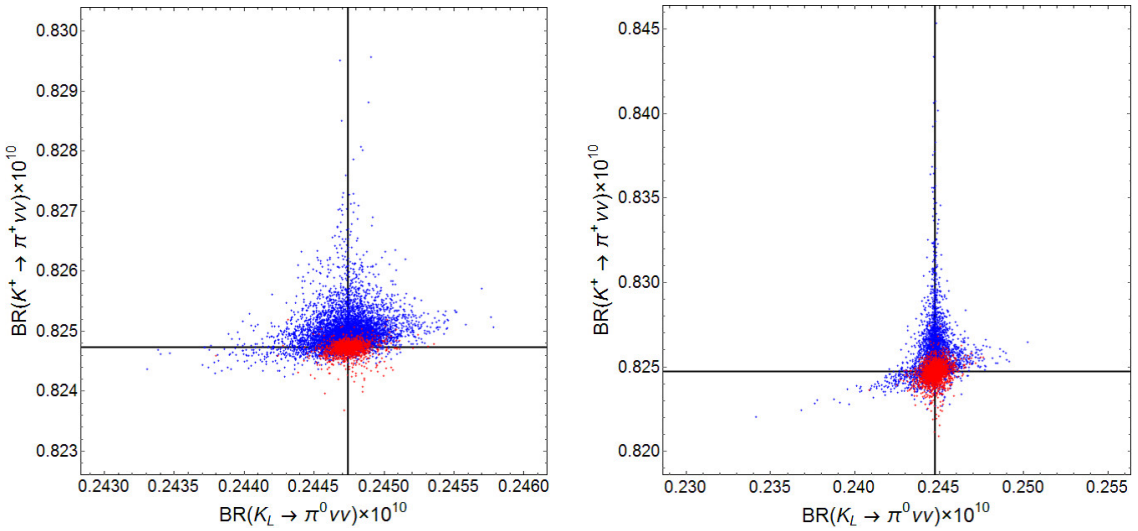

Figure 8: Our predictions for $\mathrm{BR}(K_L^0 \to \pi^0 \nu\overline{\nu})$ and $\mathrm{BR}(K^+ \to \pi^+ \nu\overline{\nu})$ with $\Lambda_{Z'} = 1400$ TeV (left) and $\Lambda_{Z'} = 500$ TeV (right) [28]. The coefficients of higher-dimensional operators satisfy $|\epsilon\, c_{ij}^d| < 10^{-2}$ (red) and $|\epsilon\, c_{ij}^d| < 10^{-3}$ (blue). Black solid lines show each SM prediction. The all points satisfy $|\delta\epsilon_K| \leq 0.3$.

a contribution because this modification is for the contribution of the one loop diagram and $\cos^2\theta \simeq 1$ in the limit $M_{Z'} \gg M_Z$.

Similar to $\mathrm{BR}(K_L^0 \to \pi^0 \nu\overline{\nu})$, the branching ratio of $K^+ \to \pi^+ \nu, \overline{\nu}$ can be estimated as

$$\mathrm{BR}(K^+ \to \pi^+ \nu\overline{\nu}) = \frac{\mathcal{A}_{ij}^+ \mathcal{A}_{ij}^{+*}}{8|(V_{CKM})_{us}|^2 G_F^2} \times r_{K^+} \times \mathrm{BR}(K^+ \to \pi^0 e^+ \nu), \tag{4.49}$$

where $\mathcal{A}_{ij}^+$ is given by

$$\mathcal{A}_{ij}^+ = \sqrt{2}\left\{\delta_{ij} C_{\mathrm{SM}} + (C_L^\nu)_{ij}\right\}. \tag{4.50}$$

The isospin breaking effect, r_{K^+}, is estimated as $r_{K^+} \simeq 0.978$ [121]. Note that the SM prediction is $\mathrm{BR}(K^+ \to \pi^+ \nu\overline{\nu}) = 7.81(75)(29) \times 10^{-11}$ [122].

Figure 8 shows our predictions of $\mathrm{BR}(K_L^0 \to \pi^0 \nu\overline{\nu})$ and $\mathrm{BR}(K^+ \to \pi^+ \nu\overline{\nu})$. We show the points which satisfy $|\delta\epsilon_K| \leq 0.3$. Black solid lines show the SM predictions, calculating from the central values in Table 5. One can see that $\mathrm{BR}(K^+ \to \pi^+ \nu\overline{\nu})$ tends to be larger than the SM prediction, while $\mathrm{BR}(K_L^0 \to \pi^0 \nu\overline{\nu})$ becomes both larger and smaller than the SM prediction. These tendencies are caused by the property of the flavor-violating coupling A_{sd}^d. The deviations of $\mathrm{BR}(K^+ \to \pi^+ \nu\overline{\nu})$ and $\mathrm{BR}(K_L^0 \to \pi^0 \nu\overline{\nu})$ are roughly proportional to $\mathrm{Re}(C_{SM} A_{sd}^d) \sim \mathrm{Re}(C_{SM})\mathrm{Re}(A_{sd}^d)$ and $\mathrm{Im}(C_{SM})\mathrm{Im}(A_{sd}^d)$, respectively. From Fig. 4, therefore, the deviations in Fig. 8 can be understood. In any case, the predictions do not largely depart from the SM prediction, as far as $\Lambda_{Z'} = 1400$ TeV. Even if $\Lambda_{Z'}$ is around 500 TeV, the deviation is at most 10 %, compared to the SM prediction.

$K_L^0 \to \ell_i\,\ell_j$ and $K_L^0 \to \pi^0\,\ell_i\,\ell_j$

The leptonic decays of K_L^0 are also induced by the Z' contribution and may be important in this model. There is a large long-distance contribution in the decay width of $K_L^0 \to \mu^+\mu^-$. By extracting the short-distance part, the new physics constraint from $K_L^0 \to \mu^+\mu^-$ is proposed in Ref. [123]: $\mathrm{BR}(K_L^0 \to \mu^+\mu^-) < 2.5 \times 10^{-9}$. In this model, it is predicted that there is extra contribution in the branching ratio of $K_L^0 \to \mu^+\mu^-$, which is described by $(C^l_{L,\,R})_{\mu\mu}$ defined in Eq. (4.40). We can estimate the deviation of this decay mode by following Refs. [110, 124, 125], although the prediction of this model cannot be largely depart from that of the SM as far as $\Lambda_{Z'} = \mathcal{O}(10^3)$. As a result, the ratio of $\mathrm{BR}(K_L^0 \to \mu^+\mu^-)$ between predictions of this model and the SM is estimated as

$$\left| \frac{\mathrm{BR}(K_L^0 \to \mu^+\mu^-)}{\mathrm{BR}(K_L^0 \to \mu^+\mu^-)_{\mathrm{SM}}} - 1 \right| \leq 0.019, \tag{4.51}$$

when $\Lambda_{Z'} = 1400$ TeV. We conclude that in the high-scale SUSY scenario, this model is safe from the bound of this decay mode.

The flavor-violating decay of K_L^0 has been experimentally investigated as well: $K_L^0 \to \mu^+e^- < 4.7 \times 10^{-12}$ [126]. This decay causes at the tree-level in this model, but the prediction cannot be large. By using typical values of A^d_{sd} and $A^l_{\mu e}$, this branching ratio is calculated as

$$\mathrm{BR}(K_L^0 \to \mu^+e^-) \simeq 4.0 \times 10^{-19} \left(\frac{1400\,\mathrm{TeV}}{\Lambda_{Z'}}\right)^4 \left(\frac{\mathrm{Re}(A^d_{sd})}{0.1}\right)^2 \left(\frac{|A^l_{\mu e}|}{0.04}\right)^2, \tag{4.52}$$

which is much below the experimental bound.

For the semi-leptonic decay of K_L^0, such as $K_L^0 \to \pi^0\,\overline{\ell}_i\,\ell_j$, the current experimental upper bounds are [127, 128]

$$\mathrm{BR}(K_L^0 \to \pi^0 e^+e^-) < 2.8 \times 10^{-10}, \tag{4.53}$$

$$\mathrm{BR}(K_L^0 \to \pi^0 \mu^+\mu^-) < 3.8 \times 10^{-10}, \tag{4.54}$$

which are about 10 times bigger than the SM predictions [129]. Therefore, large new physics effects are still allowed in these decay modes and we expect that these may be relevant to this model. However, similar to the case of $K_L^0 \to \mu^+\mu^-$, $\mathrm{BR}(K_L^0 \to \pi^0\,\overline{\ell}\,\ell)$ is dominated by SM contribution when $\Lambda_{Z'} = \mathcal{O}(10^3)$ TeV. Therefore, predictions of these modes are also below the experimental bounds.

There is also experimental constraint of the LFV decay of K_L^0, e.g. $K_L^0 \to \pi^0 e^\mp \mu^\pm$. The current bound is [130]

$$\mathrm{BR}(K_L^0 \to \pi^0 e^\mp \mu^\pm) < 7.6 \times 10^{-11}. \tag{4.55}$$

In this mode, $\mathrm{BR}(K_L^0 \to \pi^0 e^- \mu^+)$ is estimated by typical values of A_{sd}^d and $A_{\mu e}^l$ as

$$\mathrm{BR}(K_L^0 \to \pi^0 e^- \mu^+) \simeq 2.0 \times 10^{-20} \left(\frac{1400\,\mathrm{TeV}}{\Lambda_{Z'}}\right)^4 \left(\frac{\mathrm{Im}(A_{sd}^d)}{0.1}\right)^2 \left(\frac{|A_{\mu e}^l|}{0.04}\right)^2. \tag{4.56}$$

Thus, we conclude that this model is also safe and cannot be tested in this decay mode unless $\Lambda_{Z'}$ is smaller than $\mathcal{O}(10)$ TeV.

- $B^0 \to \mu^+\mu^-$ and $B_s^0 \to \mu^+\mu^-$

As we mentioned in Sec. 4.1.2, the flavor-violating Z' couplings involving the third generation, especially A_{bs}^d, become large. Therefore, this model would be constrained by the rare B decay and we expect that we can obtain some specific predictions to this model.

$B_s^0 \to \mu^+\mu^-$ and $B^0 \to \mu^+\mu^-$ have been measured at the LHC, although the errors are large: $\mathrm{BR}(B_s^0 \to \mu^+\mu^-) = 2.8^{+0.7}_{-0.6} \times 10^{-9}$ and $\mathrm{BR}(B_d^0 \to \mu^+\mu^-) = 3.9^{+1.5}_{-1.4} \times 10^{-10}$ [131]. The SM predictions are almost consistent with the experimental results as $\mathrm{BR}(B_s \to \mu^+\mu^-) = (3.66 \pm 0.23) \times 10^{-9}$ and $\mathrm{BR}(B \to \mu^+\mu^-) = (1.06 \pm 0.09) \times 10^{-10}$ [132]. In this model, the deviation of these leptonic decays from the SM predictions are estimated as [110]

$$\frac{\mathrm{BR}(B_s^0 \to \mu^+\mu^-)}{\mathrm{BR}(B_s^0 \to \mu^+\mu^-)_{\mathrm{SM}}} = \left| 1 - \frac{(C_L^{l\,B_s})_{\mu\mu}}{g_{SM}^2 \eta_Y Y_0(x_t)(V_{\mathrm{CKM}})_{tb}^*(V_{\mathrm{CKM}})_{ts}} \right|^2, \tag{4.57}$$

where $g_{SM}^2 = \sqrt{2} G_F \alpha/(\pi \sin^2\theta_W)$ and $\eta_Y = 1.012$ [115]. $(C_L^{l\,B})_{\mu\mu}$ is given by replacing A_{sd}^d with A_{bs}^d in $(C_L^l)_{\mu\mu}$. $\mathrm{BR}(B \to \mu^+\mu^-)$ is estimated in a similar expression to Eq. (4.57) by replacing A_{bs}^d and $(V_{\mathrm{CKM}})_{ts}$ to A_{bd}^d and $(V_{\mathrm{CKM}})_{td}$. Note that, as we can see in Eq. (4.41), $(C_L^{l\,B_s})_{\mu\mu}$ is also dependent on $A_{\mu\mu}^l$.

Figure 9 shows our predictions for the deviation of $\mathrm{BR}(B_s^0 \to \mu^+\mu^-)$ and $\mathrm{BR}(B^0 \to \mu^+\mu^-)$ in the each case with $\Lambda_{Z'} = 1400$ TeV (left) and $\Lambda_{Z'} = 500$ TeV (right). Because of the difference between the size of A_{bs}^d and A_{bd}^d, the deviation of $\mathrm{BR}(B_s \to \mu^+\mu^-)$ is slightly larger than that of $\mathrm{BR}(B \to \mu^+\mu^-)$. However, its deviation is at most a few % even when $\Lambda_{Z'} = 500$ TeV.

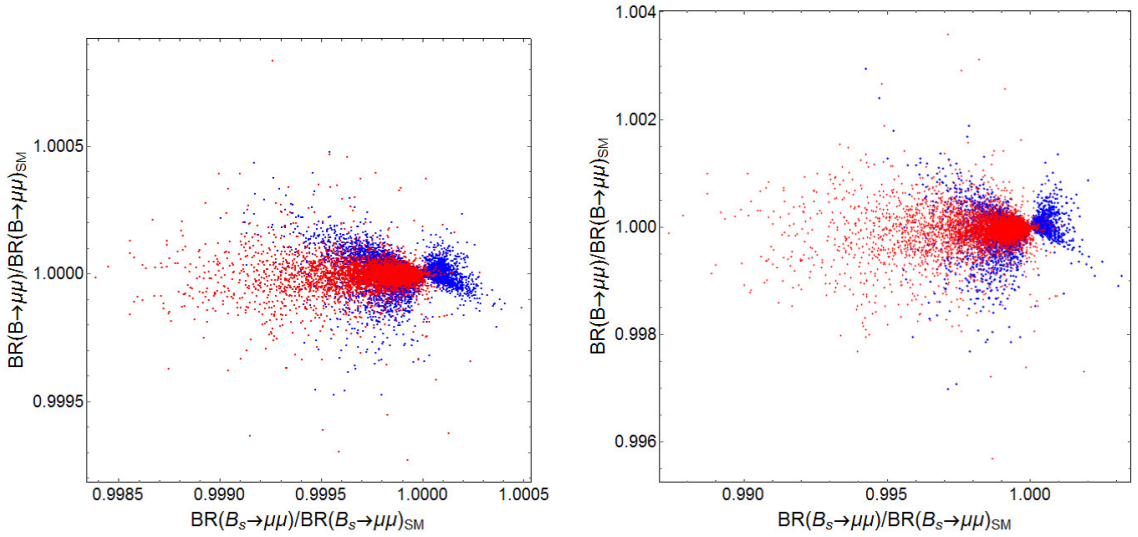

Figure 9: Our predictions for the deviation of $\mathrm{BR}(B_s^0 \to \mu^+\mu^-)$ and $\mathrm{BR}(B^0 \to \mu^+\mu^-)$ with $\Lambda_{Z'} = 1400$ TeV (left) and $\Lambda_{Z'} = 500$ TeV (right) [28]. The coefficients of higher-dimensional operators satisfy $|\epsilon\, c_{ij}^d| < 10^{-2}$ (red) and $|\epsilon\, c_{ij}^d| < 10^{-3}$ (blue). In these figures, the constraint, $|\delta\epsilon_K| \leq 0.3$, is assigned.

4.2.3 Flavor-violating processes in μ decay

There are also the Z' interactions which induce the LFV decays. It depends on the coefficients of higher-dimensional operators c_{ij}^ℓ, its couplings could be $\mathcal{O}(1)$. Therefore, in addition to $\Delta F = 1, 2$ processes, the LFV processes are important in this model. In this thesis, we focus on $\mu \to 3\,e$ and μ-e conversion which are induced at the tree-level. Note that $\mu \to e\,\gamma$ is one of the important processes for the new physics model, but it is suppressed in this model due to the largeness of the Z' mass and loop suppression.

$\underline{\mu \to 3\,e}$

We will begin with the discussion of $\mu \to 3\,e$. This process is induced by the following four-Fermi interactions:

$$\mathcal{H}^{\mu\to 3\,e} = C_L^{3\,e}(\overline{e_L}\gamma_\mu\mu_L)(\overline{e_L}\gamma^\mu e_L) + C_R^{3\,e}(\overline{e_L}\gamma_\mu\mu_L)(\overline{e_R}\gamma^\mu e_R), \tag{4.58}$$

where the coefficients are given by

$$C_L^{3\,e} = A_{e\mu}^l \left\{ \frac{A_{ee}^l}{\Lambda_{Z'}^2} - \frac{\cos 2\theta_W}{2}\frac{1}{\Lambda_Z^2} \right\}, \tag{4.59}$$

$$C_R^{3\,e} = A_{e\mu}^l \left\{ \frac{1}{\Lambda_{Z'}^2} + \sin^2\theta_W \frac{1}{\Lambda_Z^2} \right\}. \tag{4.60}$$

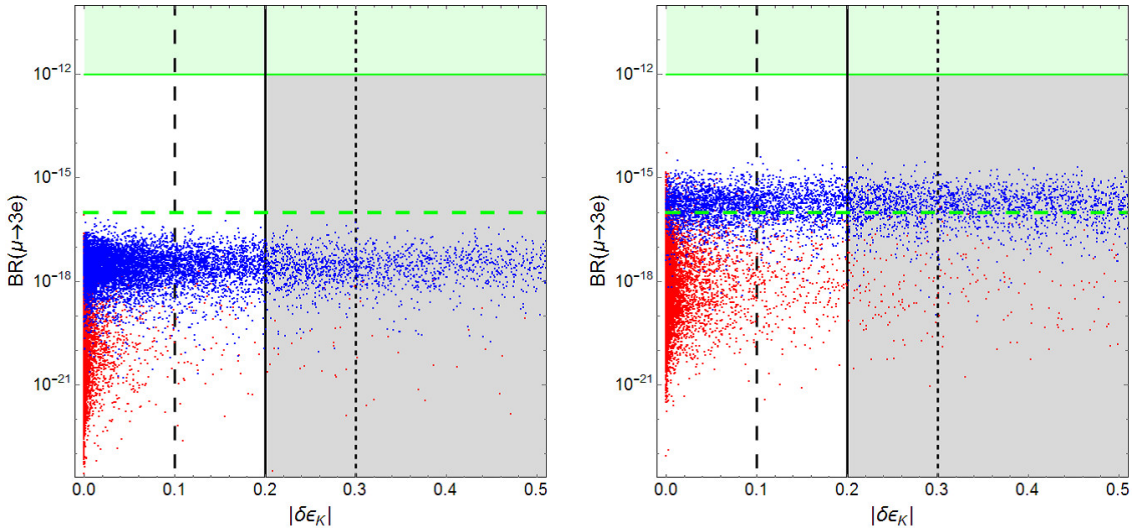

Figure 10: Our predictions for the deviation of $\mathrm{BR}(\mu \to 3\,e)$ with $\Lambda_{Z'} = 1400$ TeV (left) and $\Lambda_{Z'} = 500$ TeV (right) [28]. The coefficients of higher-dimensional operators satisfy $|\epsilon\, c^{\ell}_{ij}| < 10^{-2}$ (red) and $|\epsilon\, c^{\ell}_{ij}| < 10^{-3}$ (blue). The green region is excluded by the SINDRUM experiment [133] and the green dashed line is the future prospected bound [134].

By using these coefficients, one can evaluate the branching ratio of $\mu \to 3\,e$ as

$$\mathrm{BR}(\mu \to 3\,e) = \frac{m_\mu^5}{1536\,\pi^3\,\Gamma_\mu}\left(2\left|C_L^{3e}\right|^2 + \left|C_R^{3e}\right|^2\right) \tag{4.61}$$

$$\simeq 5.8 \times 10^{-18}\left(\frac{1400\,\mathrm{TeV}}{\Lambda_{Z'}}\right)^4\left(\frac{|A^l_{\mu e}|}{0.04}\right)^2, \tag{4.62}$$

where m_μ and Γ_μ are mass and total decay width for μ, respectively. We show the typical value of $\mathrm{BR}(\mu \to 3\,e)$ in Eq. (4.62). Note that the Z' contribution to $\mu \to e\,\nu\,\overline{\nu}$ are ignored here.

$\mu \to 3\,e$ has been investigated at the SINDRUM experiment: $\mathrm{BR}(\mu \to 3\,e) < 1.0 \times 10^{-12}$ [133]. This bound will be improved at the level of $\mathcal{O}(10^{-16})$ [134]. We show the results of this model in Fig. 10, with the correlation with $\delta(\epsilon_K)$. In the left (right) panel of Fig. 10, we take $\Lambda_{Z'} = 1400$ (500) TeV. The green region is excluded by the SINDRUM experiment [133], and the green dashed line corresponds to the expected upper bound in the Mu3e experiment [134]. From these results, we find that $\mathrm{BR}(\mu \to 3\,e) < 10^{-15}$ as far as $\Lambda_{Z'} > 500$ TeV. In the case of $\Lambda_{Z'} = 500$ TeV which corresponds to $M_{Z'} \simeq 36$ TeV, $\mathrm{BR}(\mu \to 3\,e)$ can be typically estimated as 3.5×10^{-16} from Eq. (4.62) and becomes larger than the future expected sensitivity. In such a case, $|\delta\epsilon_K|$ is also enhanced by $1/\Lambda^2_{Z'}$ as shown in Fig. 6.

μ-e conversion

Next, we focus on the μ-e conversions in nuclei. In this thesis, we assume that the coherent conversion in which the nuclei in the final state is the same as one in the initial state is dominant and therefore, we concentrate on the contributions derived from the operators,

$$\mathcal{H}^{\mu\text{-}e} = C_q^{\mu\text{-}e}(\bar{q}\gamma_\mu q)(\overline{e_L}\gamma^\mu \mu_L), \tag{4.63}$$

where the coefficients are given by

$$C_u^{\mu\text{-}e} = A_{e\mu}^l \left\{ \left(\frac{1}{4} - \frac{2}{3}\sin^2\theta_W \right) \frac{1}{\Lambda_Z^2} \right\}, \tag{4.64}$$

$$C_d^{\mu\text{-}e} = -A_{e\mu}^l \left\{ \frac{A_{dd}^d + 1}{2\Lambda_{Z'}^2} + \left(\frac{1}{4} - \frac{1}{3}\sin^2\theta_W \right) \frac{1}{\Lambda_Z^2} \right\}. \tag{4.65}$$

The conversion rate of muon, denoted as $\omega_{\rm conv}$, is

$$\omega_{\rm conv} = 4m_\mu^5 \left| (2C_u^{\mu\text{-}e} + C_d^{\mu\text{-}e})\, V^{(p)} + (C_u^{\mu\text{-}e} + 2C_d^{\mu\text{-}e})\, V^{(n)} \right|^2, \tag{4.66}$$

where $V^{(p)}$ and $V^{(n)}$ are overlap integrals which depend on the nucleus species. The branching ratio of the μ-e conversion is

$$\begin{aligned} {\rm BR}(\mu\, N \to e\, N) &= \frac{\omega_{\rm conv}}{\omega_{\rm capt}} \\ &\simeq 4.0 \times 10^{-17}\, (1.4 \times 10^{-17}) \left(\frac{1400\,{\rm TeV}}{\Lambda_{Z'}} \right)^4 \left(\frac{|A_{\mu e}^l|}{0.04} \right)^2, \end{aligned} \tag{4.67}$$

where $\omega_{\rm capt}$ is the muon capture rate. $V^{(p)}$ and $V^{(n)}$ and $\omega_{\rm capt}$ have been calculated in Ref. [135] for the each nucleus species. In Eq. (4.67), we show the typical value of ${\rm BR}(\mu\,{\rm Au} \to e\,{\rm Au})$ (${\rm BR}(\mu\,{\rm Al} \to e\,{\rm Al})$).

Figure 11 shows the results of this model and correlations on $\delta\epsilon_K$ and the μ-e conversions. The green region is excluded by the SINDRUM experiment, ${\rm BR}(\mu\,{\rm Au} \to e\,{\rm Au}) < 7 \times 10^{-13}$ [136]. The green dashed lines are the future prospects of the COMET experiment for ${\rm BR}(\mu\,{\rm Al} \to e\,{\rm Al})$: $< 7.2 \times 10^{-15}$ (phase-I) and $< 2.6 \times 10^{-17}$ (phase-II) [137, 138]. It is clear that ${\rm BR}(\mu\,{\rm Au} \to e\,{\rm Au})$ is much smaller than the current bound. There is no constraint for ${\rm BR}(\mu\,{\rm Al} \to e\,{\rm Al})$ which is slightly smaller than ${\rm BR}(\mu\,{\rm Au} \to e\,{\rm Au})$, but there is possibility to reach the future sensitivity, depending on $\Lambda_{Z'}$ and suppression factor ϵ introduced in Eqs. (4.10) and (4.11).

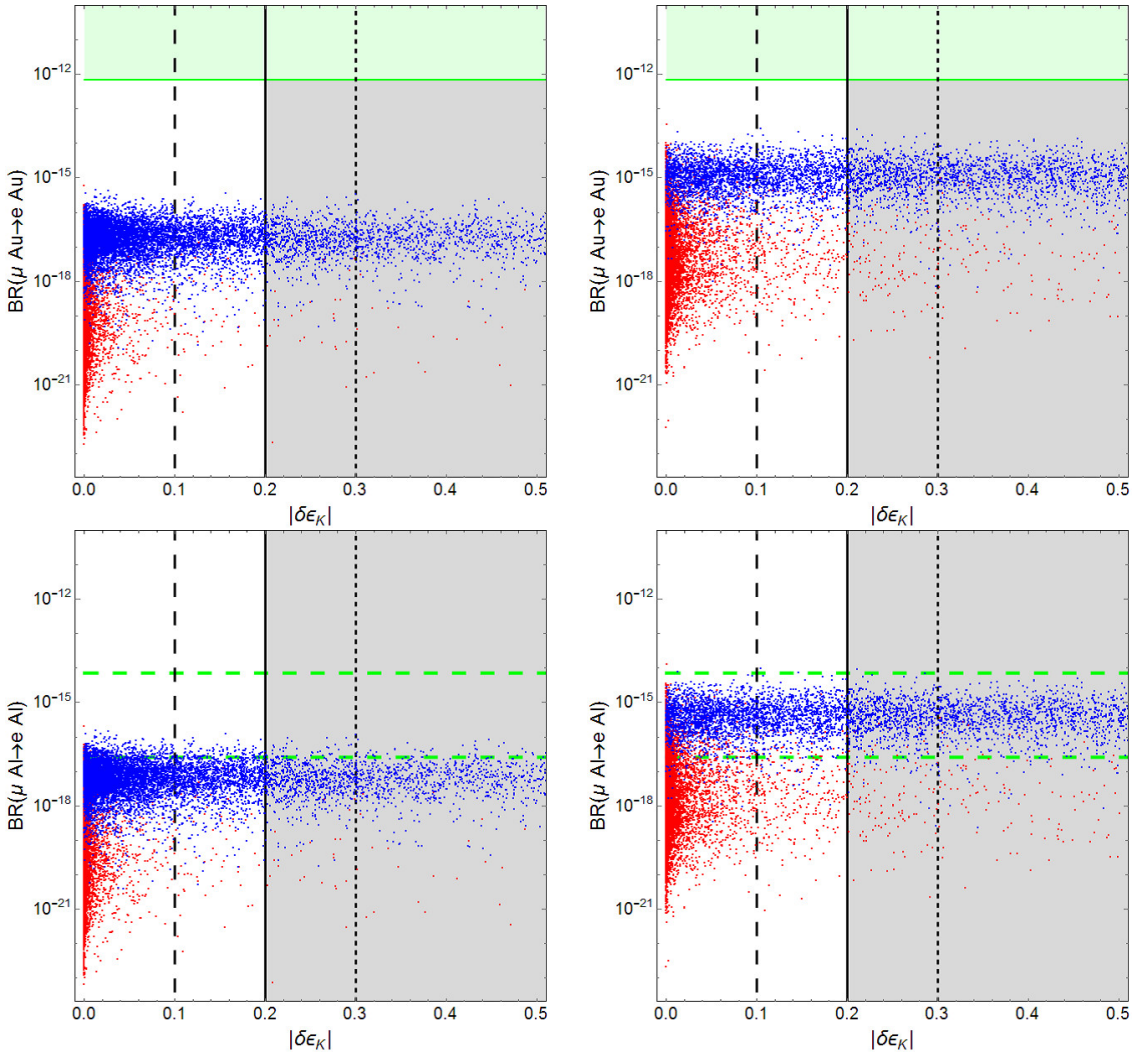

Figure 11: Our predictions for BR($\mu\,\mathrm{Au} \to e\,\mathrm{Au}$) (upper panels) and BR($\mu\,\mathrm{Al} \to e\,\mathrm{Al}$) (lower panels) [28]. We set $\Lambda_{Z'} = 1400$ TeV in left two panels and $\Lambda_{Z'} = 500$ TeV in right two panels. The coefficients of higher-dimensional operators satisfy $|\epsilon\, c_{ij}^{d,\ell}| < 10^{-2}$ (red) and $|\epsilon\, c_{ij}^{d,\ell}| < 10^{-3}$ (blue). In the upper panels, green region shows the experimental bound [136]. In the lower panels, two green dashed lines show future sensitivity from COMET-I (upper one) and COMET-II (lower one) experiment [137, 138].

4.2.4 Contributions to LFV τ decays

Finally, we discuss LFV τ decays, especially $\tau \to \ell_i\, \ell_j\, \bar{\ell}_k$ and $\tau \to \ell\, \pi^0$, $\ell\, K_S^0$, although the current constraints for these modes is still weak.

$\underline{\tau \to \ell_i\, \ell_j\, \bar{\ell}_k}$

Similar to $\mu \to 3\, e$, $\tau \to \ell_i\, \ell_j\, \bar{\ell}_k$ is caused by the following 4-Fermi interactions:

$$\mathcal{H}^{\tau \to 3\,\ell} = C_{L\ ijk}^{3\,\ell}(\overline{\ell_{Li}}\gamma_\mu \tau_L)(\overline{\ell_{Lj}}\gamma^\mu \ell_{Lk}) + C_{R\ ijk}^{3\,\ell}(\overline{\ell_{Li}}\gamma_\mu \tau_L)(\overline{\ell_{Rj}}\gamma^\mu \ell_{Rk}), \tag{4.68}$$

where the coefficients are given by

$$C_{L\ ijk}^{3\,\ell} = A_{i\tau}^{\ell}\left\{\frac{A_{jk}^{\ell}}{\Lambda_{Z'}^2} - \frac{\cos 2\theta_W}{2}\frac{\delta_{jk}}{\Lambda_Z^2}\right\}, \tag{4.69}$$

$$C_{R\ ijk}^{3\,\ell} = A_{i\tau}^{\ell}\delta_{jk}\left\{\frac{1}{\Lambda_{Z'}^2} + \sin^2\theta_W \frac{1}{\Lambda_Z^2}\right\}. \tag{4.70}$$

There are six modes in LFV τ decays. The branching ratio for the decay modes $\tau \to e^-\,\mu^+\,\mu^-$ and $\tau \to \mu^-\,e^+\,e^-$ is described as [139]

$$\mathrm{BR}(\tau \to \ell_i\, \ell_j\, \bar{\ell}_k) = \frac{m_\tau^5}{1536\,\pi^3\,\Gamma_\tau}\left(\left|C_{L\ ijk}^{3\,\ell} + C_{L\ jik}^{3\,\ell}\right|^2 + \left|C_{R\ ijk}^{3\,\ell}\right|^2 + \left|C_{R\ jik}^{3\,\ell}\right|^2\right). \tag{4.71}$$

For the other case, the branching ratio is obtained by changing $m_\mu \to m_\tau$, $\Gamma_\mu \to \Gamma_\tau$ and $C_{L,R}^{3e} \to C_{L,R_{ijk}}^{3l}$ in Eq. (4.61). We summarize the typical values of these branching ratios in Table 6 with the current experimental bounds [17, 140]. It is obvious that the predictions of this model are extremely smaller than the current experimental bounds. Even if one takes $\Lambda_{Z'} = 500$ TeV, the enhancement is only $(1400/500)^4 \simeq 61.5$. Therefore, this model is completely safe in these decay modes.

$\underline{\tau \to \ell\,\pi^0,\ \ell\,K_S^0}$

Next, we discuss the decays of $\tau \to \ell\,\pi^0$ and $\tau \to \ell\,K_S^0$. This type of decay is induced by the following interactions:

$$\mathcal{H}^{\tau \to \ell\, P^0} = C_{L\,ijk}^{\ell\,P^0}(\overline{\ell_{Li}}\gamma_\mu \tau_L)(\overline{q_{Lj}}\gamma^\mu q_{Lk}) + C_{R\,ijk}^{\ell\,P^0}(\overline{\ell_{Li}}\gamma_\mu \tau_L)(\overline{q_{Rj}}\gamma^\mu q_{Rk}), \tag{4.72}$$

where $P^0 = \pi^0, K_S^0$ and the coefficients are similar to Eq. (4.41):

$$C_{I\,ijk}^{\ell\,P^0} = A_{i\tau}^{\ell}\left\{\frac{(Q_I^q)_{jk}}{\Lambda_{Z'}^2} + \frac{\delta_{jk}}{\Lambda_Z^2}\left(\tau_I^q - Q_e^q \sin^2\theta_W\right)\right\}. \tag{4.73}$$

τ decay mode	value of BR	exp. bound ($\times 10^{-8}$) [17, 140]
$e^-e^+e^-$	1.2×10^{-18}	< 2.7
$e^-\mu^+\mu^-$	4.2×10^{-19}	< 2.7
$e^+\mu^-\mu^-$	1.5×10^{-18}	< 1.7
$\mu^-e^+e^-$	3.7×10^{-15}	< 1.8
$\mu^+e^-e^-$	2.8×10^{-22}	< 1.5
$\mu^-\mu^+\mu^-$	2.7×10^{-15}	< 2.1
$e^-\pi^0$	2.2×10^{-19}	< 8.0
$\mu^-\pi^0$	1.2×10^{-15}	< 11
$e^-K_s^0$	1.2×10^{-21}	< 2.6
$\mu^-K_s^0$	6.6×10^{-18}	< 2.3

Table 6: The typical values of each τ decay mode. In this table, we use $\Lambda_{Z'} = 1400$ TeV and typical values of A^d_{ij} and A^l_{ij}.

The branching ratios of $\tau \to \ell_i \pi^0$ and $\tau \to \ell_i K^0_s$ can be described by $C^{\ell P^0}_{I ijk}$ as [139]

$$\mathrm{BR}(\tau \to \ell_i \pi^0) = \frac{\mathrm{BR}(\tau \to \nu_\tau \pi^-)}{16\,|(V_{CKM})_{ud}|^2 G_F^2} \times \left(|C^{\ell P^0}_{L iuu} - C^{\ell P^0}_{R iuu} - C^{\ell P^0}_{L idd} + C^{\ell P^0}_{R idd}|^2 \right), \tag{4.74}$$

$$\mathrm{BR}(\tau \to \ell_i K^0_S) = \frac{\mathrm{BR}(\tau \to \nu_\tau K^-)}{16\,|(V_{CKM})_{us}|^2 G_F^2} \times \left(|C^{\ell P^0}_{R isd} - C^{\ell P^0}_{R ids}|^2 \right). \tag{4.75}$$

For the discussion of the predictions of this model, we use $\mathrm{BR}(\tau \to \nu_\tau \pi^-) = 0.1083$ and $\mathrm{BR}(\tau \to \nu_\tau K^-) = 0.007$ [17].

The results are shown in Table 6 as typical values of the branching ratios. The current experimental bounds [17] are also summarized in Table 6. As expected from the results of $\tau \to \ell_i \ell_j \bar{\ell}_k$, these decay modes are also smaller than the experimental bounds. Note that $\mathrm{BR}(\tau \to \ell_i P^0)$ is proportional to $|A^l_{i\tau}|^2$ because of Eqs. (4.73), (4.74) and (4.75). Therefore, $\mathrm{BR}(\tau \to \mu P^0)$ becomes larger than $\mathrm{BR}(\tau \to e P^0)$ in this model since roughly speaking, $|A^\ell_{e\tau}| < |A^\ell_{\mu\tau}|$.

4.3 Summary of the section

In this section, we studied the realistic $SO(10)$ SUSY GUT model in which the realistic Yukawa couplings are obtained by the mixing of the matter fields caused by introducing the extra matter fields, $\mathbf{10}_i$ of $SO(10)$. In this model, the flavor-violating Z' couplings are generated after the $U(1)'$ symmetry breaking. These couplings can be $\mathcal{O}(1)$ and cause the flavor-violating processes at the tree-level. Therefore, the flavor-violating processes

induced by Z' are important for this model even if $M_{Z'}$ is around 100 TeV. Moreover, since only $\bar{\mathbf{5}}$ fields of $SU(5)$ have the flavor-violating Z' couplings $A^{d,\ell}_{ij}$, we can expect that there are some specific predictions of this model. One of the important features of $A^{d,\ell}_{ij}$ is $A^{d,\ell}_{ij} \propto m^{d,\ell}_i m^{d,\ell}_j$, so that $(b,\, s)$ and $(\mu,\, \tau)$ elements tends to be larger than the other elements.

As a result, we found that ϵ_K is the most sensitive to this model even if $M_{Z'} = 100$ TeV. On the other hand, the mass differences of neutral meson are almost dominated by the SM prediction. When $M_{Z'} = \mathcal{O}(10)$ TeV, the deviation of ΔM_{B_s} from the SM prediction can reach 10 %, while those of ΔM_K and ΔM_B are $\mathcal{O}(1)$ %. In addition, ΔM_K and ΔM_{B_s} tend to depart from the SM prediction in the positive direction. These features are due to the predictions of A^d_{ij}.

The other important predictions are obtained from the LFV μ decays, although these predictions are much smaller than the current bounds. Since it is expected that these bounds are improved near future, this model could be tested in some experiments, e.g. the COMET and Mu2e experiments. As shown in Figs. 10 and 11, this model predicts that $\mathrm{BR}(\mu \to 3\, e)$ and $\mathrm{BR}(\mu\, \mathrm{Al} \to e\, \mathrm{Al})$ can reach the future experimental prospects without conflict with ϵ_K, when $M_{Z'}$ is $\mathcal{O}(10$ - $100)$ TeV. Now, other future experiments for μ-e conversion are planned [141–143]. If their sensitivities reach $\mathcal{O}(10^{-15})$ level, we can test our model.

In this section, we consider that the Z' scale is $\mathcal{O}(100)$ TeV to realize the 125 GeV Higgs mass in the high-scale SUSY scenario by assuming that the $U(1)'$ symmetry is broken around the SUSY scale. Important point is that although such a high scale cannot reach even at the LHC, this model can be tested indirectly by using the observables in the flavor physics.

5 D-term contributions in $E_6 \times SU(2)_F \times U(1)_A$ SUSY GUT

In this section, we introduce an E_6 SUSY GUT model with $SU(2)_F$ family symmetry and anomalous $U(1)_A$ gauge symmetry. This GUT model is based on a natural assumption in which all the interactions allowed by the symmetries are introduced. This model can solve almost all the problems which are caused in the SUSY GUT models, e.g. SUSY FCNC, SUSY CP, μ-problem and DTS problem.

5.1 $SU(2)_F$ family and anomalous $U(1)_A$ gauge symmetries

First of all, we will shortly introduce some features of $SU(2)_F$ family and anomalous $U(1)_A$ gauge symmetries. Under $SU(2)_F$ family symmetry, the first two generations are doublet, while the third generation is $SU(2)_F$ singlet. Therefore, soft SUSY-breaking mass terms for sfermions can be written as $m_0^2|\Psi_a|^2 + m_3^2|\Psi_3|^2$, where Ψ_a (Ψ_3) is E_6 fundamental and $SU(2)_F$ doublet (singlet) field. Therefore, in this model, there are mainly 2 mass parameters for sfermion masses. Because of Eq. (3.53), the sfermion mass matrix for light modes becomes

$$\tilde{m}^2_{10} = \begin{pmatrix} m_0^2 & & \\ & m_0^2 & \\ & & m_3^2 \end{pmatrix}, \quad \tilde{m}^2_{\bar{5}^0} = \begin{pmatrix} m_0^2 & & \\ & m_0^2 & \\ & & m_0^2 \end{pmatrix}. \tag{5.1}$$

Therefore, the MUSM is naturally obtained in a $E_6 \times SU(2)_F$ GUT. Note that the degeneracy of the MUSM is destroyed by the effects of the symmetry breaking. We will discuss these effects for this model later.

The anomalous $U(1)_A$ is a gauge symmetry whose anomalies are canceled by the Green-Schwarz mechanism [144]. In this framework, the Fayet-Iliopoulos term denoted as ξ^2 are introduced in the theory and its magnitude is assumed as $\xi = \lambda\Lambda$, where Λ is cutoff scale. Hereafter, we set $\Lambda = 1$. Let us consider the theory with gauge symmetry $G_{\rm other} \times U(1)_A$. A system consisting all the interactions which are allowed by $G_{\rm other} \times U(1)_A$ has a SUSY vacuum where all negatively charged fields get VEVs as follow:

$$\begin{cases} \langle Z_i^+ \rangle = 0 & (z_i^+ > 0) \\ \langle Z_i^- \rangle = \lambda^{-z_i^-} & (z_i^- < 0) \end{cases} \tag{5.2}$$

Note that $Z_i^\pm$ is a singlet under $G_{\rm other}$, while charged under $U(1)_A$ with charge $z_i^\pm$. Therefore, the VEV of Higgs is determined by its $U(1)_A$ charge in the $U(1)_A$ GUT model. The

important point is that all interactions allowed by the symmetry are introduced in the theory, including the non-renormalizable operators.

Note that the VEVs Eq. (5.2) can restrict operators in the superpotential. Usually, we introduce the superfield whose $U(1)_A$ charge is -1 in $U(1)_A$ GUTs. By using this superfield denoted as Θ, superpotential can be written by the following operators

$$\Theta^{x+y+z} XYZ, \tag{5.3}$$

if XYZ is $G_{\rm other}$ invariant. Note that x, y and z are the $U(1)_A$ charges of the superfields X, Y and Z, respectively. As we explained in Sec. 3.1.1, since we cannot use $\Theta^\dagger$ in the superpotential, the operator with $x + y + z < 0$ is forbidden by $U(1)_A$ symmetry. Therefore, we can control interactions by choosing $U(1)_A$ charges. This is called the SUSY-zero mechanism [54–58, 147].

By using these features, the DTS problem can be solved by the Dimopoulos-Wilczek mechanism [145, 146]. In this mechanism, the VEV of adjoint Higgs of $SO(10)$ becomes the following form:

$$\langle \mathbf{45}_A \rangle \sim i\sigma_2 \times \mathrm{diag}(v, v, v, 0, 0). \tag{5.4}$$

In $SO(10)$ GUT, the doublet Higgs is belonging to the vector multiplet, $\mathbf{10}$, with the color-triplet Higgs. Therefore, mass terms for these Higgs fields are obtained by the following terms:

$$W_{\rm mass} = m_H \mathbf{10}_H \mathbf{10}_H + m_{H'} \mathbf{10}'_H \mathbf{10}'_H + m_{HH'} \mathbf{10}_H \mathbf{10}'_H + \mathbf{10}_H \mathbf{45}_A \mathbf{10}'_H. \tag{5.5}$$

Note that we omit the coupling constant for $\mathbf{10}_H \mathbf{45}_A \mathbf{10}'_H$. Here, since the $\mathbf{10}$ couples to the $\mathbf{45}$ anti-symmetrically, we need another vector multiplet, $\mathbf{10}'_H$. If the mass terms $\mathbf{10}_H \mathbf{10}_H$ and $\mathbf{10}_H \mathbf{10}'_H$ are forbidden by the SUSY-zero mechanism and/or other symmetries like a Z_2 parity, the mass matrix for the Higgs fields are obtained as

$$W_{\rm mass} = \begin{pmatrix} \mathbf{5}_H & \mathbf{5}'_H \end{pmatrix} \begin{pmatrix} 0 & \langle \mathbf{45}_A \rangle \\ \langle \mathbf{45}_A \rangle & m_{H'} \end{pmatrix} \begin{pmatrix} \bar{\mathbf{5}}_H \\ \bar{\mathbf{5}}'_H \end{pmatrix}, \tag{5.6}$$

where $\mathbf{10}_H \to \mathbf{5}_H + \bar{\mathbf{5}}_H$ and $\mathbf{10}'_H \to \mathbf{5}'_H + \bar{\mathbf{5}}'_H$ in the $SO(10) \to SU(5)$ notation. Therefore, one pair of the doublets are massless since the VEV of the adjoint Higgs Eq. (5.4) means that $\langle \mathbf{45}_A \rangle = 0$ for the doublet Higgs. On the other hand, the color-triplet Higgs gets mass from $\langle \mathbf{45}_A \rangle$ (and $m_{H'}$), so that heavy color-triplet Higgs and light doublet Higgs can be realized.

If one consider $E_6 \times SU(2)_F \times U(1)_A$ SUSY GUT, spontaneous CP violation is realized.

Let us consider the following superpotential:

$$W_S = \lambda^s S \left[\sum_{n=0}^{n_f} c_n \lambda^{(f+\bar{f})n} (\bar{F}F)^n \right], \tag{5.7}$$

where S is $E_6 \times SU(2)_F$ singlet field with $U(1)_A$ charge $s(> 0)$ and F_a and $\bar{F}^a$ are E_6 singlet and $SU(2)_F$ doublet fields with $U(1)_A$ charge $f(< -1)$ and $\bar{f}(< -1)$. Here, we assume that c_n are real $\mathcal{O}(1)$ coefficients and the theory is originally CP invariant. Thus, we obtain the following condition from the F-flatness condition of Eq. (5.7) with respect to S:

$$\lambda^s \left[c_0 + c_1 \lambda^{f+\bar{f}} \langle \bar{F}F \rangle + \cdots + c_{n_f} \lambda^{n_f(f+\bar{f})} \langle \bar{F}F \rangle^{n_f} \right] = 0 \tag{5.8}$$

Therefore, if $n_f \geq 2$, $\langle \bar{F}F \rangle$ acquires an imaginary part. It leads that CP is spontaneously broken. By using $SU(2)_F$ symmetry and D-flatness condition, each VEV can be written as

$$\langle F_a \rangle \sim \begin{pmatrix} 0 \\ e^{i\rho} \lambda^{-\frac{f+\bar{f}}{2}} \end{pmatrix}, \quad \langle \bar{F}^a \rangle \sim \begin{pmatrix} 0 \\ \lambda^{-\frac{f+\bar{f}}{2}} \end{pmatrix}. \tag{5.9}$$

5.2 Contents of matters and Higgs

Table 7 shows contents of matters and Higgs and their charge assignment in the $E_6 \times SU(2)_F \times U(1)_A$ SUSY GUT model. In this section, we follow the notation in Ref. [148]. Φ

	Ψ_a	Ψ_3	F_a	$\bar{F}^a$	Φ	$\bar{\Phi}$	C	$\bar{C}$	A	Z_3	Θ
E_6	**27**	**27**	**1**	**1**	**27**	$\overline{\mathbf{27}}$	**27**	$\overline{\mathbf{27}}$	**78**	**1**	**1**
$SU(2)_F$	**2**	**1**	**2**	$\bar{\mathbf{2}}$	**1**	**1**	**1**	**1**	**1**	**1**	**1**
$U(1)_A$	4	$\frac{3}{2}$	$-\frac{3}{2}$	$-\frac{5}{2}$	-3	1	-4	-1	$-\frac{1}{2}$	$-\frac{3}{2}$	-1
Z_6	3	3	1	0	0	0	5	0	0	0	0

Table 7: Contents of chiral superfields for matters and Higgs and their charge assignment in the $E_6 \times SU(2)_F \times U(1)_A$ SUSY GUT model. Note that the discrete Z_6 symmetry is imposed in order to prohibit undesired interactions.

and C are Higgs fields which break E_6 into $SO(10)$ and $SO(10)$ into $SU(5)$, respectively. Note that $\bar{\Phi}$ and $\bar{C}$ are introduced to retain the D-flatness conditions. As we explained in Sec. 3.3.2, three **27** fundamental representations of E_6 are introduced as matter fields. The first two generations of matter fields are a doublet under $SU(2)_F$, while the third generation is a $SU(2)_F$ singlet.

In this model, the superpotential for the Yukawa couplings is written as

$$\begin{aligned} W_Y =& (a\Psi_3\Psi_3 + b\Psi_3\bar{F}^a\Psi_a + c\bar{F}^a\Psi_a\bar{F}^b\Psi_b)\Phi + d(\Psi_a, \Phi, \bar{\Phi}, A, Z_3, \Theta) \\ &+ f'\bar{F}^a\Psi_a\epsilon^{bc}F_b\Psi_c C + g'\Psi_3\epsilon^{ab}F_a\Phi_b C, \end{aligned} \tag{5.10}$$

where a, b, c, f' and g' are $\mathcal{O}(1)$ coefficients. $d(\Psi_a, \Phi, \bar{\Phi}, A, Z_3, \Theta)$ is a gauge-invariant function of $\Psi_a, \Phi, \bar{\Phi}, A, Z_3$ and Θ, which contributes to $\Psi_1\Psi_2\Phi$. After developing VEVs like $\langle\Phi\bar{\Phi}\rangle \sim \lambda^2$, $\langle C\bar{C}\rangle \sim \lambda^5$, $\langle A\rangle \sim \lambda^{1/2}$ and Eq. (5.9) for $\langle F\rangle$ and $\langle\bar{F}\rangle$, the Yukawa couplings for up-type quarks, down-type quarks and charged leptons can be obtained as

$$Y_u = \begin{pmatrix} 0 & \frac{1}{3}d_q\lambda^5 & 0 \\ -\frac{1}{3}d_q\lambda^5 & c\lambda^4 & b\lambda^2 \\ 0 & b\lambda^2 & a \end{pmatrix}, \tag{5.11}$$

$$Y_d = \begin{pmatrix} -\left(\frac{(bg-af)^2}{ac-b^2}+g^2\right)\frac{\beta_H}{a}e^{i(2\rho-\delta)}\lambda^6 & -\frac{bg-af}{ac-b^2}\frac{2}{3}d_5\beta_H e^{i(\rho-\delta)}\lambda^{5.5} & \frac{1}{3}d_q\lambda^5 \\ \left(-\frac{d_q}{3}-\frac{bg-af}{ac-b^2}\frac{b\frac{2}{3}d_5}{g}\right)\lambda^5 & \left(f\beta_H e^{i(\rho-\delta)}-\frac{(\frac{2}{3}d_5)^2}{ac-b^2}\frac{ab}{g}e^{-i\rho}\right)\lambda^{4.5} & \frac{cg-bf}{g}\lambda^4 \\ -\frac{bg-af}{ac-b^2}\frac{a\frac{2}{3}d_5}{g}\lambda^3 & \left(g\beta_H e^{i(\rho-\delta)}-\frac{(\frac{2}{3}d_5)^2}{ac-b^2}\frac{a^2}{g}e^{-i\rho}\right)\lambda^{2.5} & \frac{bg-af}{g}\lambda^2 \end{pmatrix}, \tag{5.12}$$

$$Y_e = \begin{pmatrix} -\left(\frac{(bg-af)^2}{ac-b^2}+g^2\right)\frac{\beta_H}{a}e^{i(2\rho-\delta)}\lambda^6 & d_l\lambda^5 & 0 \\ 0 & f\beta_H e^{i(\rho-\delta)}\lambda^{4.5} & g\beta_H e^{i(\rho-\delta)}\lambda^{2.5} \\ -d_l\lambda^5 & \frac{cg-bf}{g}\lambda^4 & \frac{bg-af}{g}\lambda^2 \end{pmatrix}, \tag{5.13}$$

at the GUT scale. Note that $a, b, c, d_5, d_q, d_l, f, g$ and β_H are real $\mathcal{O}(1)$ coefficients, ρ and δ are $\mathcal{O}(1)$ phases and $\lambda \sim 0.22$ is taken to be the Cabibbo angle. Therefore, we have 9 real parameters and 2 CP phases in this model.

5.3 Mass spectrum of sfermions

From the charge assignment in Table 7, the SUSY-breaking potential can be written as

$$\begin{aligned} V_{SB} =& m_0^2|\Psi_a|^2 + m_3^2|\Psi_3|^2 + m_{11}^2|\epsilon^{ab}\Psi_a F_b|^2 + m_{22}^2|\Psi_a\bar{F}^a|^2 \\ &+ (m_{23}^2\Psi_3^\dagger\Psi_a\bar{F}^a + m_{13}^2\lambda^5\Psi_3^\dagger\epsilon^{ab}\Psi_a\bar{F}_b^\dagger + m_{12}^2\lambda^5(\Psi_a\bar{F}^a)^\dagger\epsilon^{bc}\Psi_b\bar{F}_c^\dagger + \text{h.c.}) \\ &+ m^2(\Phi^\dagger\Psi^{a\dagger}\Psi_a\Phi) + (m_{12}'^2\lambda^2\bar{C}|\Psi_a|^2\bar{\Phi}^\dagger + m_{23}'^2\lambda^2\bar{C}\Psi_3^\dagger\Psi_a\bar{F}^a\bar{\Phi}^\dagger + \text{h.c.}), \end{aligned} \tag{5.14}$$

where the terms in the last line give the mass terms between $\bar{\mathbf{5}}$ and $\bar{\mathbf{5}}'$ after developing the VEVs $\langle\Phi\rangle$, $\langle\bar{\Phi}\rangle$, $\langle C\rangle$ and $\langle\bar{C}\rangle$. One can obtain the sfermion mass matrices mainly from

this potential. Another contributions are coming from the D-terms as Eq. (3.4):

$$\Delta\tilde{m}^2_\psi = \sum_a Q_a(\psi) D_a, \tag{5.15}$$

where $Q_a(\psi)$ is the $U(1)$ charge of the field ψ. In this model, there are four types of D-term contributions: D_6 for $U(1)_{V'}$, D_{10} for $U(1)_V$, D_F for $U(1)_F$ and D_A for $U(1)_A$. Here, $U(1)_F$ is the Cartan part of $SU(2)_F$. We summarize the $U(1)$ charges in Table 8. Thus, the sfermion masses for $\mathbf{10}$, $\bar{\mathbf{5}}$ and $\bar{\mathbf{5}}'$ of $SU(5)$ including the D-term contributions

ψ	$\mathbf{10}_1$	$\mathbf{10}_1$	$\mathbf{10}_3$	$\bar{\mathbf{5}}_1$	$\bar{\mathbf{5}}_2$	$\bar{\mathbf{5}}_3$	$\bar{\mathbf{5}}'_1$	$\bar{\mathbf{5}}'_2$	$\bar{\mathbf{5}}'_3$
$U(1)_{V'}$	1	1	1	1	1	1	-2	-2	-2
$U(1)_V$	1	1	1	-3	-3	-3	2	2	2
$U(1)_F$	$\frac{1}{2}$	$-\frac{1}{2}$	0	$\frac{1}{2}$	$-\frac{1}{2}$	0	$\frac{1}{2}$	$-\frac{1}{2}$	0
$U(1)_A$	4	4	$\frac{3}{2}$	4	4	$\frac{3}{2}$	4	4	$\frac{3}{2}$

Table 8: $U(1)$ charges for $\mathbf{10}_i$ and $\bar{\mathbf{5}}^{(\prime)}_i$ fields. These charges can be understood by the decomposition of $\mathbf{27}$ of E_6 (Eq. (3.47)) and Table 7.

are given from Eqs. (5.14) and (5.15) as [68]

$$\begin{aligned}\tilde{m}^2_{10} =& \begin{pmatrix} m_0^2+\lambda^4 m_{11}^2 & \lambda^9 m_{12}^2 & \lambda^7 m_{13}^2 \\ \lambda^9 m_{12}^2 & m_0^2+\lambda^4 m_{22}^2 & \lambda^2 m_{23}^2 \\ \lambda^7 m_{13}^2 & \lambda^2 m_{23}^2 & m_3^2 \end{pmatrix} + D_6 \begin{pmatrix} 1 & & \\ & 1 & \\ & & 1 \end{pmatrix} \\ &+ D_{10} \begin{pmatrix} 1 & & \\ & 1 & \\ & & 1 \end{pmatrix} + D_F \begin{pmatrix} 1 & & \\ & -1 & \\ & & 0 \end{pmatrix} + D_A \begin{pmatrix} 4 & & \\ & 4 & \\ & & \frac{3}{2} \end{pmatrix}, \end{aligned} \tag{5.16}$$

$$\begin{aligned}\tilde{m}^2_{\bar{5}} =& \begin{pmatrix} m_0^2+\lambda^4 m_{11}^2 & \lambda^9 m_{12}^2 & \lambda^7 m_{13}^2 \\ \lambda^9 m_{12}^2 & m_0^2+\lambda^4 m_{22}^2 & \lambda^2 m_{23}^2 \\ \lambda^7 m_{13}^2 & \lambda^2 m_{23}^2 & m_3^2 \end{pmatrix} + D_6 \begin{pmatrix} 1 & & \\ & 1 & \\ & & 1 \end{pmatrix} \\ &+ D_{10} \begin{pmatrix} -3 & & \\ & -3 & \\ & & -3 \end{pmatrix} + D_F \begin{pmatrix} 1 & & \\ & -1 & \\ & & 0 \end{pmatrix} + D_A \begin{pmatrix} 4 & & \\ & 4 & \\ & & \frac{3}{2} \end{pmatrix}, \end{aligned} \tag{5.17}$$

$$\tilde{m}^2_{\bar{5}'} = \begin{pmatrix} m_0^2+\lambda^2 m^2+\lambda^4 m_{11}^2 & \lambda^9 m_{12}^2 & \lambda^7 m_{13}^2 \\ \lambda^9 m_{12}^2 & m_0^2+\lambda^2 m^2+\lambda^4 m_{22}^2 & \lambda^2 m_{23}^2 \\ \lambda^7 m_{13}^2 & \lambda^2 m_{23}^2 & m_3^2 \end{pmatrix} + D_6 \begin{pmatrix} -2 & & \\ & -2 & \\ & & -2 \end{pmatrix}$$

$$+ D_{10} \begin{pmatrix} 2 & & \\ & 2 & \\ & & 2 \end{pmatrix} + D_F \begin{pmatrix} 1 & & \\ & -1 & \\ & & 0 \end{pmatrix} + D_A \begin{pmatrix} 4 & & \\ & 4 & \\ & & \frac{3}{2} \end{pmatrix}, \tag{5.18}$$

where the contribution from $m^2\Phi^\dagger\Psi^{a\dagger}\Psi_a\Phi$ to $|\mathbf{16}_{\Psi_a}|^2$ is included in m_0^2 by redefinition of m_0^2 and we just rewrite $\frac{1}{2}D_F \to D_F$. Because of the mixing of the $\bar{\mathbf{5}}$ fields like $(\bar{\mathbf{5}}_1^0, \bar{\mathbf{5}}_2^0, \bar{\mathbf{5}}_3^0) \sim (\bar{\mathbf{5}}_1, \bar{\mathbf{5}}_1', \bar{\mathbf{5}}_2)$, the sfermion mass matrix for $\bar{\mathbf{5}}_i^0$ becomes

$$\begin{aligned} \tilde{m}^2_{\bar{5}^0} \sim & \begin{pmatrix} m_0^2 + \lambda^4 m_{11}^2 & \lambda^{5.5} m_{12}'^2 & \lambda^9 m_{12}^2 \\ \lambda^{5.5} m_{12}'^2 & m_0^2 + \lambda^2 m^2 + \lambda^4 m_{11}^2 & \lambda^{7.5} m_{23}'^2 \\ \lambda^9 m_{12}^2 & \lambda^{7.5} m_{23}'^2 & m_0^2 + \lambda^4 m_{22}^2 \end{pmatrix} + D_6 \begin{pmatrix} 1 & & \\ & -2 & \\ & & 1 \end{pmatrix} \\ & + D_{10} \begin{pmatrix} -3 & & \\ & 2 & \\ & & -3 \end{pmatrix} + D_F \begin{pmatrix} 1 & & \\ & 1 & \\ & & -1 \end{pmatrix} + D_A \begin{pmatrix} 4 & & \\ & 4 & \\ & & 4 \end{pmatrix}. \end{aligned} \tag{5.19}$$

The sfermion mass matrices Eqs. (5.16) and (5.19) give interesting predictions of $E_6 \times SU(2)_F \times U(1)_A$ GUT. Even though the terms suppressed by the power of λ are dependent on the explicit model, the dominant terms in sfermion mass matrices which are

$$\tilde{m}^2_{10} \sim \begin{pmatrix} m_0^2 & & \\ & m_0^2 & \\ & & m_3^2 \end{pmatrix}, \quad \tilde{m}^2_{\bar{5}^0} \sim \begin{pmatrix} m_0^2 & & \\ & m_0^2 & \\ & & m_0^2 \end{pmatrix}, \tag{5.20}$$

are one of the important signatures of $E_6 \times SU(2)_F$ GUTs. This spectrum is known as a natural SUSY-type sfermion mass spectrum. Note that in general, the natural SUSY-type sfermion mass spectrum suffers from the CEDM problem [69–71]. In the $E_6 \times SU(2)_F \times U(1)_A$ GUT, however, the CEDM problem can be solved by considering the spontaneous CP violation [72–74] as mentioned above. We will discuss the CEDM problem in Sec. 6.

Hereafter, we neglect the terms suppressed by the power of λ. Therefore, Eqs. (5.16) and (5.19) can be rewritten as [68]

$$\begin{aligned} \tilde{m}^2_{10} &= (m_0^2 + D_6 + D_{10} + D_F + 4D_A)\,\mathbf{1}_{3\times 3} + \begin{pmatrix} 0 & & \\ & -2D_F & \\ & & -D_F - \frac{5}{2}D_A + m_3^2 - m_0^2 \end{pmatrix} \\ &\equiv (m^2_{10})_{11}\,\mathbf{1}_{3\times 3} + \begin{pmatrix} 0 & & \\ & (m^2_{10})_{22} - (m^2_{10})_{11} & \\ & & (m^2_{10})_{33} - (m^2_{10})_{11} \end{pmatrix}, \end{aligned} \tag{5.21}$$

$$\tilde{m}^2_{\bar{5}^0} = (m_0^2 + D_6 - 3D_{10} + D_F + 4D_A)\,\mathbf{1}_{3\times3} + \begin{pmatrix} 0 & & \\ & -3D_6 + 5D_{10} & \\ & & -2D_F \end{pmatrix}$$
$$\equiv (m^2_{\bar{5}^0})_{11}\,\mathbf{1}_{3\times3} + \begin{pmatrix} 0 & & \\ & (m^2_{\bar{5}^0})_{22} - (m^2_{\bar{5}^0})_{11} & \\ & & (m^2_{\bar{5}^0})_{33} - (m^2_{\bar{5}^0})_{11} \end{pmatrix}, \tag{5.22}$$

where $\mathbf{1}_{3\times3}$ is a 3×3 unit matrix. From these rewrites, we find a non-trivial prediction of this model, $(m^2_{10})_{22} - (m^2_{10})_{11} = (m^2_{\bar{5}^0})_{33} - (m^2_{\bar{5}^0})_{11}$ [68]. If this relation is observed in future experiments, strong evidence for this model is obtained, and we can know the size of D_F. Furthermore, the size of D_6 and D_{10} can be determined when $(m^2_{10})_{11} - (m^2_{\bar{5}^0})_{11}$ and $(m^2_{\bar{5}^0})_{22} - (m^2_{\bar{5}^0})_{11}$ are observed. If these small modifications from Eq. (5.20) are observed in addition to the relation $(m^2_{10})_{22} - (m^2_{10})_{11} = (m^2_{\bar{5}^0})_{33} - (m^2_{\bar{5}^0})_{11}$, it is thought that the $E_6 \times SU(2)_F \times U(1)_A$ model can be established.

However, these modifications are constrained by the FCNCs. In the next subsection, we study the constraints to the D-terms from the FCNC processes. As we mentioned in Sec. 4, the K^0-$\overline{K^0}$ mixing is most sensitive to the new physics and gives the strongest constraints. Therefore, we focus on the constraint from ϵ_K parameter in K^0-$\overline{K^0}$ mixing.

5.4 FCNC constraints to D-terms

For the discussion of the size of the D-terms from the FCNC constraints, we focus on the natural SUSY-type sfermion masses, i.e. $m_0 \gg m_3$. Since the D-terms are expected to be small for the FCNC constraints, we can fix $|(m^2_{10})_{33} - (m^2_{10})_{11}| = m_0^2$ from Eq. (5.21). In order to obtain the 125 GeV Higgs mass, m_3 must be larger than 1 TeV. Therefore we take $m_3 \sim \mathcal{O}(1)$ TeV because of the naturalness. The upper bound for the ratio m_0/m_3 is known to be roughly 5 in order not to be negative stop mass square through two loop RGE [61, 149]. Therefore, we expect that $m_0 \sim O(10)$ TeV. Note that since the upper bound of m_0/m_3 is dependent on the explicit models between the GUT scale and the SUSY-breaking scale, we do not discuss it explicitly.

If the D-term contributions can be negligible, almost all experimental bounds from FCNC processes are satisfied because of the sfermion mass spectrum in this model [150–153]. When the D-terms become sizable, the strongest constraints can be given from the CP-violating parameter ϵ_K in K^0-$\overline{K^0}$ mixing. Since the other FCNC constraints are basically satisfied if the constraints from K^0-$\overline{K^0}$ mixing are satisfied, we consider the constraints on the size of D-terms from the bounds of ϵ_K.

For the calculation of constraints from the FCNC processes with the basis in which quarks and leptons are mass eigenstates, diagonalizing matrices for the Yukawa couplings

are needed. we define it as follow:

$$\psi'_{Li}(Y_\psi)_{ij}\psi'^c_{Rj} = (L^\dagger_\psi \psi'_L)_i (L^T_\psi Y_\psi R_\psi)_{ij} (R^\dagger_\psi \psi'^c_R)_j \equiv \psi_{Li}(Y^D_\psi)_{ij}\psi^c_{Rj}, \tag{5.23}$$

where ψ' is a flavor eigenstate, ψ is a mass eigenstate and Y^D_ψ is a diagonalized Yukawa matrix of ψ. We show the rough expressions of the diagonalizing matrices for up-type quarks, down-type quarks and charged leptons without $O(1)$ coefficients, which are obtained from Eqs. (5.11), (5.12) and (5.13):

$$L_u \sim \begin{pmatrix} 1 & \frac{1}{3}\lambda & 0 \\ \frac{1}{3}\lambda & 1 & \lambda^2 \\ \frac{1}{3}\lambda^3 & \lambda^2 & 1 \end{pmatrix}, \; R_u \sim \begin{pmatrix} 1 & \frac{1}{3}\lambda & 0 \\ \frac{1}{3}\lambda & 1 & \lambda^2 \\ \frac{1}{3}\lambda^3 & \lambda^2 & 1 \end{pmatrix}, \tag{5.24}$$

$$L_d \sim \begin{pmatrix} 1 & (\frac{2}{3}+i\frac{4}{27})\lambda & \frac{1}{3}\lambda^3 \\ (\frac{2}{3}+i\frac{4}{27})\lambda & 1 & \lambda^2 \\ (\frac{2}{3}+i\frac{4}{27})\lambda^3 & \lambda^2 & 1 \end{pmatrix}, \; R_d \sim \begin{pmatrix} 1 & \frac{2}{3}(1+i)\lambda^{0.5} & \frac{2}{3}\lambda \\ \frac{2}{3}(1+i)\lambda^{0.5} & 1 & (1+i)\lambda^{0.5} \\ \frac{2}{3}(1+i)\lambda & (1+i)\lambda^{0.5} & 1 \end{pmatrix}, \tag{5.25}$$

$$L_e \sim \begin{pmatrix} 1 & (1+i)\lambda^{0.5} & 0 \\ (1+i)\lambda^{0.5} & 1 & (1+i)\lambda^{0.5} \\ \lambda & (1+i)\lambda^{0.5} & 1 \end{pmatrix}, \; R_e \sim \begin{pmatrix} 1 & \lambda & \lambda^3 \\ \lambda & 1 & \lambda^2 \\ \lambda^3 & \lambda^2 & 1 \end{pmatrix}, \tag{5.26}$$

$$L_\nu \sim \begin{pmatrix} 1 & (1+i)\lambda^{0.5} & (1+i)\lambda \\ (1+i)\lambda^{0.5} & 1 & (1+i)\lambda^{0.5} \\ (1+i)\lambda & (1+i)\lambda^{0.5} & 1 \end{pmatrix}. \tag{5.27}$$

Note that the detailed expressions of these diagonalizing matrices with the explicit $\mathcal{O}(1)$ coefficients are summarized in Appendix D. We have two types for the diagonalizing matrices for **10** of $SU(5)$ sfermions and for $\bar{\mathbf{5}}$ sfermions as

$$U_{\text{CKM-type}} \equiv \begin{pmatrix} 1 & a_{12}\lambda & a_{13}\lambda^3 \\ a_{21}\lambda & 1 & a_{23}\lambda^2 \\ a_{31}\lambda^3 & a_{32}\lambda^2 & 1 \end{pmatrix} \qquad (\text{for } L_u,\, L_d,\, R_u \text{ and } R_e) \tag{5.28}$$

$$U_{\text{MNS-type}} \equiv \begin{pmatrix} b_{11} & b_{12}\lambda^{0.5} & b_{13}\lambda \\ b_{21}\lambda^{0.5} & b_{22} & b_{23}\lambda^{0.5} \\ b_{31}\lambda & b_{32}\lambda^{0.5} & b_{33} \end{pmatrix} \qquad (\text{for } L_e,\, L_\nu \text{ and } R_d), \tag{5.29}$$

where a_{ij} and b_{ij} are generically complex $O(1)$ coefficients, respectively. The mass inser-

tion parameters are defined as

$$(\delta^{\psi}_{\Gamma\Gamma})_{ij} \equiv \frac{(\Gamma^{\dagger}_{\psi}\tilde{m}^2_{\psi_\Gamma}\Gamma_{\psi})_{ij}}{m^2_{\tilde{\psi}}} \quad (\Gamma = L, R^*), \tag{5.30}$$

where $m_{\tilde{\psi}}$ is the averaged sfermion mass of $\psi = u, d, e, \nu$ and is taken m_0 in many cases in this thesis. These can be calculated as

$$(\delta^{\psi}_{\Gamma\Gamma})_{12} = a^*_{21}\lambda\left((m^2_{10})_{22} - (m^2_{10})_{11}\right) + a^*_{31}a_{32}\lambda^5\left((m^2_{10})_{33} - (m^2_{10})_{11}\right) \tag{5.31}$$

$$(\delta^{\psi}_{\Gamma\Gamma})_{13} = \left[a^*_{21}a_{23}\left((m^2_{10})_{22} - (m^2_{10})_{11}\right) + a^*_{31}\left((m^2_{10})_{33} - (m^2_{10})_{11}\right)\right]\lambda^3 \tag{5.32}$$

$$(\delta^{\psi}_{\Gamma\Gamma})_{23} = \left[a_{23}\left((m^2_{10})_{22} - (m^2_{10})_{11}\right) + a^*_{32}\left((m^2_{10})_{33} - (m^2_{10})_{11}\right)\right]\lambda^2 \tag{5.33}$$

for **10** fields and

$$(\delta^{\psi}_{\Gamma\Gamma})_{12} = b^*_{21}b_{22}\lambda^{0.5}\left((m^2_{\bar{5}^0})_{22} - (m^2_{\bar{5}^0})_{11}\right) + b^*_{31}b_{32}\lambda^{1.5}\left((m^2_{\bar{5}^0})_{33} - (m^2_{\bar{5}^0})_{11}\right) \tag{5.34}$$

$$(\delta^{\psi}_{\Gamma\Gamma})_{13} = \left[b^*_{21}b_{23}\left((m^2_{\bar{5}^0})_{22} - (m^2_{\bar{5}^0})_{11}\right) + b^*_{31}b_{33}\left((m^2_{\bar{5}^0})_{33} - (m^2_{\bar{5}^0})_{11}\right)\right]\lambda \tag{5.35}$$

$$(\delta^{\psi}_{\Gamma\Gamma})_{23} = \left[b^*_{22}b_{23}\left((m^2_{\bar{5}^0})_{22} - (m^2_{\bar{5}^0})_{11}\right) + b^*_{32}b_{33}\left((m^2_{\bar{5}^0})_{33} - (m^2_{\bar{5}^0})_{11}\right)\right]\lambda^{0.5} \tag{5.36}$$

for $\bar{\mathbf{5}}$ fields. In Appendix E, we show each mass insertion parameter in this model with explicit $O(1)$ coefficients.

Let us calculate the constraints from the ϵ_K parameter in K^0-$\overline{K^0}$ mixing. In Refs. [154, 155], the constraints for $(\delta^d_{LL})_{12}$ and $(\delta^d_{RR})_{12}$ are studied by including the SM contribution and NLO calculation of QCD. Their bounds are

$$\sqrt{|\mathrm{Im}(\delta^d_{LL})^2_{12}|} < 2.9\times10^{-3}\left(\frac{m_{\tilde{d}}}{500\mathrm{GeV}}\right), \tag{5.37}$$

$$\sqrt{|\mathrm{Im}(\delta^d_{RR})^2_{12}|} < 2.9\times10^{-3}\left(\frac{m_{\tilde{d}}}{500\mathrm{GeV}}\right), \tag{5.38}$$

$$\sqrt{|\mathrm{Im}(\delta^d_{LL})_{12}(\delta^d_{RR})_{12}|} < 1.1\times10^{-4}\left(\frac{m_{\tilde{d}}}{500\mathrm{GeV}}\right). \tag{5.39}$$

These parameters can roughly be calculated as

$$(\delta^d_{LL})_{12} \sim \left(\frac{2}{3} + i\frac{4}{27}\right)\left(\lambda\frac{(m^2_{10})_{22} - (m^2_{10})_{11}}{m^2_{\tilde{d}}} + \lambda^5\frac{(m^2_{10})_{33} - (m^2_{10})_{11}}{m^2_{\tilde{d}}}\right), \tag{5.40}$$

$$(\delta^d_{RR})_{12} \sim \frac{2}{3}(1+i)\left(\lambda^{0.5}\frac{(m^2_{\bar{5}^0})_{22} - (m^2_{\bar{5}^0})_{11}}{m^2_{\tilde{d}}} + \lambda^{1.5}\frac{(m^2_{\bar{5}^0})_{33} - (m^2_{\bar{5}^0})_{11}}{m^2_{\tilde{d}}}\right), \tag{5.41}$$

in this model [68]. By taking $|(m^2_{10})_{33} - (m^2_{10})_{11}| = m^2_0 = m^2_{\tilde{d}}$, we can obtain the allowed re-

gion in ($\sqrt{|(m^2_{\bar{5}^0})_{22} - (m^2_{\bar{5}^0})_{11}|}/m_{\tilde{d}}$, $\sqrt{|(m^2_{10})_{22} - (m^2_{10})_{11}|}/m_{\tilde{d}} = \sqrt{|(m^2_{\bar{5}^0})_{33} - (m^2_{\bar{5}^0})_{11}|}/m_{\tilde{d}}$) space. we show the results in Fig. 12. Note that $(m^2_{10})_{22} - (m^2_{10})_{11} = (m^2_{\bar{5}^0})_{33} - (m^2_{\bar{5}^0})_{11}$ is one of the predictions in the $E_6 \times SU(2)_F \times U(1)_A$ model.

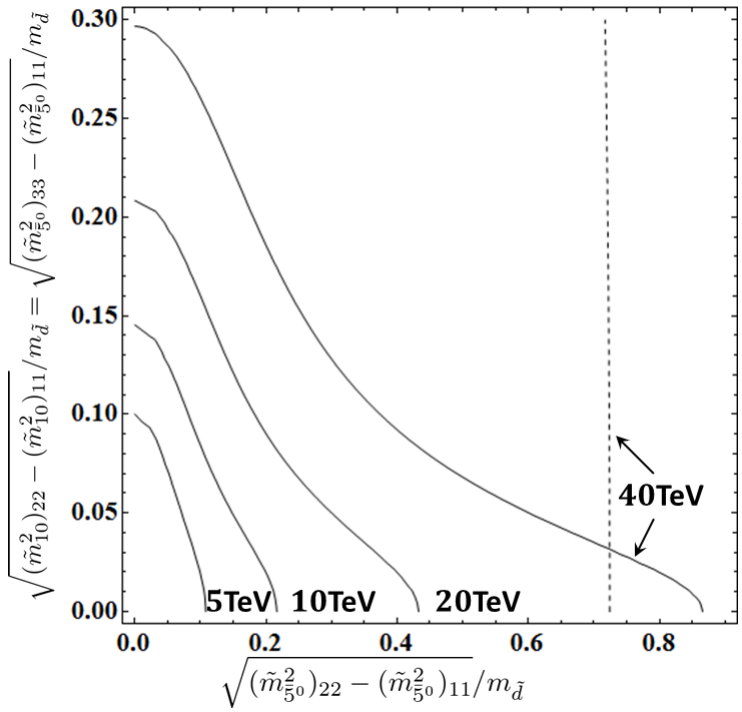

Figure 12: Allowed region in ($\sqrt{|(m^2_{\bar{5}^0})_{22} - (m^2_{\bar{5}^0})_{11}|}/m_{\tilde{d}}$, $\sqrt{|(m^2_{10})_{22} - (m^2_{10})_{11}|}/m_{\tilde{d}} = \sqrt{|(m^2_{\bar{5}^0})_{33} - (m^2_{\bar{5}^0})_{11}|}/m_{\tilde{d}}$) space [68]. The allowed region for the condition of $\sqrt{|\mathrm{Im}(\delta^d_{LL})_{12}(\delta^d_{RR})_{12}|}$ is obtained below the solid lines for various $m_{\tilde{d}} = 5$ TeV, 10 TeV, 20 TeV and 40 TeV. The allowed region for $\sqrt{|\mathrm{Im}(\delta^d_{RR})^2_{12}|}$ is the left side of the dotted line for $m_{\tilde{d}} = 40$ TeV. The other conditions are satisfied in the allowed region for $\sqrt{|\mathrm{Im}(\delta^d_{LL})_{12}(\delta^d_{RR})_{12}|}$.

Note that we neglected the contributions to the sfermion masses which are suppressed by power of λ in Eqs. (5.16) and (5.19) in the above arguments. Almost all these terms can be neglected because of the power of λ. However, $\lambda^2 m^2$ term in Eq. (5.19) can give non-vanishing contribution to $\sqrt{|(m^2_{\bar{5}^0})_{22} - (m^2_{\bar{5}^0})_{11}|}/m_{\tilde{d}}$ if $m \sim m_0$. In such a case, we can easily extract the FCNC constraints from Fig. 12.

5.5 Summary of the section

In this section, we introduced the interesting SUSY GUT models based on the $E_6 \times SU(2)_F \times U(1)_A$ SUSY GUT. These models can solve almost all the problems which are caused in SUSY GUT model under the natural assumption which all the interactions

allowed by the symmetries are introduced. One of the important signatures of the $E_6 \times SU(2)_F \times U(1)_A$ SUSY GUT is the MUSM. This structure can suppress the contributions to SUSY FCNC processes and stabilize the weak scale at the same time [54–58, 156–158].

However, the universality of the MUSM is destroyed by non-vanishing D-term contributions predicted in the $E_6 \times SU(2)_F \times U(1)_A$ SUSY GUT. Therefore, these contributions are strongly constrained by the FCNC processes, especially the CP-violating parameter ϵ_K in K^0-$\overline{K^0}$ mixing. We searched the size of D-term contributions from the constraint of ϵ_K and found that sizable contributions are allowed as shown in Fig. 12, which is $\mathcal{O}(1)$ TeV. Moreover, we obtained the novel relation, $(m^2_{10})_{22} - (m^2_{10})_{11} = (m^2_{\bar{5}^0})_{33} - (m^2_{\bar{5}^0})_{11}$ which is specific to this model. Therefore, if this relation can be observed in the future experiments in addition to the small modifications from the MUSM, we may establish the $E_6 \times SU(2)_F \times U(1)_A$ SUSY GUT.

6 CEDM constraints in natural SUSY-type sfermion spectrum

In the previous section, we introduced the SUSY GUT model with the natural SUSY-type sfermion mass spectrum. This type of spectrum suffers from the CEDM constraints because of the light stop mass. In this section, we focus on the sfermion mass spectrum obtained in Eq. (5.20) [150, 151, 159],

$$\tilde{m}_{10}^2 = \begin{pmatrix} m_0^2 & & \\ & m_0^2 & \\ & & m_3^2 \end{pmatrix}, \quad \tilde{m}_{\bar{5}0}^2 = \begin{pmatrix} m_0^2 & & \\ & m_0^2 & \\ & & m_0^2 \end{pmatrix}, \tag{6.1}$$

and investigate the lower bound of the sfermion masses from the EDM bounds.

6.1 CEDM and rough estimation

The effective Lagrangian for the quark CEDM can be calculated by the diagram shown in Fig. 13, and described as

$$\mathcal{L}_{\text{CEDM}} = -\frac{ig_s}{2} d_q^C \bar{q}(G \cdot \sigma)\gamma_5 q, \tag{6.2}$$

where g_s is the QCD coupling, $G \cdot \sigma = G_{\mu\nu}^A T^A \sigma^{\mu\nu}$, $G_{\mu\nu}^A$ is field strength of gluon, T^A $(A = 1, 2, \cdots, 8)$ are $SU(3)$ generators and $\sigma^{\mu\nu} = \frac{i}{2}[\gamma^\mu, \gamma^\nu]$. d_q^C denotes a quark CEDM

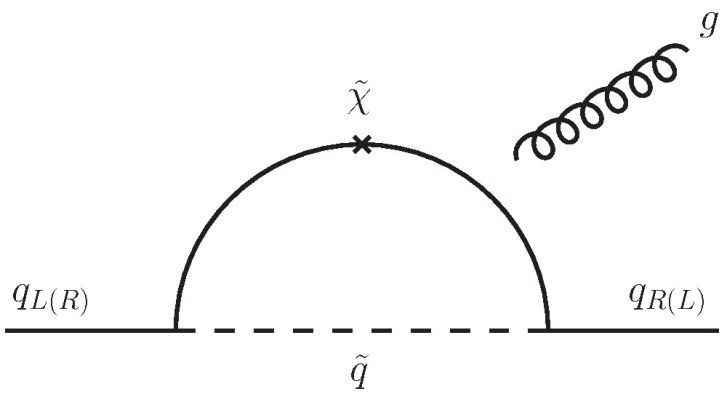

Figure 13: An one-loop diagram for the quark CEDM. $\tilde{\chi}$ denotes fermionic superpartners, such as gluinos, charginos and neutralinos.

and particularly, it is dominated by gluino contributions. Therefore, we focus on the gluino contributions to the quark CEDMs in this thesis.

If one consider the natural SUSY-type sfermion spectrum, such as Eq. (6.1), the diagram shown in Fig. 14 becomes dominant contribution to up-quark CEDM, d_u^C [69, 72, 160, 161]. This contribution is enhanced when the stop mass is light to be around 1

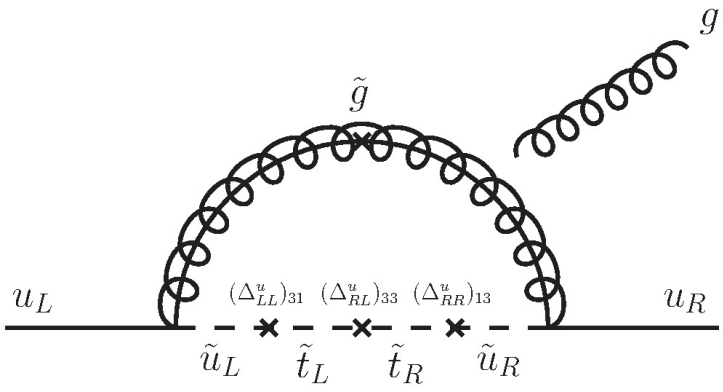

Figure 14: A diagram which dominantly contributes to d_u^C. $(\Delta^u_{AB})_{ij}$ $(A, B = L \text{ or } R,\ i, j = 1, 2, 3)$ is the element of 6×6 sfermion mass matrix (see Eq. (6.3)).

TeV and in general, its size is severely constrained by the CEDM constraints even if all SUSY-breaking parameters and the Higgsino mass parameter μ are taken to be real. In order to explain the enhancement and constraints, let us estimate this diagram by using mass insertion approximation (MIA) [162].

We define the 6×6 mass matrix for up-type sfermions as follow:

$$M^2_{\tilde{u}} = \begin{pmatrix} L_u^\dagger(m_Q^2 + v_u^2 Y_u^* Y_u^T)L_u & L_u^\dagger(v_u A_u^* - \mu v_d Y_u^*)R_u^* \\ R_u^T(v_u A_u^T - \mu v_d Y_u^T)L_u & R_u^T(m_u^2 + v_u^2 Y_u^T Y_u^*)R_u^* \end{pmatrix} \equiv \begin{pmatrix} (\Delta^u_{LL}) & (\Delta^u_{LR}) \\ (\Delta^u_{RL}) & (\Delta^u_{RR}) \end{pmatrix}, \quad (6.3)$$

where A_u is a 3×3 matrix for scalar three point vertex and m_Q^2 and m_u^2 are 3×3 soft SUSY-breaking mass matrices. Hereafter, we assume that Y_u has the hierarchical structure for the observed masses as follow:

$$Y_u \sim \begin{pmatrix} \lambda^6 & \lambda^5 & \lambda^3 \\ \lambda^5 & \lambda^4 & \lambda^2 \\ \lambda^3 & \lambda^2 & 1 \end{pmatrix} \quad (\lambda = 0.22). \quad (6.4)$$

Here, we omit the $\mathcal{O}(1)$ coefficients for each element. In this case, the diagonalizing matrices, L_u and R_u, can be the CKM-type matrix:

$$L_u, R_u \sim V_{\rm CKM} \sim \begin{pmatrix} 1 & \lambda & \lambda^3 \\ \lambda & 1 & \lambda^2 \\ \lambda^3 & \lambda^2 & 1 \end{pmatrix}. \quad (6.5)$$

The diagonalized Yukawa coupling is obtained as $L_u^T Y_u R_u = Y_u^D$ as in Eq. (5.23). By using these equations, we can estimate the contribution of Fig. 14 to d_u^C as

$$\begin{aligned} d_u^C &\simeq \frac{\alpha_s}{4\pi} F_{\rm MIA}(r_{\tilde g}, r_{\tilde t}) {\rm Im}\left[\frac{M_{\tilde g}}{m_{\tilde t}^2}\frac{(\Delta_{RL}^u)_{33}}{m_{\tilde t}^2}\frac{(\Delta_{LL}^u)_{31}}{m_{\tilde u}^2}\frac{(\Delta_{RR}^u)_{13}}{m_{\tilde u}^2}\right] \\ &\sim \frac{\alpha_s}{4\pi} F(r_{\tilde g}, r_{\tilde t}) \frac{M_{\tilde g} A_{u33} v_u}{m_{\tilde t}^4} {\rm Im}\left[(\delta_{LL}^u)_{31}(\delta_{RR}^u)_{13}\right], \end{aligned} \tag{6.6}$$

where $M_{\tilde g}$ is the gluino mass, $r_{\tilde g} = M_{\tilde g}^2/m_{\tilde u}^2$, $r_{\tilde t} = m_{\tilde t}^2/m_{\tilde u}^2$ and $F_{\rm MIA}(x,y)$ is a loop function. Note that in notation of Eq. (6.3), the mass insertion parameters $(\delta_{AB}^u)_{ij}$ are

$$(\delta_{AB}^u)_{ij} = \frac{(\Delta_{AB}^u)_{ij}}{m_{\tilde u}^2} \ (A, B = L \,{\rm or}\, R,\ i,j = 1,2,3). \tag{6.7}$$

In Eq. (6.6), we assume that $M_{\tilde g}$ and $(\Delta_{RL}^u)_{33} \sim A_{u33} v_u$ are real. Therefore, d_u^C is proportional to the imaginary part of the $(\delta_{LL}^u)_{31}(\delta_{RR}^u)_{13}$ which includes the diagonalizing matrices, L_u and R_u. Since these diagonalizing matrices are complex to obtain the KM phase, the contribution of Eq. (6.6) are induced even if all SUSY-breaking parameters and μ are real.

To obtain the CEDM constraints, one should use the relations between the EDM and CEDM. In this thesis, we use the following relations: $d_{\rm Hg} \sim 2.2 \times 10^{-3}\, e(d_u^C - d_d^C)$ [163] for the mercury EDM and $d_{\rm N} \sim -0.3\, e(d_u^C - d_d^C)$ [164] for the neutron EDM. The current upper bound for these EDMs [76, 77] are

$$d_N < 3.0 \times 10^{-26}\, e\,{\rm cm}, \tag{6.8}$$

$$d_{Hg} < 7.4 \times 10^{-30}\, e\,{\rm cm}. \tag{6.9}$$

By taking $m_{\tilde t} \sim A_{u33} \sim 2$ TeV, $m_{\tilde g} \sim 1.5 m_{\tilde t} \sim 3$ TeV and $m_{\tilde u} \sim 10$ TeV and using these relations and constraints, we obtain the following bounds for the mass insertion parameters[7]:

$${\rm Im}\left[(\delta_{LL}^u)_{31}(\delta_{RR}^u)_{13}\right] < \left\{ \begin{array}{c} 5.3 \times 10^{-6}\,({\rm Hg}) \\ 1.6 \times 10^{-4}\,({\rm neutron}) \end{array} \right\} \left(\frac{m_{\tilde t}}{2\,{\rm TeV}}\right)^2. \tag{6.10}$$

Note that the loop integral in this case is $F_{\rm MIA}(0.09, 0.04) \simeq 0.079$. We summarize the value of $F_{\rm MIA}(r_{\tilde g}, r_{\tilde t})$ with different $r_{\tilde g}$ and $r_{\tilde t}$ in Appendix F. The left-hand side of Eq. (6.10)

[7] For the bound of d_u^C, we consider the situation that $m_0 \gg m_3$. In such a case, the down quark CEDM d_d^C is decoupled and can be ignored. In this thesis, we just use the bound for $d_u^C - d_d^C$ obtained from the relations between the EDM and CEDM as that for d_u^C and d_d^C.

can be calculated by Eqs. (6.1) and (6.5) as

$$\mathrm{Im}\left[(\delta^u_{LL})_{31}(\delta^u_{RR})_{13}\right] \simeq \left(\frac{m^2_{\tilde{t}} - m^2_{\tilde{u}}}{m^2_{\tilde{u}}}\right)^2 \times \lambda^6. \tag{6.11}$$

Clearly, this does not decouple when $m_{\tilde{u}} \to \infty$ which correspond to $m_0 \to \infty$, and its size is about $\lambda^6 \sim 10^{-4}$. Therefore, the stop mass is needed to be larger than roughly 10 TeV in order to avoid the Hg EDM bound obtained in this approximation.

Note that the down quark CEDM d^C_d decouples in the limit of $m_0 \to \infty$ because the mass of the right-handed sbottom becomes heavy in the natural SUSY-type sfermion spectrum Eq. (6.1). Therefore, by calculating the approximate expression for d^C_d in a similar way, we expected that $m_{\tilde{d}} > 10$ TeV is needed to satisfy the CEDM bounds if the decoupling feature of d^C_d for $m_{\tilde{d}}$ is similar to that of d^C_u for $m_{\tilde{u}}$.

In the point of view of the naturalness, it is preferable that the stop mass is $\mathcal{O}(1)$ TeV. In order to satisfy the CEDM bounds in such a light stop case, an interesting solution is to assume that Y_u and A_u are real at the GUT scale, while Y_d is complex to obtain the KM phase. In this solution, diagonalizing matrices for Y_u are also real, and d^C_u is strongly suppressed as understood from Eq. (6.6). In fact, Y_u becomes complex at the low energy scale through the RGE running. However, since there is a loop suppression in the imaginary part of Y_u, the current CEDM bounds are satisfied in this case.

6.2 Calculational method

In order to discuss the CEDM constraints for the model with the natural SUSY-type sfermion spectrum and compare the lower bound of the sfermion masses in different Yukawa structure, we calculate the CEDMs numerically. Before showing the results, let us explain the detail of the calculation.

For the calculation, the input parameters are given at the GUT scale, $\Lambda_{\rm GUT} = 2 \times 10^{16}$ GeV. For simplicity, we assume that the model is the MSSM with the natural SUSY-type sfermion spectrum. Therefore, the input parameters are gauge couplings g_i, gaugino masses M_i, Yukawa couplings Y_f, scalar cubic couplings A_f which are called A-parameters in this thesis, sfermion mass matrices and doublet Higgs masses. These values or structures are[8]

$$g_1(\Lambda_{\rm GUT}) = g_2(\Lambda_{\rm GUT}) = g_3(\Lambda_{\rm GUT}) = g_{\rm GUT} = 0.7, \tag{6.12}$$

$$M_1(\Lambda_{\rm GUT}) = M_2(\Lambda_{\rm GUT}) = M_3(\Lambda_{\rm GUT}) = M_{1/2}, \tag{6.13}$$

[8]We consider that hierarchies of A-parameters are the similar to those of corresponding Yukawa couplings. This situation can be realized if one consider the model in which the Froggatt-Nielsen mechanism [165, 166] is considered.

$$Y_u = \begin{pmatrix} y_{u11}\lambda^6 & y_{u12}\lambda^5 & y_{u13}\lambda^3 \\ y_{u21}\lambda^5 & y_{u22}\lambda^4 & y_{u23}\lambda^2 \\ y_{u31}\lambda^3 & y_{u32}\lambda^2 & y_{u33} \end{pmatrix}, \qquad A_u = A_0 \begin{pmatrix} a_{u11}\lambda^6 & a_{u12}\lambda^5 & a_{u13}\lambda^3 \\ a_{u21}\lambda^5 & a_{u22}\lambda^4 & a_{u23}\lambda^2 \\ a_{u31}\lambda^3 & a_{u32}\lambda^2 & a_{u33} \end{pmatrix}, \tag{6.14}$$

$$Y_d = \begin{pmatrix} y_{d11}\lambda^6 & y_{d12}\lambda^{5.5} & y_{d13}\lambda^5 \\ y_{d21}\lambda^5 & y_{d22}\lambda^{4.5} & y_{d23}\lambda^4 \\ y_{d31}\lambda^3 & y_{d32}\lambda^{2.5} & y_{d33}\lambda^2 \end{pmatrix}, \qquad A_d = A_0 \begin{pmatrix} a_{d11}\lambda^6 & a_{d12}\lambda^{5.5} & a_{d13}\lambda^5 \\ a_{d21}\lambda^5 & a_{d22}\lambda^{4.5} & a_{d23}\lambda^4 \\ a_{d31}\lambda^3 & a_{d32}\lambda^{2.5} & a_{d33}\lambda^2 \end{pmatrix}, \tag{6.15}$$

$$Y_e = \begin{pmatrix} y_{e11}\lambda^6 & y_{e12}\lambda^5 & y_{e13}\lambda^3 \\ y_{e21}\lambda^{5.5} & y_{e22}\lambda^{4.5} & y_{e23}\lambda^{2.5} \\ y_{e31}\lambda^5 & y_{e32}\lambda^4 & y_{e33}\lambda^2 \end{pmatrix}, \qquad A_e = A_0 \begin{pmatrix} a_{e11}\lambda^6 & a_{e12}\lambda^5 & a_{e13}\lambda^3 \\ a_{e21}\lambda^{5.5} & a_{e22}\lambda^{4.5} & a_{e23}\lambda^{2.5} \\ a_{e31}\lambda^5 & a_{e32}\lambda^4 & a_{e33}\lambda^2 \end{pmatrix}, \tag{6.16}$$

$$\tilde{m}^2_{10} = \begin{pmatrix} m_0^2 & & \\ & m_0^2 & \\ & & m_3^2 \end{pmatrix}, \quad \tilde{m}^2_{\bar{5}0} = \begin{pmatrix} m_0^2 & & \\ & m_0^2 & \\ & & m_0^2 \end{pmatrix}, \tag{6.17}$$

$$m^2_{H_u}(\Lambda_{\rm GUT}) = m^2_{H_d}(\Lambda_{\rm GUT}) = (500\,{\rm GeV})^2, \tag{6.18}$$

where y_{fij} and a_{fij} $(f = u, d, e)$ are the $\mathcal{O}(1)$ coefficients and A_0 is the typical scale of A-parameters. The other parameter of the MSSM is the Higgsino mass parameter, μ. In this calculation, it is fixed by the Z boson mass M_Z. Note that we do not mind the largeness of the value of μ because it does not contribute much to d_u^C, although μ becomes $\mathcal{O}(1)$ TeV and it may lead to destabilization of the weak scale.

In the calculation, we assume that Yukawa couplings and A-parameters have the hierarchies composed of $\lambda = 0.22$, but have three different types of $\mathcal{O}(1)$ coefficients at the GUT scale for the comparison:

(i) *complex Y_u type*
All y_{fij} and a_{fij} $(f = u, d, e)$ are complex $\mathcal{O}(1)$ coefficients $(i, j = 1, 2, 3)$.

(ii) *real Y_u type*
y_{uij} and a_{uij} are real $\mathcal{O}(1)$ coefficients, while y_{dij}, a_{dij}, y_{eij} and a_{eij} are complex $\mathcal{O}(1)$ coefficients $(i, j = 1, 2, 3)$.

(iii) *E_6 model* (with family symmetry and spontaneous CP violation)
y_{uij}, y_{dij} and y_{eij} have the special structures obtained in Eqs. (5.11), (5.12) and (5.13) [73–75]: $y_{u11} = y_{u13} = y_{u31} = y_{e13} = y_{e21} = 0$, $y_{u12} = -y_{u21} = y_{d13} = \frac{1}{3}d_q$, $y_{u23} = y_{u32}$, $y_{d23} = y_{e32}$, $y_{d33} = y_{e33}$ and $y_{e12} = -y_{e31}$. y_{d11}, y_{d12}, y_{d22}, y_{d32}, y_{e11}, y_{e22} and y_{e23} are complex $\mathcal{O}(1)$ coefficients, and d_q, y_{u22}, y_{u23}, y_{u33}, y_{d21}, y_{d23}, y_{d31}, y_{d33} and y_{e12} are real $\mathcal{O}(1)$ coefficients. A-parameters have same structures.

Note that the real or complex $\mathcal{O}(1)$ coefficient in this thesis is defined as follow. The $\mathcal{O}(1)$ coefficient C can be written by its radius and phase as $C = |C|\exp(i\theta^{(C)})$. We fix the

range of the radius as $0.5 \leq |C| \leq 1.5$. If C is the real $\mathcal{O}(1)$ coefficient, the phase $\theta^{(C)}$ is randomly chosen by 0 or π. If C is the complex $\mathcal{O}(1)$ coefficient, the phase $\theta^{(C)}$ is random number in the range of $0 \leq \theta^{(C)} \leq 2\pi$.

For all three types, we assume that $M_{1/2}$, μ, $A_{u33} = A_0$ and $y_{u33} = 0.8$ are real at the GUT scale, in which most of the usual contributions to EDMs are strongly suppressed when $m_0 \to \infty$. In addition, we consider that the SUSY-breaking scale is 1 TeV and $\tan\beta = 7$.

We obtain the low energy parameters from above inputs by using two-loop RGEs of the MSSM[9] [167]. The CEDMs for light quarks (u, d, s) can be calculated by the one-loop formulas for the gluino contributions as

$$d_u^C = c\frac{\alpha_s}{4\pi}\sum_{j=1}^{6}\frac{M_{\tilde{g}}}{(\hat{M}_{\tilde{u}}^2)_{jj}}\left\{\left(-\frac{1}{3}F_1(x_j^u) - 3F_2(x_j^u)\right)\mathrm{Im}[(U_{\tilde{u}}^\dagger)_{1j}(U_{\tilde{u}})_{j4}]\right\}, \tag{6.19}$$

$$d_d^C = c\frac{\alpha_s}{4\pi}\sum_{j=1}^{6}\frac{M_{\tilde{g}}}{(\hat{M}_{\tilde{d}}^2)_{jj}}\left\{\left(-\frac{1}{3}F_1(x_j^d) - 3F_2(x_j^d)\right)\mathrm{Im}[(U_{\tilde{d}}^\dagger)_{1j}(U_{\tilde{d}})_{j4}]\right\}, \tag{6.20}$$

$$d_s^C = c\frac{\alpha_s}{4\pi}\sum_{j=1}^{6}\frac{M_{\tilde{g}}}{(\hat{M}_{\tilde{d}}^2)_{jj}}\left\{\left(-\frac{1}{3}F_1(x_j^d) - 3F_2(x_j^d)\right)\mathrm{Im}[(U_{\tilde{d}}^\dagger)_{2j}(U_{\tilde{d}})_{j5}]\right\}, \tag{6.21}$$

where $c \sim 0.9$ is QCD correction. $\hat{M}_{\tilde{q}}^2\,(q = u, d)$ are diagonalized squark mass matrices which is defined as $\hat{M}_{\tilde{q}}^2 = U_{\tilde{q}} M_{\tilde{q}}^2 U_{\tilde{q}}^\dagger$. $M_{\tilde{q}}^2$ is 6×6 sfermion mass matrices and $U_{\tilde{q}}$ are their diagonalizing matrices. $F_1(x) = (x^2 - 4x + 3 + 2\mathrm{ln}x)/2(1-x)^3$ and $F_2(x) = (x^2 - 1 - 2x\mathrm{ln}x)/2(1-x)^3$ are coming from loop integrals and $x_j^q = \frac{M_{\tilde{g}}^2}{(\hat{M}_{\tilde{q}}^2)_{jj}}$. The current bounds for each quark CEDM [69, 76, 77, 160] are

$$|d_q^C| < 3.4 \times 10^{-27}\,\mathrm{cm} \quad (q = u, d),\ (\text{from Hg EDM}) \tag{6.22}$$

$$|d_q^C| < 1.0 \times 10^{-25}\,\mathrm{cm} \quad (q = u, d),\ (\text{from neutron EDM}) \tag{6.23}$$

$$|d_s^C| < 1.1 \times 10^{-25}\,\mathrm{cm}. \tag{6.24}$$

In the next subsection, we will show the results by calculating CEDMs above method. We generate $\mathcal{O}(100)$ model points with different $\mathcal{O}(1)$ coefficients and obtain the mean value and standard deviation of $\log_{10}|d_q^C|$. Note that we do not fit the observed fermion masses and the CKM matrix strictly. However, these are roughly realized by the Yukawa hierarchies in Eqs. (6.14), (6.15) and (6.16).

[9] We do not consider one-loop threshold corrections in this calculation since their effects to CEDMs are much smaller than that of $\mathcal{O}(1)$ coefficients, although one-loop threshold corrections should be taken into account when one calculate RGEs at two-loop level.

m_0	$M_{\tilde{g}}$	$\lvert A_{u33}\rvert$
5 TeV	2.7 TeV	2.0 TeV
10 TeV	2.8 TeV	2.1 TeV
20 TeV	4.3 TeV	3.1 TeV
30 TeV	6.2 TeV	4.4 TeV
40 TeV	8.4 TeV	5.8 TeV

Table 9: $M_{\tilde{g}}$ and $|A_{u33}|$ at the SUSY scale (1 TeV) in each m_0 value for calculation in Fig. 15.

6.3 Numerical results

The first result is shown in Fig. 15. The vertical axis is $\log_{10}|d_u^C|$ (left panel) and $\log_{10}|d_d^C|$

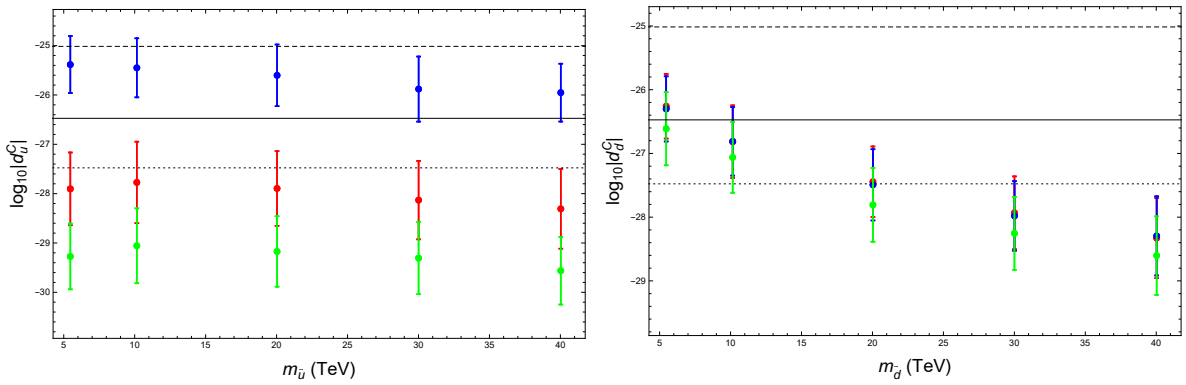

Figure 15: $m_{\tilde{u},\tilde{d}}$ dependence of d_u^C (left panel) and d_d^C (right panel) [78]. Blue, red and green plots are *complex* Y_u *type*, *real* Y_u *type* and E_6 *model*, respectively. Each error bar shows the standard deviation for the value of $\log_{10}|d_q^C|$ $(q = u, d)$. Black solid line is current bound from Hg EDM and allowed region is lower area. Dashed line shows the current bound from neutron EDM, and the dotted line is the bound expected in future experiments of neutron EDM. We choose m_3 and $M_{1/2}$ to become light stop at the SUSY scale (1 TeV), and in these figures, we set $m_{\tilde{t}} = (2000 \pm 250)$ GeV. We also set $A_0 = -1$ TeV.

(right panel) and the horizontal axis is heavy sfermion mass at low energy denoted as $m_{\tilde{u},\tilde{d}}$. Blue, red and green plots are corresponding to *complex* Y_u *type*, *real* Y_u *type* and E_6 *model*, respectively. For these plots, we set $A_0 = -1$ TeV at the GUT scale and the stop mass at low energy is about 2 TeV by choosing the values of $M_{1/2}$ and m_3. The current bounds are shown as black solid line (Hg EDM, Eq. (6.22)) and dashed line (neutron EDM, Eq. (6.23)). We also plotted the future expected bound in the experiments of neutron EDM [168–172] as dotted line. The values of $M_{\tilde{g}}$ and $|A_{u33}|$ at the low energy are listed in Table 9. From Fig. 15, one can see that d_u^C does not depend on the $m_{\tilde{u}}$ (and hence m_0),

while d_d^C is decoupled when m_0 become large. Roughly speaking, the Hg EDM bound leads to $m_{\tilde{d}} > 7$ TeV from d_d^C plots, which corresponds to $m_0 > 7$ TeV at the GUT scale. Note that hereafter, we discuss the sfermion mass bound by using the center value in each distribution. From d_u^C plots, when $m_{\tilde{t}} \simeq 2$ TeV, *complex* Y_u *type* cannot satisfy the current $d_{\rm Hg}$ bound, while *real* Y_u *type* and E_6 *model* can satisfy it. This means that the assumption which Y_u and A_u at the GUT scale are real is a good solution for the CEDM problem. Note that E_6 *model* predicts smaller values of d_u^C than the results of *real* Y_u *type*. This is caused by the special structure in Y_u at the GUT scale, especially $y_{u11} = y_{u13} = y_{u31} = 0$ and the factor of $1/3$ in $y_{u12} = -y_{u21}$.

Next, we show how large stop mass is needed in Fig. 16. The horizontal axis is $m_{\tilde{t}}$.

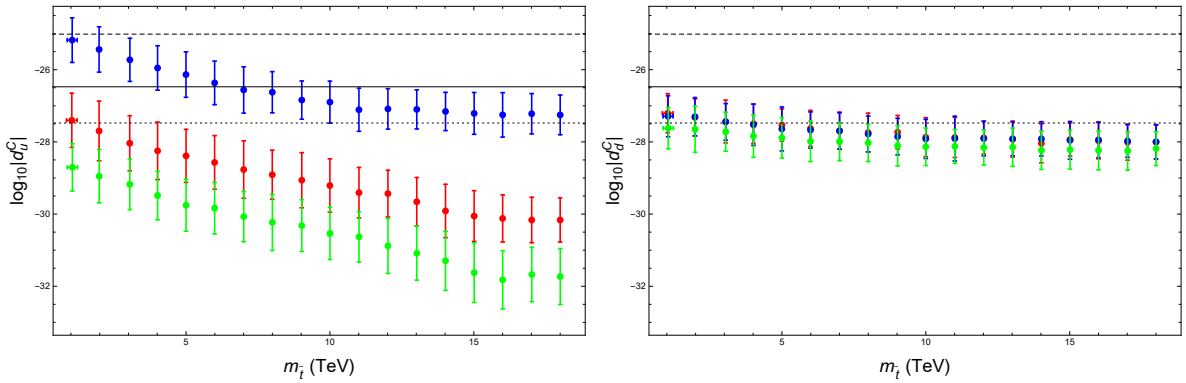

Figure 16: $m_{\tilde{t}}$ dependence of d_u^C (left panel) and d_d^C (right panel) [78]. Blue, red and green plots are *complex* Y_u *type*, *real* Y_u *type* and E_6 *model*, respectively. Each vertical error bar shows the standard deviation for the value of $\log_{10}|d_q^C|$ $(q = u, d)$. Horizontal error bar shows the distribution of stop masses by variation of $O(1)$ coefficients of Yukawa couplings and A parameters. Black solid line is current bound from Hg EDM and allowed region is lower area. Dashed line shows the current bound from neutron EDM, and the dotted line is the bound expected in future experiments of neutron EDM. In these figures, we set $m_0 = 10$ TeV and $A_0 = -1$ TeV.

The vertical axis, colors of plots and shapes of lines are the same meaning as in Fig. 15. For these plots, we set $m_0 = 20$ TeV and $A_0 = -1$ TeV at the GUT scale. At the low energy, $M_{\tilde{g}} = 3$ TeV and stop mass is given by the eigenvalues of the matrix of the stop mass square as $m_{\tilde{t}} \equiv \sqrt{m_{\tilde{t}_1} m_{\tilde{t}_2}}$. It is obvious that d_u^C is strongly dependent on $m_{\tilde{t}}$ and roughly, $m_{\tilde{t}} > 7$ TeV is needed to satisfy the current bounds in *complex* Y_u *type*, which is not so far from the lower bound obtained by the MIA. However, it may not be permissible to be such a large stop mass from the point of view of naturalness. On the other hand, *real* Y_u *type* and E_6 *model* can satisfy the d_u^C bound even if $m_{\tilde{t}} \lesssim 1$ TeV. Therefore, to satisfy the d_u^C bound with $\mathcal{O}(1)$ TeV stop mass, real Y_u at GUT scale can be an important condition. Note that the flat regions appeared in the large stop mass area are caused by

the contributions from the first two generation squarks. This is because we fix $m_0 = 20$ TeV. These regions are expected to disappear if $m_0 \gg 20$ TeV.

Note that we have also calculated the strange quark CEDM and investigated its $m_{\tilde{d},\tilde{t}}$ dependences. The results are very similar to d_d^C results and the current bound is almost satisfied. Therefore, we do not discuss the constraints of d_s^C. The weakness of the constraint of d_s^C can be understood from Fig. 17.

In the last of this subsection, we will mention about the 125 GeV Higgs mass. We have checked whether the Higgs mass is really obtained in this setup by using `FeynHiggs-2.10` [173–177]. Table 10 shows the values of GUT scale parameters we used. These values are chosen to obtain positive squared masses for all sfermions at the SUSY-breaking scale. We show the values of $m_{\tilde{t}}$ and $|A_{u33}|$ at the SUSY-breaking scale for each m_0 case in Table 11. We found that the 125 GeV Higgs mass is realized by these parameters in all

m_0	m_3	$M_{1/2}$	A_0
5 TeV	1.2 TeV	1.5 TeV	-5 TeV
10 TeV	1.5 TeV	1.8 TeV	-4.5 TeV
20 TeV	2 TeV	2.4 TeV	-2.5 TeV
40 TeV	3.5 TeV	4.5 TeV	-3.5 TeV

Table 10: GUT scale parameters which we use for obtaining the 125 GeV Higgs mass in each m_0 value.

m_0	$m_{\tilde{t}}$	$\lvert A_{u33}\rvert$
5 TeV	1.9 TeV	3.4 TeV
10 TeV	2.3 TeV	3.7 TeV
20 TeV	2.6 TeV	4.1 TeV
40 TeV	4.3 TeV	7.4 TeV

Table 11: $m_{\tilde{t}}$ and $|A_{u33}|$ at SUSY scale in each m_0 value.

three types. The CEDM values in these cases are shown in Fig. 17.

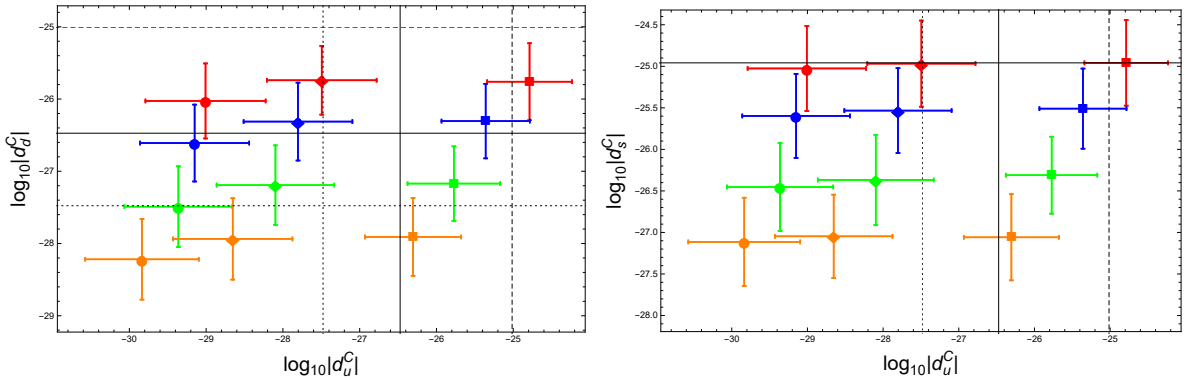

Figure 17: Up, down and strange quark CEDM in three type of boundary condition of Y_u [78]. Left panel is up and down quark CEDM and right panel is up and strange quark CEDM. Square, diamond and circle plots are *complex* Y_u *type*, *real* Y_u *type* and E_6 *model*,, respectively. Red, blue, green and orange mean that m_0 is 5 TeV, 10 TeV, 20 TeV and 40 TeV. Each error bar shows the standard deviation for the value of $\log_{10}|d_q^C|$ $(q = u, d, s)$. Black solid line is the current bound from Hg EDM and allowed region is lower left area. Dashed line shows the current bound from neutron EDM, and the dotted line is the bound expected in future experiments of neutron EDM.

The left (right) panel shows d_u^C versus d_d^C (d_u^C versus d_s^C). In these figures, square, diamond and circle plots are corresponding to *complex* Y_u *type*, *real* Y_u *type* and E_6 *model*, respectively. Red, blue, green and orange means that m_0 is 5 TeV, 10 TeV, 20 TeV and 40 TeV. The current bounds are shown as black solid line (Hg EDM, Eq. (6.22)) and dashed line (neutron EDM, Eq. (6.23)). We also plotted the future expected bound in the experiments of neutron EDM [168–172] as dotted line. The lower left area of each line is allowed region. From Fig. 17, d_u^C bound for *complex* Y_u *type* is still severe even these cases. Interestingly, for *real* Y_u *type* and E_6 *model*, we can expect some signals from the down quark CEDM d_d^C in future experiments of neutron EDM when $m_0 = \mathcal{O}(10)$ TeV.

6.4 Comment on electron EDM

The electron EDM bound is recently improved at the ACME EDM Experiment [178]. It may be important for the discussion of the lower bounds of the sfermion masses. Therefore, we also calculate the electron EDM denoted as d_e and search its constraints in the same situations discussed above. We will show the results for the sum of four neutralino contributions by using the expressions in Ref. [71]. Note that although there are another contributions, the chargino contributions, to d_e, we just ignore such contributions since these are much smaller than the neutralino contributions because of the largeness of the

chargino masses. We checked that in the setup discussed here, the results are not changed if the chargino contributions are included.

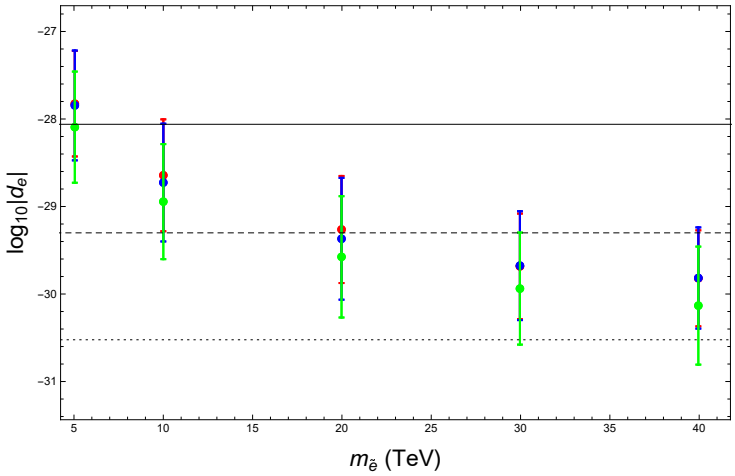

Figure 18: $m_{\tilde{e}}$ dependence of d_e in three type of boundary condition of Y_u [78]. Blue, red and green plots are *complex* Y_u *type*, *real* Y_u *type* and E_6 *model*, respectively. Each error bar show standard deviation for the value of $\log_{10}|d_e|$. Black solid line is current bound and allowed region is lower area. Other input parameters are same as for the Fig. 15. The dashed (dotted) line shows the future bound expected by ACME II (III) [179, 180].

The vertical and horizontal axes in Fig. 18 are $\log_{10}|d_e|$ and the heavy slepton masses, respectively. The colors of plots show the same meaning as in Fig. 15. Black solid line shows the current bound, $|d_e| < 8.7 \times 10^{-29}\, e$ cm, and lower area is allowed. Dashed (Dotted) line is the future expected bound at ACME II (III) [179, 180]. The input parameters used for this result are the same are for Fig. 15. In Table 12, we show the neutralino masses in each m_0 case.

m_0	m_{N_1}	m_{N_2}	m_{N_3}, m_{N_4}
5 TeV	0.5 TeV	0.9 TeV	2.1 TeV
10 TeV	0.6 TeV	1.0 TeV	2.4 TeV
20 TeV	0.8 TeV	1.5 TeV	3.3 TeV
30 TeV	1.2 TeV	2.2 TeV	4.2 TeV
40 TeV	1.6 TeV	3.0 TeV	5.2 TeV

Table 12: Neutralino masses at SUSY scale in each m_0 case. In this calculation, the masses of two of heavy neutralinos, m_{N_3} and m_{N_4}, are almost degenerated.

From Figs. 15 and 18, we found that the current constraint of d_e is slightly weaker than that of d_q^C. The lower bounds of the slepton mass for *real* Y_u *type* and *complex* Y_u

type are roughly 6 TeV, while that of E_6 *model* is 5 TeV. This difference is caused by the structure of Y_e in E_6 *model* (see Eq. (5.13)). Note that since electron EDM experiments will be improved in a few years [180], some signals are expected in d_e when $m_0 = \mathcal{O}(10)$ TeV. If there is no signal, the lower bound of m_0 becomes 20 TeV.

6.5 Summary of the section

In this section, we focused on the natural SUSY-type sfermion mass spectrum, Eq. (6.1). This type of spectrum is strongly constrained by the CEDM constraints because of the light stop contributions. In general, sfermion masses, including the stop mass, are needed to be larger than 10 TeV to satisfy these constraints. It causes the destabilization of the weak scale.

An interesting solution shown in this section is the up-type Yukawa couplings are set to be real at the GUT scale. For comparison, we calculated the CEDMs and discussed the lower bounds of sfermion masses in three different types of Yukawa structure, *complex* Y_u *type*, *real* Y_u *type* and E_6 *model*. As a result, we found that real Y_u at the GUT scale is one of the good solutions for the CEDM constraints with light ($\mathcal{O}(1)$ TeV) stop mass. We summarized the lower bound of sfermion masses from Hg EDM bound in each type in Table 13. From this table, we can conclude that if the stop mass is observed in future experiments and its size is $\mathcal{O}(1)$ TeV, it may be able to constrain the structure of Y_u at GUT scale by using the CEDM constraints.

	complex Y_u *type*	*real* Y_u *type*	E_6 *model*
m_0	7 TeV (20 TeV)	7 TeV (20 TeV)	5 TeV (15 TeV)
$m_{\tilde{t}}$	7 TeV (20 TeV)	No constraint (1 TeV)	No constraint (No constraint)

Table 13: The lower bounds from Hg EDM bound. In this table, we also show the bounds from the future expected sensitivity of neutron EDM in parentheses. "No constraint" means that the bound is smaller than 1 TeV.

Actually, there are large uncertainties in the theoretical calculation of the relation between $d_{\rm Hg}$ and d_q^C [163, 181]. Therefore, the other EDM bounds, such as neutron and electron EDM bounds, are also important to discuss the lower bounds of sfermion masses conservatively. However, there are almost no constraints from the current d_n bound even in *complex* Y_u *type*. The current d_e bound constrains the heavy sfermion mass as $m_0 >$ 5-6 TeV. In a near future, the electron EDM experiments are improved and we expect that strong constraint to m_0 is given or some signals are observed in future experiments. On the other hand, $m_{\tilde{t}}$ is not constrained by d_e. Therefore, an improvement of the neutron EDM is needed to constrain the stop mass. Of course, not only the experimental improvement but also the theoretical improvement in the calculation of Hg EDM are important.

7 Conclusion

The scale of GUTs ($10^{15\text{-}16}$ GeV) is much higher than the weak scale. Therefore, direct searches for the GUT are difficult in the current (and maybe future) experiments, and to search for predictions of GUT models, which can be observed at low energy, is important for testing such a model. In this thesis, we have obtained such predictions in the realistic SUSY GUT models which can realize the observed fermion mass hierarchies and CKM matrix.

We especially focused on the method in which the SM matter fields are given by linear combinations of matter fields considered in the model. Because of this field mixing, undesired relations predicted in some GUT models are modified and realistic mass spectrum can be obtained. In some of models, flavor-violating couplings are obtained by this mixing and induce FCNC in specific processes.

One of such models is our $SO(10)$ SUSY GUT model discussed in Sec. 4. In this model, we introduced three additional fields, $\mathbf{10}$, as matters in addition to $\mathbf{16}_i$ matter fields. Therefore, we have six $\bar{\mathbf{5}}$ matter fields and these fields mix with each other after extra $U(1)'$ gauge symmetry is broken. We considered that this symmetry breaking is caused around the SUSY breaking scale which is $\mathcal{O}(100)$ TeV in this model. Therefore, a scale of extra gauge boson Z' is also $\mathcal{O}(100)$ TeV. Since there are flavor-violating Z' couplings induced by the field mixing, FCNC processes mediated by Z' are induced at tree-level and important for this model even when $m_{Z'} \simeq 100$ TeV. Moreover, since this flavor-violating couplings are only for matter fields belonging to $\bar{\mathbf{5}}$ field, some prediction specific to this model would be obtained. Therefore, we have investigated our predictions from the current FCNC bounds.

As a result, our model is most sensitive to the CP-violating parameter ϵ_K in K^0-$\overline{K^0}$ mixing. We found that its deviation can be larger than 10 %. Another predictions are obtained from LFV μ decays, $\mu \to 3\,e$ and μ-e conversion. We can conclude that our model is still safe for the bounds of these processes. Moreover, if $m_{Z'}$ is $\mathcal{O}(10)$ TeV, our predictions can reach future expected bounds. One of the important features of our flavor-violating couplings is that its (b, s)-element tends to be large because $A^d_{bs} \propto m^d_s m^d_b$. Therefore, some predictions are expected in B physics. However, the deviation from the SM predictions for $B^0_{(s)}$-$\overline{B^0_{(s)}}$ are smaller than 10 % unless $m_{Z'}$ is around $\mathcal{O}(10)$ TeV. The important point is that our model can be tested indirectly, even though the SUSY breaking scale and hence Z' scale are $\mathcal{O}(100)$ TeV which is too high scale to reach at the LHC.

We have also discussed the E_6 model with $SU(2)_F$ family and anomalous $U(1)_A$ gauge symmetries in Sec. 5. In such a model, almost all the problems caused in a SUSY GUT model are solved in the natural assumption. One of the interesting features of this model

is the sfermion mass spectrum. Since all the sfermion masses other than stop mass are degenerated in this spectrum called MUSM in this thesis, SUSY contributions to FCNC processes are suppressed without destabilizing the weak scale.

In this model, however, there are non-vanishing D-term contributions to the MUSM. Since these contributions are dependent on the flavor, the degeneracy of the MUSM is destroyed, and D-terms are constrained by FCNC processes. Therefore, we have discussed the size of D-term contributions. If the stop mass is around 1 TeV and the other sfermion masses are $\mathcal{O}(10)$ TeV, we found that these contributions can be sizable even when the most strongest constraint in FCNC processes are considered. Therefore, small but sizable contributions to the MUSM may become the evidence of this model if all the sfermion masses are observed in future experiments and almost degenerated except for the stop mass. In addition, we found the novel relation $(m^2_{10})_{22} - (m^2_{10})_{11} = (m^2_{\bar{5}^0})_{33} - (m^2_{\bar{5}^0})_{11}$ which is specific to this model, so that to verify this relation is also important to test this model.

In fact, the natural SUSY-type sfermion mass spectrum like the MUSM is severely constrained by CEDMs. This is caused by the smallness of the stop mass. A simple solution is that one takes stop mass to be heavy, though it leads to destabilization of the weak scale. Moreover, the constraint of up quark CEDM is still severe even if all the SUSY-breaking parameters are set to be real. To satisfy the CEDM constraints with light stop mass, real Y_u at the GUT scale is a good solution. Therefore, we have searched the lower bounds of sfermion masses and discussed the difference of the lower bounds in three types of structures of Yukawa couplings in Sec. 6.

We found that when we assume that Y_u is real at the GUT scale, the CEDM bounds are satisfied even when the stop mass is 1 TeV. On the other hand, roughly speaking, the stop mass should be larger than 7 TeV when Y_u is complex at the GUT scale. We obtained these bounds from the current mercury EDM bound, although there are still large uncertainties in the theoretical calculation of $d_{\rm Hg}$. Therefore, we also investigated the lower bounds from the neutron EDM bound. However in such case, we did not obtain any constraints even when Y_u is complex at the GUT scale. If the neutron EDM bound is improved in future, heavy sfermion masses are constrained as $m_0 > 20$ TeV. To satisfy the future expected d_n bound, the stop mass should be much larger than 10 TeV in the case of complex Y_u at the GUT scale, while the light stop mass ($\sim \mathcal{O}(1)$ TeV) is still allowed if Y_u is real at the GUT scale. Note that at present, the bound from electron EDM may be also important to discuss the lower bounds of sfermion masses. However, we cannot obtain the stop mass bound from d_e bound, so that theoretical and/or experimental improvement is needed to constrain the stop mass.

Acknowledgements

First of all, I am deeply grateful to Nobuhiro Maekawa for supervising my work, for instructive discussions, for his various advices and continuous encouragement. I am also very grateful to thank Junji Hisano and Pyungwon Ko for kindly discussing with me, for instructive suggestions and for continuous encouragement.

Furthermore, I am also grateful to Kazuhiro Tobe, Yuji Omura, Yu Muramatsu and Chaehyun Yu for fruitful discussions, for instructive suggestions and for giving me much constructive advice.

I would like to thank Ken Kikuchi and Shohei Okawa for instructive suggestions and for fruitful discussions. I would also like to thank Manabu Yoshida and Shuhei Iguro for collaborating new works and for fruitful discussions.

I also thank my good friends, Satoshi Akagi, Taishi Ikeda, Meguru Komada, Sosuke Noda, Kazuhisa Okamoto, Daiki Suenaga and many others for sharing wonderful time with me.

Finally, I owe my deepest gratitude to my parents for their endless support.

This work is supported by the Japan Society for the Promotion of Science (JSPS) Research Fellowships for Young Scientists, No. 16J08299.

A Notation

In this section, we list a notation for this thesis.

$$\sigma^\mu = \left(\mathbf{1}, \sigma^i\right) \qquad (i = 1, 2, 3), \tag{A.1}$$

where $\mathbf{1}$ is a 2×2 unit matrix. The Pauli matrices are

$$\sigma^1 = \begin{pmatrix} 0 & 1 \\ 1 & 0 \end{pmatrix}, \quad \sigma^2 = \begin{pmatrix} 0 & -i \\ i & 0 \end{pmatrix}, \quad \sigma^3 = \begin{pmatrix} 1 & 0 \\ 0 & -1 \end{pmatrix}. \tag{A.2}$$

The gamma matrices are

$$\gamma^0 = \begin{pmatrix} \mathbf{0} & \mathbf{1} \\ \mathbf{1} & \mathbf{0} \end{pmatrix}, \quad \gamma^1 = \begin{pmatrix} \mathbf{0} & \sigma^1 \\ -\sigma^1 & \mathbf{0} \end{pmatrix}, \quad \gamma^2 = \begin{pmatrix} \mathbf{0} & \sigma^2 \\ -\sigma^2 & \mathbf{0} \end{pmatrix}, \quad \gamma^3 = \begin{pmatrix} \mathbf{0} & \sigma^3 \\ -\sigma^3 & \mathbf{0} \end{pmatrix}, \tag{A.3}$$

where $\mathbf{0}$ is a 2×2 zero matrix. γ^5 matrix is defined as

$$\gamma^5 \equiv i\gamma^0\gamma^1\gamma^2\gamma^3 = \begin{pmatrix} \mathbf{-1} & \mathbf{0} \\ \mathbf{0} & \mathbf{1} \end{pmatrix}. \tag{A.4}$$

Projection operators are written by γ^5 as

$$P_L = \frac{1 - \gamma^5}{2}, \qquad P_R = \frac{1 + \gamma^5}{2}. \tag{A.5}$$

Charge conjugation is defined as

$$\psi^c \equiv \mathcal{C}\psi\mathcal{C} = -i\gamma^2\psi^* = -i\gamma^2\gamma^0\bar{\psi}^T = C\bar{\psi}^T, \tag{A.6}$$

where $C \equiv -i\gamma^2\gamma^0 = i\gamma^0\gamma^2$.

B RGEs for the $\Delta F = 2$ processes

The one-loop RGE for $\widetilde{Q}_1^q$ is given by

$$\mu \frac{d}{d\mu} \widetilde{C}_1^q = -\frac{\alpha_s}{2\pi} \left(\frac{3}{N_c} - 3 \right) \widetilde{C}_1^q. \tag{B.1}$$

Using the one-loop description of the RGE running of α_s, we can estimate the one-loop Wilson coefficients in the each process: for the K^0-$\overline{K^0}$ mixing,

$$\widetilde{C}_1^K(m_K) = \left(\frac{\alpha_s(m_c)}{\alpha_s(m_K)} \right)^{\frac{2}{9}} \left(\frac{\alpha_s(m_b)}{\alpha_s(m_c)} \right)^{\frac{6}{25}} \left(\frac{\alpha_s(m_t)}{\alpha_s(m_b)} \right)^{\frac{6}{23}} \left(\frac{\alpha_s(M_{Z'})}{\alpha_s(m_t)} \right)^{\frac{2}{7}} \widetilde{C}_1^K(M_{Z'}), \tag{B.2}$$

and for the $B^0_{(s)}$-$\overline{B^0_{(s)}}$ mixing,

$$\widetilde{C}_1^{B_{(s)}}(m_b) = \left(\frac{\alpha_s(m_t)}{\alpha_s(m_b)} \right)^{\frac{6}{23}} \left(\frac{\alpha_s(M_{Z'})}{\alpha_s(m_t)} \right)^{\frac{2}{7}} \widetilde{C}_1^{B_{(s)}}(M_{Z'}). \tag{B.3}$$

C Functions

The functions which appear in the K^0-$\overline{K^0}$ and $B^0_{(s)}$-$\overline{B^0_{(s)}}$ mixing are given by

$$S_0(x) = \frac{4x - 11x^2 + x^3}{4(1-x)^2} - \frac{3x^3 \log x}{2(1-x)^3}, \tag{C.1}$$

$$\begin{aligned} S(x,y) &= \frac{-3xy}{4(y-1)(x-1)} - \frac{xy(4 - 8y + y^2)\log y}{4(y-1)^2(x-y)} \\ &\quad + \frac{xy(4 - 8x + x^2)\log x}{4(x-1)^2(x-y)}. \end{aligned} \tag{C.2}$$

The function for the short-distance contribution to $K_L \to \pi\overline{\nu}\nu$ is defined as

$$X(x) = \frac{x}{8} \left\{ \frac{x+2}{x-1} + \frac{3x-6}{(x-1)^2} \log x \right\}. \tag{C.3}$$

The function for $B_{s(d)} \to \mu^+\mu^-$ is defined as

$$Y_0(x) = \frac{x}{8} \left\{ \frac{x-4}{x-1} + \frac{3x}{(x-1)^2} \ln x \right\}. \tag{C.4}$$

D The coefficients of diagonalizing matrices

In Appendix A in Ref. [148], we show how to diagonalize the 3×3 matrix Y_{ij}. Here we show the diagonalizing matrices for up-type quarks, down-type quarks and charged leptons in the leading order. The diagonalizing matrices L_ψ and R_ψ come from mixing angles $s_{ij}^{\psi L/R} \equiv \sin\theta_{ij}^{\psi L/R} e^{i\chi_{ij}^{\psi L/R}}$ and $c_{ij}^{\psi L/R} \equiv \cos\theta_{ij}^{\psi L/R}$. In our calculation we use the approximation that the mixing angles are small, i.e. $|s_{ij}^{\psi L/R}| \sim |\theta_{ij}^{\psi L/R}| \ll 1$ ($s_{ij}^{\psi L/R} \sim \theta_{ij}^{\psi L/R} e^{i\chi_{ij}^{\psi L/R}}$) and $c_{ij}^{\psi L/R} \simeq 1$. In this approximation the diagonalizing matrices are

$$L_\psi \simeq \begin{pmatrix} 1 & s_{12}^{\psi L*} & s_{13}^{\psi L*} \\ -s_{12}^{\psi L} & 1 & s_{23}^{\psi L*} \\ -s_{13}^{\psi L} + s_{23}^{\psi L} s_{12}^{\psi L} & -s_{23}^{\psi L} & 1 \end{pmatrix}, \tag{D.1}$$

$$R_\psi \simeq \begin{pmatrix} 1 & s_{12}^{\psi R} & s_{13}^{\psi R} \\ -s_{12}^{\psi R*} & 1 & s_{23}^{\psi R} \\ -s_{13}^{\psi R*} + s_{23}^{\psi R*} s_{12}^{\psi R*} & -s_{23}^{\psi R*} & 1 \end{pmatrix}. \tag{D.2}$$

From Eq. (5.11), the mixing angles for up-type quarks are calculated as

$$s_{23}^{uL} = s_{23}^{uR*} \simeq \frac{b}{a}\lambda^2 \equiv R_{23}^{uL}\lambda^2,\ s_{13}^{uL} = s_{13}^{uR*} \simeq 0,\ s_{12}^{uL} = -s_{12}^{uR*} \simeq \frac{\frac{1}{3}ad_q}{ac-b^2}\lambda \equiv \frac{1}{3}R_{12}^{uL}\lambda. \tag{D.3}$$

From Eq. (5.12), the mixing angles for down-type quarks are calculated as

$$s_{23}^{dL} \simeq \frac{cg-bf}{bg-af}\lambda^2 \equiv R_{23}^{dL}\lambda^2, s_{13}^{dL} \simeq \frac{1}{3}\frac{d_q g}{bg-af}\lambda^3 \equiv \frac{1}{3}R_{13}^{dL}\lambda^3, \tag{D.4}$$

$$\begin{aligned} s_{12}^{dL} &\simeq -\frac{2}{3}\frac{(bg-af)^2 d_5}{(ac-b^2)\{f(bg-af)-g(cg-bf)\}}\lambda \\ &\quad + \frac{4}{27}\frac{a^2 d_q d_5^2}{(ac-b^2)\{f(bg-af)-g(cg-bf)\}\beta_H} e^{-i(2\rho-\delta)}\lambda \\ &\equiv \left(\frac{2}{3}R_{12}^{dL} + \frac{4}{27}I_{12}^{dL} e^{-i(2\rho-\delta)}\right)\lambda, \end{aligned}$$

$$s_{23}^{dR*} \simeq \frac{g^2\beta_H}{bg-af} e^{i(\rho-\delta)}\lambda^{0.5} - \frac{4}{9}\frac{d_5^2 a^2}{(ac-b^2)(bg-af)} e^{-i\rho}\lambda^{0.5} \tag{D.5}$$

$$\equiv I_{23}^{dR} e^{i(\rho-\delta)}\lambda^{0.5} - \frac{4}{9} I_{23}^{\prime dR} e^{-i\rho}\lambda^{0.5}, \tag{D.6}$$

$$s_{13}^{dR*} \simeq -\frac{2}{3}\frac{ad_5}{ac-b^2}\lambda \equiv \frac{2}{3}R_{13}^{dR}\lambda,$$

$$s_{12}^{dR*} \simeq \frac{2}{3}\frac{d_5(bg-af)}{\{f(bg-af)-g(cg-bf)\}\beta_H}e^{-i(\rho-\delta)}\lambda^{0.5} \equiv \frac{2}{3}I_{12}^{dR}e^{-i(\rho-\delta)}\lambda^{0.5}.$$

From Eq. (5.13), the mixing angles for charged lepton are calculated as

$$s_{23}^{eL} \simeq \frac{g^2\beta_H}{bg-af}e^{i(\rho-\delta)}\lambda^{0.5} \equiv I_{23}^{dR}e^{i(\rho-\delta)}\lambda^{0.5},\ s_{13}^{eL} \simeq 0, \tag{D.7}$$

$$s_{12}^{eL} \simeq \frac{d_l(bg-af)}{\{f(bg-af)-g(cg-bf)\}\beta_H}e^{-i(\rho-\delta)}\lambda^{0.5} \equiv I_{12}^{eL}e^{-i(\rho-\delta)}\lambda^{0.5}$$

$$s_{23}^{eR*} \simeq s_{23}^{dL} \equiv R_{23}^{dL}\lambda^2,\ s_{13}^{eR*} \simeq -\frac{d_l g}{bg-af}\lambda^3 \equiv R_{13}^{eR}\lambda^3, \tag{D.8}$$

$$s_{12}^{eR*} \simeq \frac{d_l g^2}{\{f(bg-af)-g(cg-bf)\}}\lambda \equiv R_{12}^{eR}\lambda.$$

The diagonalizing matrices for up-type quarks, down-type quarks and charged leptons are calculated as

$$L_u \sim \begin{pmatrix} 1 & \frac{1}{3}R_{12}^{uL}\lambda & 0 \\ -\frac{1}{3}R_{12}^{uL}\lambda & 1 & R_{23}^{uL}\lambda^2 \\ \frac{1}{3}R_{23}^{uL}R_{12}^{uL}\lambda^3 & -R_{23}^{uL}\lambda^2 & 1 \end{pmatrix}, \tag{D.9}$$

$$R_u \sim \begin{pmatrix} 1 & -\frac{1}{3}R_{12}^{uL}\lambda & 0 \\ \frac{1}{3}R_{12}^{uL}\lambda & 1 & R_{23}^{uL}\lambda^2 \\ -\frac{1}{3}R_{23}^{uL}R_{12}^{uL}\lambda^3 & -R_{23}^{uL}\lambda^2 & 1 \end{pmatrix}, \tag{D.10}$$

$$L_d = \begin{pmatrix} 1 & (\frac{2}{3}R_{12}^{dL} + \frac{4}{27}I_{12}^{dL}e^{i(2\rho-\delta)})\lambda & \frac{1}{3}R_{13}^{dL}\lambda^3 \\ -(\frac{2}{3}R_{12}^{dL} + \frac{4}{27}I_{12}^{dL}e^{-i(2\rho-\delta)})\lambda & 1 & R_{23}^{dL}\lambda^2 \\ (-\frac{1}{3}R_{13}^{dL} + \frac{2}{3}R_{23}^{dL}R_{12}^{dL} + \frac{4}{27}R_{23}^{dL}I_{12}^{dL}e^{-i(2\rho-\delta)})\lambda^3 & -R_{23}^{dL}\lambda^2 & 1 \end{pmatrix},$$

$$R_d = \begin{pmatrix} 1 & \frac{2}{3}I_{12}^{dR}e^{i(\rho-\delta)}\lambda^{0.5} & \frac{2}{3}R_{13}^{dR}\lambda \\ -\frac{2}{3}I_{12}^{dR}e^{-i(\rho-\delta)}\lambda^{0.5} & 1 & I_{23}^{dR}e^{-i(\rho-\delta)}\lambda^{0.5} \\ (-\frac{2}{3}R_{13}^{dR} + \frac{2}{3}I_{23}^{dR}I_{12}^{dR} - \frac{8}{27}I_{23}^{\prime dR}I_{12}^{dR}e^{-i(2\rho-\delta)})\lambda & -I_{23}^{dR}e^{i(\rho-\delta)}\lambda^{0.5} & 1 \end{pmatrix}$$

$$L_e \sim \begin{pmatrix} 1 & I_{12}^{eL}e^{i(\rho-\delta)}\lambda^{0.5} & 0 \\ -I_{12}^{eL}e^{-i(\rho-\delta)}\lambda^{0.5} & 1 & I_{23}^{dR}e^{-i(\rho-\delta)}\lambda^{0.5} \\ I_{23}^{dR}I_{12}^{eL}\lambda & -I_{23}^{dR}e^{i(\rho-\delta)}\lambda^{0.5} & 1 \end{pmatrix}, \tag{D.11}$$

$$R_e \sim \begin{pmatrix} 1 & R_{12}^{eR}\lambda & R_{13}^{eR}\lambda^3 \\ -R_{12}^{eR}\lambda & 1 & R_{23}^{dL}\lambda^2 \\ (-R_{13}^{eR} + R_{23}^{dL}R_{12}^{eR})\lambda^3 & -R_{23}^{dL}\lambda^2 & 1 \end{pmatrix}. \tag{D.12}$$

In this model the Majorana neutrino mass matrix has a lot of other real parameters and

CP phases, and therefore, we cannot constrain the diagonalizing matrix for neutrino. The diagonalizing matrix for neutrino is written as

$$L_\nu \sim \begin{pmatrix} 1 & \lambda^{0.5} & \lambda \\ \lambda^{0.5} & 1 & \lambda^{0.5} \\ \lambda & \lambda^{0.5} & 1 \end{pmatrix}, \tag{D.13}$$

where we have omitted the complex $O(1)$ coefficients. In this model we can obtain realistic CKM and MNS matrices as

$$\begin{aligned} V_{\rm CKM} &= L_u^\dagger L_d \\ &\sim \begin{pmatrix} 1 & (-\frac{1}{3}R_{12}^{uL} + \frac{2}{3}R_{12}^{dL} + \frac{4}{27}I_{12}^{dL}e^{i(\rho-\delta)})\lambda & O(\lambda^4) \\ (\frac{1}{3}R_{12}^{uL} - \frac{2}{3}R_{12}^{dL} - \frac{4}{27}I_{12}^{dL}e^{-i(2\rho-\delta)})\lambda & 1 & (-R_{23}^{uL} + R_{23}^{dL})\lambda^2 \\ \{-\frac{2}{3}R_{23}^{uL}R_{12}^{dL} - \frac{1}{3}R_{13}^{dL} + \frac{2}{3}I_{23}^{dL}I_{12}^{dL} - \frac{4}{27}(R_{23}^{uL} - R_{23}^{dL})I_{12}^{dL}e^{-i(2\rho-\delta)}\}\lambda^3 & (R_{23}^{uL} - R_{23}^{dL})\lambda^2 & 1 \end{pmatrix}, \end{aligned} \tag{D.14}$$

$$|V_{\rm MNS}| = \left|L_\nu^\dagger L_e\right| \sim \begin{pmatrix} 1 & \lambda^{0.5} & \lambda \\ \lambda^{0.5} & 1 & \lambda^{0.5} \\ \lambda & \lambda^{0.5} & 1 \end{pmatrix}. \tag{D.15}$$

As discussed in Ref. [72–75], the leading contribution to the component $(V_{\rm CKM})_{13}$ is cancelled and the sub-leading contribution $O(\lambda^4)$ dominates $(V_{\rm CKM})_{13}$.

E Mass insertion parameters

In this appendix, we just show all mass insertion parameters in the $E_6 \times SU(2)_F \times U(1)_A$ SUSY GUT model.

$$(\delta_{12}^u)_{LL} = -(\delta_{12}^u)_{RR} \simeq \left\{-\frac{1}{3}R_{12}^{uL}\lambda\Delta m_{10,2}^2 - \frac{1}{3}(R_{23}^{uL})^2 R_{12}^{uL}\lambda^5\Delta m_{10,3}^2\right\}/m_{\tilde{u}}^2 \tag{E.1}$$

$$(\delta_{13}^u)_{LL} = -(\delta_{13}^u)_{RR} \simeq \left\{-\frac{1}{3}R_{23}^{uL}R_{12}^{uL}\Delta m_{10,2}^2 + \frac{1}{3}R_{23}^{uL}R_{12}^{uL}\Delta m_{10,3}^2\right\}\lambda^3/m_{\tilde{u}}^2 \tag{E.2}$$

$$(\delta_{23}^u)_{LL} = (\delta_{23}^u)_{RR} \simeq R_{23}^{uL}\{\Delta m_{10,2}^2 - \Delta m_{10,3}^2\}\lambda^2/m_{\tilde{u}}^2 \tag{E.3}$$

$$(\delta_{12}^d)_{LL} \simeq \left\{-\left(\frac{2}{3}R_{12}^{dL} + \frac{4}{27}I_{12}^{dL}e^{i(2\rho-\delta)}\right)\lambda\Delta m_{10,2}^2 \right. \tag{E.4}$$

$$-R_{23}^{dL}\left(-\frac{1}{3}R_{13}^{dL}+\frac{2}{3}R_{23}^{dL}R_{12}^{dL}+\frac{4}{27}R_{23}^{dL}I_{12}^{dL}e^{i(2\rho-\delta)}\right)\lambda^5\Delta m_{10,3}^2\Bigg\}/m_{\tilde{d}}^2$$

$$(\delta_{13}^d)_{LL}\simeq\Bigg\{-R_{23}^{dL}\left(\frac{2}{3}R_{12}^{dL}+\frac{4}{27}I_{12}^{dL}e^{i(2\rho-\delta)}\right)\Delta m_{10,2}^2 \tag{E.5}$$
$$+\left(-\frac{1}{3}R_{13}^{dL}+\frac{2}{3}R_{23}^{dL}R_{12}^{dL}+\frac{4}{27}R_{23}^{dL}I_{12}^{dL}e^{i(2\rho-\delta)}\right)\Delta m_{10,3}^2\Bigg\}\lambda^3/m_{\tilde{d}}^2$$

$$(\delta_{23}^d)_{LL}\simeq R_{23}^{dL}\{\Delta m_{10,2}^2-\Delta m_{10,3}^2\}\lambda^2/m_{\tilde{d}}^2 \tag{E.6}$$

$$(\delta_{12}^d)_{RR}\simeq\left\{-\frac{2}{3}I_{12}^{dR}e^{i(\rho-\delta)}\lambda^{0.5}\Delta m_{\bar{5},2}^2-I_{23}^{dR}\left(-\frac{2}{3}R_{13}^{dR}+\frac{2}{3}I_{23}^{dR}I_{12}^{dR}\right)e^{i(\rho-\delta)}\lambda^{1.5}\Delta m_{\bar{5},3}^2\right\}/m_{\tilde{d}}^2 \tag{E.7}$$

$$(\delta_{13}^d)_{RR}\simeq\Bigg\{\left(-\frac{2}{3}I_{23}^{dR}I_{12}^{dR}+\frac{8}{27}I_{12}^{dR}I_{23}^{\prime dR}e^{i(2\rho-\delta)}\right)\Delta m_{\bar{5},2}^2 \tag{E.8}$$
$$+\left(-\frac{2}{3}R_{13}^{dR}+\frac{2}{3}I_{23}^{dR}I_{12}^{dR}-\frac{8}{27}I_{23}^{\prime dR}I_{12}^{dR}e^{i(2\rho-\delta)}\right)\Delta m_{\bar{5},3}^2\Bigg\}\lambda/m_{\tilde{d}}^2$$

$$(\delta_{23}^d)_{RR}\simeq I_{23}^{dR}e^{-i(\rho-\delta)}\{\Delta m_{\bar{5},2}^2-\Delta m_{\bar{5},3}^2\}\lambda^{0.5}/m_{\tilde{d}}^2 \tag{E.9}$$

$$(\delta_{12}^e)_{LL}\simeq-I_{12}^{eL}e^{i(\rho-\delta)}\{\lambda^{0.5}\Delta m_{\bar{5},2}^2+(I_{23}^{dR})^2\lambda^{1.5}\Delta m_{\bar{5},3}^2\}/m_{\tilde{e}}^2 \tag{E.10}$$

$$(\delta_{13}^e)_{LL}\simeq-I_{23}^{dR}I_{12}^{eL}\{\Delta m_{\bar{5},2}^2-\Delta m_{\bar{5},3}^2\}\lambda/m_{\tilde{e}}^2 \tag{E.11}$$

$$(\delta_{23}^e)_{LL}\simeq I_{23}^{dR}e^{-i(\rho-\delta)}\{\Delta m_{\bar{5},2}^2-\Delta m_{\bar{5},3}^2\}\lambda^{0.5}/m_{\tilde{e}}^2 \tag{E.12}$$

$$(\delta_{12}^e)_{RR}\simeq\{-R_{12}^{eR}\lambda\Delta m_{10,2}^2-R_{23}^{dL}(-R_{13}^{eR}+R_{23}^{dL}R_{12}^{eR})\lambda^5\Delta m_{10,3}^2\}/m_{\tilde{e}}^2 \tag{E.13}$$

$$(\delta_{13}^e)_{RR}\simeq\{-R_{23}^{dL}R_{12}^{eR}\Delta m_{10,2}^2+(-R_{13}^{eR}+R_{23}^{dL}R_{12}^{eR})\Delta m_{10,3}^2\}\lambda^3/m_{\tilde{e}}^2 \tag{E.14}$$

$$(\delta_{23}^e)_{RR}\simeq R_{23}^{dL}\{\Delta m_{10,2}^2-\Delta m_{10,3}^2\}\lambda^2/m_{\tilde{e}}^2 \tag{E.15}$$

F Loop integral for the dominant diagram to d_u^C

The expression of up quark CEDM d_u^C in mass insertion approximation is

$$d_u^C = \frac{\alpha_s}{4\pi}\frac{M_{\tilde{g}}}{m_{\tilde{t}}^2}\mathrm{Im}\left[(\delta_{LL}^u)_{31}(\delta_{RL}^u)_{33}(\delta_{RR}^u)_{13}\right]\times F_{\mathrm{MIA}}(r_{\tilde{g}},r_{\tilde{t}}) \tag{F.1}$$

$$F_{\mathrm{MIA}}(r_{\tilde{g}},r_{\tilde{t}}) \equiv 6\,r_{\tilde{t}}^2\left(-3I_G(r_{\tilde{g}},r_{\tilde{t}})+\frac{1}{3}I_{S_1}(r_{\tilde{g}},r_{\tilde{t}})+\frac{1}{3}I_{S_2}(r_{\tilde{g}},r_{\tilde{t}})+\frac{1}{3}I_{S_3}(r_{\tilde{g}},r_{\tilde{t}})+\frac{1}{3}I_{S_4}(r_{\tilde{g}},r_{\tilde{t}})\right) \tag{F.2}$$

where $r_{\tilde{g}} = \frac{M_{\tilde{g}}^2}{m_{\tilde{u}}^2}$, $r_{\tilde{t}} = \frac{m_{\tilde{t}}^2}{m_{\tilde{u}}^2}$ and $I_i(r_{\tilde{g}}, r_{\tilde{t}})$ are loop integrals. Each integral are

$$I_G(r_{\tilde{g}}, r_{\tilde{t}}) = \int_0^1 dx_1 \cdots dx_4 \delta(\Sigma_i x_i - 1) \frac{2x_1 x_3 x_4}{[r_{\tilde{g}}(x_1 + x_2) + x_3 + r_{\tilde{t}} x_4]^4}, \tag{F.3}$$

$$I_{S_1}(r_{\tilde{g}}, r_{\tilde{t}}) = \int_0^1 dx_1 \cdots dx_4 \delta(\Sigma_i x_i - 1) \frac{(2x_3 + 2x_4 - 1)x_3 x_4}{[r_{\tilde{g}} x_1 + x_2 + x_3 + r_{\tilde{t}} x_4]^4}, \tag{F.4}$$

$$I_{S_2}(r_{\tilde{g}}, r_{\tilde{t}}) = \int_0^1 dx_1 \cdots dx_5 \delta(\Sigma_i x_i - 1) \frac{(2x_3 + 2x_5 - 1)x_5}{[r_{\tilde{g}} x_1 + x_2 + x_3 + r_{\tilde{t}}(x_4 + x_5)]^4}, \tag{F.5}$$

$$I_{S_3}(r_{\tilde{g}}, r_{\tilde{t}}) = \int_0^1 dx_1 \cdots dx_5 \delta(\Sigma_i x_i - 1) \frac{(2x_3 + 2x_5 - 1)x_4}{[r_{\tilde{g}} x_1 + x_2 + x_3 + r_{\tilde{t}}(x_4 + x_5)]^4}, \tag{F.6}$$

$$I_{S_4}(r_{\tilde{g}}, r_{\tilde{t}}) = \int_0^1 dx_1 \cdots dx_4 \delta(\Sigma_i x_i - 1) \frac{(2x_3 - 1)x_2 x_4}{[r_{\tilde{g}} x_1 + x_2 + x_3 + r_{\tilde{t}} x_4]^4}. \tag{F.7}$$

We show the values of $F_{\rm MIA}(r_{\tilde{g}}, r_{\tilde{t}})$ with several values of mass ratio, $r_{\tilde{g}}$ and $r_{\tilde{t}}$.

$r_{\tilde{t}} \setminus r_{\tilde{g}}$	0.2^2	0.3^2	0.5^2	1^2	2^2	5^2
0.1^2	4.1×10^{-2}	1.1×10^{-2}	1.8×10^{-3}	1.2×10^{-4}	6.9×10^{-6}	1.6×10^{-7}
0.2^2	2.4×10^{-1}	7.9×10^{-2}	1.6×10^{-2}	1.2×10^{-3}	6.9×10^{-5}	1.5×10^{-6}
0.3^2	5.3×10^{-1}	2.0×10^{-1}	4.6×10^{-2}	4.0×10^{-3}	2.4×10^{-4}	5.1×10^{-6}
0.4^2	8.5×10^{-1}	3.6×10^{-1}	9.1×10^{-2}	8.8×10^{-3}	5.6×10^{-4}	1.2×10^{-5}
0.5^2	1.2	5.2×10^{-1}	1.4×10^{-1}	1.5×10^{-2}	1.0×10^{-3}	2.1×10^{-5}
0.6^2	1.4	6.8×10^{-1}	2.0×10^{-1}	2.3×10^{-2}	1.6×10^{-3}	3.4×10^{-5}
0.7^2	1.7	8.2×10^{-1}	2.6×10^{-1}	3.2×10^{-2}	2.3×10^{-3}	5.0×10^{-5}
0.8^2	1.9	9.6×10^{-1}	3.2×10^{-1}	4.1×10^{-2}	3.2×10^{-3}	6.8×10^{-5}
0.9^2	2.1	1.1	3.7×10^{-1}	5.1×10^{-2}	4.1×10^{-3}	8.9×10^{-5}
1^2	2.3	1.2	4.2×10^{-1}	6.1×10^{-2}	5.0×10^{-3}	1.1×10^{-4}
2^2	3.2	1.8	7.6×10^{-1}	1.4×10^{-1}	1.5×10^{-2}	4.0×10^{-4}
5^2	3.7	2.3	1.0	2.4×10^{-1}	3.3×10^{-2}	1.2×10^{-3}

Table 14: The values of $F_{\rm MIA}(r_{\tilde{g}}, r_{\tilde{t}})$ with several values of $r_{\tilde{g}}$ and $r_{\tilde{t}}$.

References

[1] G. Aad *et al.* [ATLAS Collaboration], "Observation of a new particle in the search for the Standard Model Higgs boson with the ATLAS detector at the LHC," Phys. Lett. B **716**, 1 (2012) [arXiv:1207.7214 [hep-ex]].

[2] S. Chatrchyan *et al.* [CMS Collaboration], "Observation of a new boson at a mass of 125 GeV with the CMS experiment at the LHC," Phys. Lett. B **716**, 30 (2012) [arXiv:1207.7235 [hep-ex]].

[3] Q. R. Ahmad *et al.* [SNO Collaboration], "Direct evidence for neutrino flavor transformation from neutral current interactions in the Sudbury Neutrino Observatory," Phys. Rev. Lett. **89**, 011301 (2002) [nucl-ex/0204008].

[4] S. Fukuda *et al.* [Super-Kamiokande Collaboration], "Determination of solar neutrino oscillation parameters using 1496 days of Super-Kamiokande I data," Phys. Lett. B **539**, 179 (2002) [hep-ex/0205075].

[5] K. Eguchi *et al.* [KamLAND Collaboration], "First results from KamLAND: Evidence for reactor anti-neutrino disappearance," Phys. Rev. Lett. **90**, 021802 (2003) [hep-ex/0212021].

[6] Y. Ashie *et al.* [Super-Kamiokande Collaboration], "Evidence for an oscillatory signature in atmospheric neutrino oscillation," Phys. Rev. Lett. **93**, 101801 (2004) [hep-ex/0404034].

[7] B. Aharmim *et al.* [SNO Collaboration], "Electron energy spectra, fluxes, and day-night asymmetries of ^{8}B solar neutrinos from measurements with NaCl dissolved in the heavy-water detector at the Sudbury Neutrino Observatory," Phys. Rev. C **72**, 055502 (2005) [nucl-ex/0502021].

[8] T. Araki *et al.* [KamLAND Collaboration], "Measurement of neutrino oscillation with KamLAND: Evidence of spectral distortion," Phys. Rev. Lett. **94**, 081801 (2005) [hep-ex/0406035].

[9] M. H. Ahn *et al.* [K2K Collaboration], "Measurement of Neutrino Oscillation by the K2K Experiment," Phys. Rev. D **74**, 072003 (2006) [hep-ex/0606032].

[10] D. G. Michael *et al.* [MINOS Collaboration], "Observation of muon neutrino disappearance with the MINOS detectors and the NuMI neutrino beam," Phys. Rev. Lett. **97**, 191801 (2006) [hep-ex/0607088].

[11] P. Adamson *et al.* [MINOS Collaboration], "Measurement of Neutrino Oscillations with the MINOS Detectors in the NuMI Beam," Phys. Rev. Lett. **101**, 131802 (2008) [arXiv:0806.2237 [hep-ex]].

[12] K. Abe *et al.* [T2K Collaboration], "Indication of Electron Neutrino Appearance from an Accelerator-produced Off-axis Muon Neutrino Beam," Phys. Rev. Lett. **107**, 041801 (2011) [arXiv:1106.2822 [hep-ex]].

[13] K. Abe *et al.* [T2K Collaboration], "First Muon-Neutrino Disappearance Study with an Off-Axis Beam," Phys. Rev. D **85**, 031103 (2012) [arXiv:1201.1386 [hep-ex]].

[14] F. P. An *et al.* [Daya Bay Collaboration], "Observation of electron-antineutrino disappearance at Daya Bay," Phys. Rev. Lett. **108**, 171803 (2012) [arXiv:1203.1669 [hep-ex]].

[15] K. Abe *et al.* [T2K Collaboration], "Measurement of Neutrino Oscillation Parameters from Muon Neutrino Disappearance with an Off-axis Beam," Phys. Rev. Lett. **111**, no. 21, 211803 (2013) [arXiv:1308.0465 [hep-ex]].

[16] N. Agafonova *et al.* [OPERA Collaboration], "Evidence for $\nu_\mu \to \nu_\tau$ appearance in the CNGS neutrino beam with the OPERA experiment," Phys. Rev. D **89**, no. 5, 051102 (2014) [arXiv:1401.2079 [hep-ex]].

[17] K. A. Olive *et al.* [Particle Data Group], "Review of Particle Physics," Chin. Phys. C **38**, 090001 (2014).

[18] G. 't Hooft, "Naturalness, chiral symmetry, and spontaneous chiral symmetry breaking," NATO Sci. Ser. B **59**, 135 (1980).

[19] H. Georgi and S. L. Glashow, "Unity of All Elementary Particle Forces," Phys. Rev. Lett. **32**, 438 (1974).

[20] J. E. Kim and H. P. Nilles, "The μ-Problem and the Strong CP-Problem," Phys. Lett. **138B**, 150 (1984).

[21] H. Georgi, "The State of the Art—Gauge Theories," AIP Conf. Proc. **23**, 575 (1975).

[22] H. Fritzsch and P. Minkowski, "Unified Interactions of Leptons and Hadrons," Annals Phys. **93**, 193 (1975).

[23] H. Georgi and C. Jarlskog, "A New Lepton - Quark Mass Relation in a Unified Theory," Phys. Lett. **86B**, 297 (1979).

[24] J. R. Ellis and M. K. Gaillard, "Fermion Masses and Higgs Representations in SU(5)," Phys. Lett. **88B**, 315 (1979).

[25] G. Lazarides, Q. Shafi and C. Wetterich, "Proton Lifetime and Fermion Masses in an SO(10) Model," Nucl. Phys. B **181**, 287 (1981).

[26] S. M. Barr, "An SO(10) Model of Fermion Masses," Phys. Rev. D **24**, 1895 (1981).

[27] J. Hisano, Y. Muramatsu, Y. Omura and M. Yamanaka, "Flavor violating Z' from $SO(10)$ SUSY GUT in High-Scale SUSY," Phys. Lett. B **744**, 395 (2015) [arXiv:1503.06156 [hep-ph]].

[28] J. Hisano, Y. Muramatsu, Y. Omura and Y. Shigekami, "Flavor physics induced by light Z' from $SO(10)$ GUT," JHEP **1611** (2016) 018 [arXiv:1607.05437 [hep-ph]].

[29] J. Hisano, D. Kobayashi and N. Nagata, "Enhancement of Proton Decay Rates in Supersymmetric SU(5) Grand Unified Models," Phys. Lett. B **716**, 406 (2012) [arXiv:1204.6274 [hep-ph]].

[30] J. Hisano, D. Kobayashi, Y. Muramatsu and N. Nagata, "Two-loop Renormalization Factors of Dimension-six Proton Decay Operators in the Supersymmetric Standard Models," Phys. Lett. B **724**, 283 (2013) [arXiv:1302.2194 [hep-ph]].

[31] J. Hisano, T. Kuwahara and Y. Omura, "Threshold Corrections to Baryon Number Violating Operators in Supersymmetric $SU(5)$ GUTs," Nucl. Phys. B **898** (2015) 1 Erratum: [Nucl. Phys. B **907** (2016) 476] [arXiv:1503.08561 [hep-ph]].

[32] B. Bajc, J. Hisano, T. Kuwahara and Y. Omura, "Threshold corrections to dimension-six proton decay operators in non-minimal SUSY SU(5) GUTs," Nucl. Phys. B **910** (2016) 1 [arXiv:1603.03568 [hep-ph]].

[33] F. Gürsey, P. Ramond and P. Sikivie, "A Universal Gauge Theory Model Based on E_6," Phys. Lett. **60B**, 177 (1976).

[34] Y. Achiman and B. Stech, "Quark Lepton Symmetry and Mass Scales in an E_6 Unified Gauge Model," Phys. Lett. **77B**, 389 (1978).

[35] R. Barbieri and D. V. Nanopoulos, "An Exceptional Model for Grand Unification," Phys. Lett. **91B**, 369 (1980).

[36] T. Kugo and J. Sato, "Dynamical symmetry breaking in an E_6 GUT model," Prog. Theor. Phys. **91**, 1217 (1994) [hep-ph/9402357].

[37] N. Irges, S. Lavignac and P. Ramond, "Predictions from an anomalous U(1) model of Yukawa hierarchies," Phys. Rev. D **58**, 035003 (1998) [hep-ph/9802334].

[38] M. Bando and T. Kugo, "Neutrino masses in E_6 unification," Prog. Theor. Phys. **101**, 1313 (1999) [hep-ph/9902204].

[39] M. Bando, T. Kugo and K. Yoshioka, "Mass matrices in E_6 unification," Prog. Theor. Phys. **104**, 211 (2000) [hep-ph/0003220].

[40] M. Dine, R. G. Leigh and A. Kagan, "Flavor symmetries and the problem of squark degeneracy," Phys. Rev. D **48**, 4269 (1993) [hep-ph/9304299].

[41] A. Pomarol and D. Tommasini, "Horizontal symmetries for the supersymmetric flavor problem," Nucl. Phys. B **466**, 3 (1996) [hep-ph/9507462].

[42] R. Barbieri, G. R. Dvali and L. J. Hall, "Predictions from a U(2) flavor symmetry in supersymmetric theories," Phys. Lett. B **377**, 76 (1996) [hep-ph/9512388].

[43] R. Barbieri and L. J. Hall, "A Grand unified supersymmetric theory of flavor," Nuovo Cim. A **110**, 1 (1997) [hep-ph/9605224].

[44] K. S. Babu and S. M. Barr, "Gauged SO(3) family symmetry and squark mass degeneracy," Phys. Lett. B **387**, 87 (1996) [hep-ph/9606384].

[45] R. Barbieri, L. J. Hall, S. Raby and A. Romanino, "Unified theories with U(2) flavor symmetry," Nucl. Phys. B **493**, 3 (1997) [hep-ph/9610449].

[46] Z. Berezhiani, "Unified picture of the particle and sparticle masses in SUSY GUT," Phys. Lett. B **417**, 287 (1998) [hep-ph/9609342].

[47] G. Eyal, "Models of supersymmetric $U(2) \times U(1)$ flavor symmetry," Phys. Lett. B **441**, 191 (1998) [hep-ph/9807308].

[48] R. Barbieri, P. Creminelli and A. Romanino, "Neutrino mixings from a U(2) flavor symmetry," Nucl. Phys. B **559**, 17 (1999) [hep-ph/9903460].

[49] S. F. King and G. G. Ross, "Fermion masses and mixing angles from SU(3) family symmetry," Phys. Lett. B **520**, 243 (2001) [hep-ph/0108112].

[50] E. Witten, "Some Properties of O(32) Superstrings," Phys. Lett. **149B**, 351 (1984).

[51] M. Dine, N. Seiberg and E. Witten, "Fayet-Iliopoulos Terms in String Theory," Nucl. Phys. B **289**, 589 (1987).

[52] J. J. Atick, L. J. Dixon and A. Sen, "String Calculation of Fayet-Iliopoulos D-terms in Arbitrary Supersymmetric Compactifications," Nucl. Phys. B **292**, 109 (1987).

[53] M. Dine, I. Ichinose and N. Seiberg, "F Terms and D Terms in String Theory," Nucl. Phys. B **293**, 253 (1987).

[54] N. Maekawa, "Neutrino masses, anomalous U(1) gauge symmetry and doublet - triplet splitting," Prog. Theor. Phys. **106**, 401 (2001) [hep-ph/0104200].

[55] N. Maekawa, "Gauge coupling unification with anomalous $\mathrm{U}(1)_A$ gauge symmetry," Prog. Theor. Phys. **107**, 597 (2002) [hep-ph/0111205].

[56] N. Maekawa and T. Yamashita, "Gauge coupling unification in GUT with anomalous U(1) symmetry," Phys. Rev. Lett. **90**, 121801 (2003) [hep-ph/0209217].

[57] N. Maekawa and T. Yamashita, "E_6 unification, doublet-triplet splitting and anomalous $U(1)_A$ symmetry," Prog. Theor. Phys. **107**, 1201 (2002) [hep-ph/0202050].

[58] N. Maekawa and T. Yamashita, "Simple E_6 unification with anomalous $U(1)_A$ symmetry," Prog. Theor. Phys. **110**, 93 (2003) [hep-ph/0303207].

[59] N. Maekawa, "A Natural solution for the μ problem with anomalous $U(1)_A$ gauge symmetry," Phys. Lett. B **521**, 42 (2001) [hep-ph/0107313].

[60] S. Dimopoulos and G. F. Giudice, "Naturalness constraints in supersymmetric theories with nonuniversal soft terms," Phys. Lett. B **357**, 573 (1995) [hep-ph/9507282].

[61] N. Arkani-Hamed and H. Murayama, "Can the supersymmetric flavor problem decouple?," Phys. Rev. D **56**, R6733 (1997) [hep-ph/9703259].

[62] J. Hisano, K. Kurosawa and Y. Nomura, "Natural effective supersymmetry," Nucl. Phys. B **584**, 3 (2000) [hep-ph/0002286].

[63] J. S. Hagelin and S. Kelley, "Sparticle Masses as a Probe of GUT Physics," Nucl. Phys. B **342**, 95 (1990).

[64] Y. Kawamura, H. Murayama and M. Yamaguchi, "Probing symmetry breaking pattern using sfermion masses," Phys. Lett. B **324**, 52 (1994) [hep-ph/9402254].

[65] Y. Kawamura, H. Murayama and M. Yamaguchi, "Low-energy effective Lagrangian in unified theories with nonuniversal supersymmetry breaking terms," Phys. Rev. D **51**, 1337 (1995) [hep-ph/9406245].

[66] Y. Kawamura and M. Tanaka, "Scalar mass spectrum as a probe of E_6 gauge symmetry breaking," Prog. Theor. Phys. **91**, 949 (1994).

[67] K. Inoue, K. Kojima and K. Yoshioka, "Probing flavor structure in unified theory with scalar spectroscopy," JHEP **0707**, 027 (2007) [hep-ph/0703253].

[68] N. Maekawa, Y. Muramatsu and Y. Shigekami, "Sizable D-term contribution as a signature of $E_6 \times SU(2)_F \times U(1)_A$ SUSY GUT model," PTEP **2014** (2014) no.11, 113B02 [arXiv:1405.4193 [hep-ph]].

[69] J. Hisano and Y. Shimizu, "Hadronic EDMs induced by the strangeness and constraints on supersymmetric CP phases," Phys. Rev. D **70**, 093001 (2004) [hep-ph/0406091].

[70] K. V. P. Latha, D. Angom, B. P. Das and D. Mukherjee, "Probing CP violation with the electric dipole moment of atomic mercury," Phys. Rev. Lett. **103**, 083001 (2009) Erratum: [Phys. Rev. Lett. **115**, no. 5, 059902 (2015)] [arXiv:0902.4790 [physics.atom-ph]].

[71] J. R. Ellis, J. S. Lee and A. Pilaftsis, "Electric Dipole Moments in the MSSM Reloaded," JHEP **0810**, 049 (2008) [arXiv:0808.1819 [hep-ph]].

[72] M. Ishiduki, S.-G. Kim, N. Maekawa and K. Sakurai, "CEDM constraints on modified sfermion universality and spontaneous CP violation," Prog. Theor. Phys. **122**, 659 (2009) [arXiv:0901.3400 [hep-ph]].

[73] M. Ishiduki, S.-G. Kim, N. Maekawa and K. Sakurai, "Spontaneous CP violation in E_6 SUSY GUT with SU(2) flavor and anomalous U(1) symmetries," Phys. Rev. D **80**, 115011 (2009) Erratum: [Phys. Rev. D **81**, 039901 (2010)] [arXiv:0910.1336 [hep-ph]].

[74] H. Kawase and N. Maekawa, "Flavor structure of E_6 GUT models," Prog. Theor. Phys. **123**, 941 (2010) [arXiv:1005.1049 [hep-ph]].

[75] N. Maekawa and K. Takayama, "Neutrino properties in $E_6 \times SU(2)_F$ SUSY GUT with spontaneous CP violation," Phys. Rev. D **85**, 095015 (2012) [arXiv:1202.5816 [hep-ph]].

[76] J. M. Pendlebury *et al.*, "Revised experimental upper limit on the electric dipole moment of the neutron," Phys. Rev. D **92**, no. 9, 092003 (2015) [arXiv:1509.04411 [hep-ex]].

[77] B. Graner, Y. Chen, E. G. Lindahl and B. R. Heckel, "Reduced Limit on the Permanent Electric Dipole Moment of ^{199}Hg," Phys. Rev. Lett. **116**, no. 16, 161601 (2016) Erratum: [Phys. Rev. Lett. **119**, no. 11, 119901 (2017)] [arXiv:1601.04339 [physics.atom-ph]].

[78] N. Maekawa, Y. Muramatsu and Y. Shigekami, "Constraints of chromoelectric dipole moments to natural SUSY type sfermion spectrum," Phys. Rev. D **95** (2017) no.11, 115021 [arXiv:1702.01527 [hep-ph]].

[79] C. Patrignani *et al.* [Particle Data Group], "Review of Particle Physics," Chin. Phys. C **40**, no. 10, 100001 (2016).

[80] N. Cabibbo, "Unitary Symmetry and Leptonic Decays," Phys. Rev. Lett. **10**, 531 (1963).

[81] M. Kobayashi and T. Maskawa, "CP Violation in the Renormalizable Theory of Weak Interaction," Prog. Theor. Phys. **49**, 652 (1973).

[82] L. L. Chau and W. Y. Keung, "Comments on the Parametrization of the Kobayashi-Maskawa Matrix," Phys. Rev. Lett. **53**, 1802 (1984).

[83] L. Wolfenstein, "Parametrization of the Kobayashi-Maskawa Matrix," Phys. Rev. Lett. **51**, 1945 (1983).

[84] M. Gell-Mann, P. Ramond and R. Slansky, "Complex Spinors and Unified Theories," Conf. Proc. C **790927**, 315 (1979) [arXiv:1306.4669 [hep-th]].

[85] T. Yanagida, "Horizontal Symmetry And Masses Of Neutrinos," Conf. Proc. C **7902131**, 95 (1979).

[86] H. Georgi, H. R. Quinn and S. Weinberg, "Hierarchy of Interactions in Unified Gauge Theories," Phys. Rev. Lett. **33**, 451 (1974).

[87] L. Randall and C. Csaki, "The Doublet-triplet splitting problem and Higgses as pseudoGoldstone bosons," [hep-ph/9508208].

[88] N. Arkani-Hamed and S. Dimopoulos, "Supersymmetric unification without low energy supersymmetry and signatures for fine-tuning at the LHC," JHEP **0506**, 073 (2005) [hep-th/0405159].

[89] G. F. Giudice and A. Romanino, "Split supersymmetry," Nucl. Phys. B **699**, 65 (2004) Erratum: [Nucl. Phys. B **706**, 487 (2005)] [hep-ph/0406088].

[90] N. Arkani-Hamed, S. Dimopoulos, G. F. Giudice and A. Romanino, "Aspects of split supersymmetry," Nucl. Phys. B **709**, 3 (2005) [hep-ph/0409232].

[91] J. D. Wells, "PeV-scale supersymmetry," Phys. Rev. D **71**, 015013 (2005) [hep-ph/0411041].

[92] G. F. Giudice and A. Strumia, "Probing High-Scale and Split Supersymmetry with Higgs Mass Measurements," Nucl. Phys. B **858**, 63 (2012) [arXiv:1108.6077 [hep-ph]].

[93] L. J. Hall and Y. Nomura, "Spread Supersymmetry," JHEP **1201**, 082 (2012) [arXiv:1111.4519 [hep-ph]].

[94] M. Ibe and T. T. Yanagida, "The Lightest Higgs Boson Mass in Pure Gravity Mediation Model," Phys. Lett. B **709**, 374 (2012) [arXiv:1112.2462 [hep-ph]].

[95] M. Ibe, S. Matsumoto and T. T. Yanagida, "Pure Gravity Mediation with $m_{3/2} =$ 10-100TeV," Phys. Rev. D **85**, 095011 (2012) [arXiv:1202.2253 [hep-ph]].

[96] N. Arkani-Hamed, A. Gupta, D. E. Kaplan, N. Weiner and T. Zorawski, "Simply Unnatural Supersymmetry," arXiv:1212.6971 [hep-ph].

[97] H. Abe, T. Kobayashi and Y. Omura, "Relaxed fine-tuning in models with non-universal gaugino masses," Phys. Rev. D **76**, 015002 (2007) [hep-ph/0703044 [HEP-PH]].

[98] H. Abe, J. Kawamura and H. Otsuka, "The Higgs boson mass in a natural MSSM with nonuniversal gaugino masses at the GUT scale," PTEP **2013**, 013B02 (2013) [arXiv:1208.5328 [hep-ph]].

[99] J. L. Feng and D. Sanford, "A Natural 125 GeV Higgs Boson in the MSSM from Focus Point Supersymmetry with A-Terms," Phys. Rev. D **86**, 055015 (2012) [arXiv:1205.2372 [hep-ph]].

[100] H. Baer, V. Barger, P. Huang, A. Mustafayev and X. Tata, "Radiative natural SUSY with a 125 GeV Higgs boson," Phys. Rev. Lett. **109**, 161802 (2012) [arXiv:1207.3343 [hep-ph]].

[101] CKMfitter group, `http://ckmfitter.in2p3.fr/www/results/plots_eps15/num/ckmEval_results_eps15.html`

[102] K. G. Chetyrkin, J. H. Kuhn and M. Steinhauser, "RunDec: A Mathematica package for running and decoupling of the strong coupling and quark masses," Comput. Phys. Commun. **133**, 43 (2000) [hep-ph/0004189].

[103] H. Arason, D. J. Castano, B. Keszthelyi, S. Mikaelian, E. J. Piard, P. Ramond and B. D. Wright, "Renormalization group study of the standard model and its extensions. 1. The Standard model," Phys. Rev. D **46**, 3945 (1992).

[104] S. P. Martin and M. T. Vaughn, "Regularization dependence of running couplings in softly broken supersymmetry," Phys. Lett. B **318**, 331 (1993) [hep-ph/9308222].

[105] R. N. Mohapatra and J. W. F. Valle, "Neutrino Mass and Baryon Number Nonconservation in Superstring Models," Phys. Rev. D **34**, 1642 (1986).

[106] M. C. Gonzalez-Garcia and J. W. F. Valle, "Fast Decaying Neutrinos and Observable Flavor Violation in a New Class of Majoron Models," Phys. Lett. B **216**, 360 (1989).

[107] F. Deppisch and J. W. F. Valle, "Enhanced lepton flavor violation in the supersymmetric inverse seesaw model," Phys. Rev. D **72**, 036001 (2005) [hep-ph/0406040].

[108] R. D. Peccei and H. R. Quinn, "Constraints Imposed by CP Conservation in the Presence of Instantons," Phys. Rev. D **16**, 1791 (1977).

[109] R. D. Peccei and H. R. Quinn, "CP Conservation in the Presence of Instantons," Phys. Rev. Lett. **38**, 1440 (1977).

[110] A. J. Buras, F. De Fazio and J. Girrbach, "The Anatomy of Z' and Z with Flavour Changing Neutral Currents in the Flavour Precision Era," JHEP **1302**, 116 (2013) [arXiv:1211.1896 [hep-ph]].

[111] J. Brod and M. Gorbahn, "Next-to-Next-to-Leading-Order Charm-Quark Contribution to the CP Violation Parameter ϵ_K and ΔM_K," Phys. Rev. Lett. **108**, 121801 (2012) [arXiv:1108.2036 [hep-ph]].

[112] A. J. Buras, M. Jamin and P. H. Weisz, "Leading and Next-to-leading QCD Corrections to ϵ-Parameter and $B^0 - \bar{B}^0$ Mixing in the Presence of a Heavy Top Quark," Nucl. Phys. B **347**, 491 (1990).

[113] J. Brod and M. Gorbahn, "ϵ_K at Next-to-Next-to-Leading Order: The Charm-Top-Quark Contribution," Phys. Rev. D **82**, 094026 (2010) [arXiv:1007.0684 [hep-ph]].

[114] J. Laiho, E. Lunghi and R. S. Van de Water, "Lattice QCD inputs to the CKM unitarity triangle analysis," Phys. Rev. D **81**, 034503 (2010) [arXiv:0910.2928 [hep-ph]].

[115] G. Buchalla and A. J. Buras, "The rare decays $K \to \pi\nu\bar{\nu}$, $B \to X\nu\bar{\nu}$ and $B \to l^+l^-$: An Update," Nucl. Phys. B **548**, 309 (1999) [hep-ph/9901288].

[116] J. Charles, S. Descotes-Genon, Z. Ligeti, S. Monteil, M. Papucci and K. Trabelsi, "Future sensitivity to new physics in B_d, B_s, and K mixings," Phys. Rev. D **89**, no. 3, 033016 (2014) [arXiv:1309.2293 [hep-ph]].

[117] A. Bazavov *et al.* [Fermilab Lattice and MILC Collaborations], "$B^0_{(s)}$-mixing matrix elements from lattice QCD for the Standard Model and beyond," Phys. Rev. D **93**, no. 11, 113016 (2016) [arXiv:1602.03560 [hep-lat]].

[118] J. K. Ahn *et al.* [E391a Collaboration], "Experimental study of the decay $K^0_L \to \pi^0\nu\bar{\nu}$," Phys. Rev. D **81**, 072004 (2010) [arXiv:0911.4789 [hep-ex]].

[119] A. V. Artamonov *et al.* [BNL-E949 Collaboration], "Study of the decay $K^+ \to \pi^+ \nu\bar{\nu}$ in the momentum region $140 < P_\pi < 199$ MeV/c," Phys. Rev. D **79**, 092004 (2009) [arXiv:0903.0030 [hep-ex]].

[120] A. J. Buras, D. Buttazzo, J. Girrbach-Noe and R. Knegjens, "$K^+ \to \pi^+ \nu\bar{\nu}$ and $K_L \to \pi^0 \nu\bar{\nu}$ in the Standard Model: status and perspectives," JHEP **1511**, 033 (2015) [arXiv:1503.02693 [hep-ph]].

[121] F. Mescia and C. Smith, "Improved estimates of rare K decay matrix-elements from $K_{\ell 3}$ decays," Phys. Rev. D **76**, 034017 (2007) [arXiv:0705.2025 [hep-ph]].

[122] J. Brod, M. Gorbahn and E. Stamou, "Two-Loop Electroweak Corrections for the $K \to \pi\nu\bar{\nu}$ Decays," Phys. Rev. D **83**, 034030 (2011) [arXiv:1009.0947 [hep-ph]].

[123] G. Isidori and R. Unterdorfer, "On the short distance constraints from $K_{L,S} \to \mu^+\mu^-$," JHEP **0401**, 009 (2004) [hep-ph/0311084].

[124] A. J. Buras, R. Fleischer, S. Recksiegel and F. Schwab, "Anatomy of prominent B and K decays and signatures of CP violating new physics in the electroweak penguin sector," Nucl. Phys. B **697**, 133 (2004) [hep-ph/0402112].

[125] M. Gorbahn and U. Haisch, "Charm Quark Contribution to $K_L \to \mu^+\mu^-$ at Next-to-Next-to-Leading," Phys. Rev. Lett. **97**, 122002 (2006) [hep-ph/0605203].

[126] D. Ambrose *et al.* [BNL Collaboration], "New limit on muon and electron lepton number violation from $K_L^0 \to \mu^\pm e^\mp$ decay," Phys. Rev. Lett. **81**, 5734 (1998) [hep-ex/9811038].

[127] A. Alavi-Harati *et al.* [KTeV Collaboration], "Search for the rare decay $K_L \to \pi^0 e^+ e^-$," Phys. Rev. Lett. **93**, 021805 (2004) [hep-ex/0309072].

[128] A. Alavi-Harati *et al.* [KTeV Collaboration], "Search for the Decay $K_L \to \pi^0 \mu^+ \mu^-$," Phys. Rev. Lett. **84**, 5279 (2000) [hep-ex/0001006].

[129] F. Mescia, C. Smith and S. Trine, "$K_L \to \pi^0 e^+ e^-$ and $K_L \to \pi^0 \mu^+ \mu^-$: A Binary star on the stage of flavor physics," JHEP **0608**, 088 (2006) [hep-ph/0606081].

[130] E. Abouzaid *et al.* [KTeV Collaboration], "Search for lepton flavor violating decays of the neutral Kaon," Phys. Rev. Lett. **100**, 131803 (2008) [arXiv:0711.3472 [hep-ex]].

[131] V. Khachatryan *et al.* [CMS and LHCb Collaborations], "Observation of the rare $B_s^0 \to \mu^+\mu^-$ decay from the combined analysis of CMS and LHCb data," Nature **522**, 68 (2015) [arXiv:1411.4413 [hep-ex]].

[132] C. Bobeth, M. Gorbahn, T. Hermann, M. Misiak, E. Stamou and M. Steinhauser, "$B_{s,d} \to \ell^+\ell^-$ in the Standard Model with Reduced Theoretical Uncertainty," Phys. Rev. Lett. **112**, 101801 (2014) [arXiv:1311.0903 [hep-ph]].

[133] U. Bellgardt *et al.* [SINDRUM Collaboration], "Search for the Decay $\mu^+ \to e^+e^+e^-$," Nucl. Phys. B **299**, 1 (1988).

[134] A. Blondel *et al.*, "Research Proposal for an Experiment to Search for the Decay $\mu \to eee$," arXiv:1301.6113 [physics.ins-det].

[135] R. Kitano, M. Koike and Y. Okada, "Detailed calculation of lepton flavor violating muon-electron conversion rate for various nuclei," Phys. Rev. D **66**, 096002 (2002) Erratum: [Phys. Rev. D **76**, 059902 (2007)] [hep-ph/0203110].

[136] W. H. Bertl *et al.* [SINDRUM II Collaboration], "A Search for μ-e conversion in muonic gold," Eur. Phys. J. C **47**, 337 (2006).

[137] Y. Kuno [COMET Collaboration], "A search for muon-to-electron conversion at J-PARC: The COMET experiment," PTEP **2013**, 022C01 (2013).

[138] COMET Collaboration, http://comet.kek.jp/Documents_files/IPNS-Review-2014.pdf (2014).

[139] P. Langacker and M. Plumacher, "Flavor changing effects in theories with a heavy Z' boson with family nonuniversal couplings," Phys. Rev. D **62**, 013006 (2000) [hep-ph/0001204].

[140] K. Hayasaka *et al.*, "Search for Lepton Flavor Violating Tau Decays into Three Leptons with 719 Million Produced Tau+Tau- Pairs," Phys. Lett. B **687**, 139 (2010) [arXiv:1001.3221 [hep-ex]].

[141] H. Natori [DeeMe Collaboration], "DeeMe experiment - An experimental search for a mu-e conversion reaction at J-PARC MLF," Nucl. Phys. Proc. Suppl. **248-250**, 52 (2014).

[142] Mu2e Collaboration, "Proposal to search for $\mu^- + N \to e^- N$ with a single-event sensitivity below 10^{-16}," http://mu2e-docdb.fnal.gov/cgi-bin/ShowDocument?docid=388 (2008).

[143] PRISM Collaboration, "An exprimental search for a μ^--e^- conversion at sensitivity of the order of 10^{-18} with a highly intense muon sourse," http://www-ps.kek.jp/jhf-np/LOIlist/pdf/L25.pdf (2003).

[144] M. B. Green and J. H. Schwarz, "Anomaly Cancellation in Supersymmetric D=10 Gauge Theory and Superstring Theory," Phys. Lett. **149B**, 117 (1984).

[145] S. Dimopoulos and F. Wilczek, "Incomplete Multiplets in Supersymmetric Unified Models," Print-81-0600 (SANTA BARBARA), NSF-ITP-82-07 (1981).

[146] M. Srednicki, "Supersymmetric Grand Unified Theories and the Early Universe," Nucl. Phys. B **202**, 327 (1982).

[147] Y. Nir and N. Seiberg, "Should squarks be degenerate?," Phys. Lett. B **309**, 337 (1993) [hep-ph/9304307].

[148] N. Maekawa and Y. Muramatsu, "Nucleon decay via dimension-6 operators in $E_6 \times SU(2)_F \times U(1)_A$ SUSY GUT model," PTEP **2014**, no. 11, 113B03 (2014) [arXiv:1401.2633 [hep-ph]].

[149] A. G. Cohen, D. B. Kaplan and A. E. Nelson, "The More minimal supersymmetric standard model," Phys. Lett. B **388**, 588 (1996) [hep-ph/9607394].

[150] N. Maekawa, "NonAbelian horizontal symmetry and anomalous U(1) symmetry for supersymmetric flavor problem," Phys. Lett. B **561**, 273 (2003) [hep-ph/0212141].

[151] N. Maekawa, "E_6 unification, large neutrino mixings, and SUSY flavor problem," Prog. Theor. Phys. **112**, 639 (2004) [hep-ph/0402224].

[152] S.-G. Kim, N. Maekawa, A. Matsuzaki, K. Sakurai and T. Yoshikawa, "Lepton flavor violation in SUSY GUT model with non-universal sfermion masses," Phys. Rev. D **75**, 115008 (2007) [hep-ph/0612370].

[153] S.-G. Kim, N. Maekawa, A. Matsuzaki, K. Sakurai and T. Yoshikawa, "CP asymmetries of $B \to \phi K_S$ and $B \to \eta' K_S$ in SUSY GUT Model with Non-universal Sfermion Masses," Prog. Theor. Phys. **121**, 49 (2009) [arXiv:0803.4250 [hep-ph]].

[154] F. Gabbiani, E. Gabrielli, A. Masiero and L. Silvestrini, "A Complete analysis of FCNC and CP constraints in general SUSY extensions of the standard model," Nucl. Phys. B **477**, 321 (1996) [hep-ph/9604387].

[155] M. Ciuchini *et al.*, "ΔM_K and ϵ_K in SUSY at the next-to-leading order," JHEP **9810**, 008 (1998) [hep-ph/9808328].

[156] K. S. Babu and S. M. Barr, "Large neutrino mixing angles in unified theories," Phys. Lett. B **381**, 202 (1996) [hep-ph/9511446].

[157] S. M. Barr, "Predictive models of large neutrino mixing angles," Phys. Rev. D **55**, 1659 (1997) [hep-ph/9607419].

[158] M. Bando and N. Maekawa, "E_6 Unification with Bi-Large Neutrino Mixing," Prog. Theor. Phys. **106**, 1255 (2001) [hep-ph/0109018].

[159] K. Hamaguchi, M. Kakizaki and M. Yamaguchi, "Democratic (S)fermions and lepton flavor violation," Phys. Rev. D **68**, 056007 (2003) [hep-ph/0212172].

[160] S. Dimopoulos and L. J. Hall, "Electric dipole moments as a test of supersymmetric unification," Phys. Lett. B **344**, 185 (1995) [hep-ph/9411273].

[161] F. Sala, "A bound on the charm chromo-EDM and its implications," JHEP **1403**, 061 (2014) [arXiv:1312.2589 [hep-ph]].

[162] L. J. Hall, V. A. Kostelecky and S. Raby, "New Flavor Violations in Supergravity Models," Nucl. Phys. B **267**, 415 (1986).

[163] M. Jung and A. Pich, "Electric Dipole Moments in Two-Higgs-Doublet Models," JHEP **1404**, 076 (2014) [arXiv:1308.6283 [hep-ph]].

[164] K. Fuyuto, J. Hisano and N. Nagata, "Neutron electric dipole moment induced by strangeness revisited," Phys. Rev. D **87**, no. 5, 054018 (2013) [arXiv:1211.5228 [hep-ph]].

[165] C. D. Froggatt and H. B. Nielsen, "Hierarchy of Quark Masses, Cabibbo Angles and CP Violation," Nucl. Phys. B **147**, 277 (1979).

[166] L. E. Ibanez and G. G. Ross, "Fermion masses and mixing angles from gauge symmetries," Phys. Lett. B **332**, 100 (1994) [hep-ph/9403338].

[167] S. P. Martin and M. T. Vaughn, "Two-loop renormalization group equations for soft supersymmetry breaking couplings," Phys. Rev. D **50**, 2282 (1994) Erratum: [Phys. Rev. D **78**, 039903 (2008)] [hep-ph/9311340].

[168] K. Bodek *et al.*, "An Improved Neutron Electric Dipole Moment Experiment," arXiv:0806.4837 [nucl-ex].

[169] I. Altarev *et al.*, "Towards a new measurement of the neutron electric dipole moment," Nucl. Instrum. Meth. A **611**, 133 (2009).

[170] C. A. Baker *et al.*, "CryoEDM: A cryogenic experiment to measure the neutron electric dipole moment," J. Phys. Conf. Ser. **251**, 012055 (2010).

[171] D. H. Beck *et al.* [nEDM Collaboration], "From yeV to TeV: Search for the Neutron Electric Dipole Moment," arXiv:1111.1273 [nucl-ex].

[172] I. Altarev *et al.*, "A next generation measurement of the electric dipole moment of the neutron at the FRM II," Nuovo Cim. C **035N04**, 122 (2012).

[173] S. Heinemeyer, W. Hollik and G. Weiglein, "The Masses of the neutral CP-even Higgs bosons in the MSSM: Accurate analysis at the two-loop level," Eur. Phys. J. C **9**, 343 (1999) [hep-ph/9812472].

[174] S. Heinemeyer, W. Hollik and G. Weiglein, "FeynHiggs: A Program for the calculation of the masses of the neutral CP-even Higgs bosons in the MSSM," Comput. Phys. Commun. **124**, 76 (2000) [hep-ph/9812320].

[175] G. Degrassi, S. Heinemeyer, W. Hollik, P. Slavich and G. Weiglein, "Towards high precision predictions for the MSSM Higgs sector," Eur. Phys. J. C **28**, 133 (2003) [hep-ph/0212020].

[176] M. Frank, T. Hahn, S. Heinemeyer, W. Hollik, H. Rzehak and G. Weiglein, "The Higgs Boson Masses and Mixings of the Complex MSSM in the Feynman-Diagrammatic Approach," JHEP **0702**, 047 (2007) [hep-ph/0611326].

[177] T. Hahn, S. Heinemeyer, W. Hollik, H. Rzehak and G. Weiglein, "FeynHiggs: A program for the calculation of MSSM Higgs-boson observables - Version 2.6.5," Comput. Phys. Commun. **180**, 1426 (2009).

[178] J. Baron *et al.* [ACME Collaboration], "Order of Magnitude Smaller Limit on the Electric Dipole Moment of the Electron," Science **343**, 269 (2014) [arXiv:1310.7534 [physics.atom-ph]].

[179] T. Chupp and M. Ramsey-Musolf, "Electric Dipole Moments: A Global Analysis," Phys. Rev. C **91**, no. 3, 035502 (2015) [arXiv:1407.1064 [hep-ph]].

[180] J. Doyle, "Search for the Electric Dipole Moment of the Electron with Thorium Monoxide-The ACME Experiment," `http://online.kitp.ucsb.edu/online/nuclear_c16/doyle/` (2016).

[181] J. Engel, M. J. Ramsey-Musolf and U. van Kolck, "Electric Dipole Moments of Nucleons, Nuclei, and Atoms: The Standard Model and Beyond," Prog. Part. Nucl. Phys. **71**, 21 (2013) [arXiv:1303.2371 [nucl-th]].